JAIST Repository
https://dspace.jaist.ac.jp/

Title	薬剤及び細胞の放出制御を目指したポリペプチド系の構築
Author(s)	Patel, Monika
Citation	
Issue Date	2017-09
Type	Thesis or Dissertation
Text version	ETD
URL	http://hdl.handle.net/10119/14837
Rights	
Description	Supervisor:松村　和明，マテリアルサイエンス研究科，博士

JAIST
JAPAN
ADVANCED INSTITUTE OF
SCIENCE AND TECHNOLOGY

Japan Advanced Institute of Science and Technology

Doctoral Dissertation

Tunable polypeptide systems and their application in controlled delivery of drugs and cells.

Monika Patel

Supervisor: Assoc. Prof. Dr. Kazuaki Matsumura

School of Materials Science

Japan Advanced Institute of Science and Technology

September 2017

Thesis Title	Tunable polypeptide systems and their application in controlled delivery of drugs and cells.
Submitted by	Monika Patel
Thesis Advisor	Assoc. Prof Kazuaki Matsumura
Thesis Co-advisor	Professor Takahiro Hohsaka

THESIS COMMITTEE

Chairman **Assoc. Prof. Dr. Kazuaki Matsumura**

Japan Advanced Institute of Science and Technology

Referee **Professor Dr. Tatsuo Kaneko**

Japan Advanced Institute of Science and Technology

Referee **Professor Dr. Yuzuru Takamura**

Japan Advanced Institute of Science and Technology

Referee **Assoc. Prof. Dr. Toshiaki *Taniike***

Japan Advanced Institute of Science and Technology

External Referee **Assoc. Prof. Dr. Tadashi Nakaji-Hirabayashi**

University of Toyama

ACKNOWLEDGEMENTS

Numerous people over the years have helped me get here and made it happen. So I take immense pleasure to thank everyone who made this thesis possible.

First and foremost, I take this opportunity to convey my deepest gratitude and respect for my thesis advisor Professor Kazuaki MATSUMURA for his constant support, motivation and advice throughout this project. He has always encouraged me to develop as an independent researcher and helped me realize the power of critical reasoning. He has always been a supporting mentor and an extraordinary advisor. With his enthusiasm, inspiration, and his great efforts to explain things clearly and simply, he helped to make research fun for me. Throughout my dissertation period, he provided encouragement, sound advice, critical comments and lots of good ideas.

My earnest thanks must also go to all the members of my thesis advisory and exam committee: *Professor Tatsuo KANEKO, Professor Yuzuru TAKAMURA, Associate Professor Toshiaki TANIIKE* and external referee *Assoc. Prof. Tadashi NAKAJI-HIRABAYASHI* not only for their insightful comments and encouragement, but also for the questions which guided me to widen my research from various viewpoints. They generously gave their time to offer me valuable comments toward improving my work and provided me constructive criticism which helped me develop a broader perspective to my thesis.

My sincere thanks again goes to my minor research supervisor Professor Tatsuo KANEKO, without his precious support it would not be possible to complete my doctoral thesis. Also his support with the glove box facility of his lab have been crucial to this thesis. I would also like to express deep gratitude towards sub supervisor Assoc. Professor Takahiro HOHSAKA for their kind support.

There is no way to express how much it meant to me and to this thesis to have such cooperative and supporting lab members. I would like to thank all members of TAKAMURA lab for their help and all the good times we had together. This would be incomplete without mentioning the

indispensable support from Japan Advanced Institute of Science and Technology (JAIST) and MEXT that bought this entire affair to a successful end.

On a personal note I would like to dedicate this thesis to my family. No word could thank them for always being the support system and standing with me no matter what the case is. I owe an earnest thanks to my parents, my sister and my grandparents for their unconditional love and endless patience. It was their love that raised me up again when I got enervated. And finally I would thank all my friends in JAIST who helped me get through this agonizing period in the most positive way, and has been a family away from home.

Monika Patel

CONTENTS

PREFACE

Over the past several decades, synthetic polypeptides, poly- (amino acid)s, have received increasing attention in terms of controlled synthesis, structure–property relationships, and bio-related applications. Polypeptide-based copolymers can self-assemble into diverse aggregate structures, such as spherical micelles, cylindrical micelles, vesicles, and hierarchical structures in selective solvents. Due to their good biocompatibility, polypeptides and their assemblies are especially promising candidates as delivery systems for various therapeutic payloads, for example, drugs and DNA. The hydrophilic shell stabilizes the aggregates in blood circulation, and the hydrophobic core acts as a nano-reservoir for therapeutic agents. In addition, mimicking the role of mineral proteins, polypeptide aggregates have been applied as modifiers to mediate the internalization of inorganics in recent research. For bio-related applications such as delivery vehicles and bio-mineralization additives, it is essential to control the morphology, structure, and functionality of polypeptide self-assemblies. The molecular architecture is a basic factor determining the self-assembly behavior of copolymers in solution. Copolymers with various topologies, including block, graft, and dendrimer-like, display diverse self-assembly behaviors in selective solvents. However, synthesis of copolymers with various topologies and defined chemical compositions is a daunting task. The cooperative self-assembly of copolymers with secondary components, such as homopolymers, copolymers, nanoparticles (NPs), and small molecules, has therefore emerged as an appealing strategy for constructing various aggregates. In addition, copolymer self-assembly behavior is highly dependent on the preparation conditions such as the nature of the solvent and the polymer concentration. For the polypeptide based copolymers, the ordering of polypeptide rods and the rod–coil chain conformation transition induce distinct self-assembly behaviors. Owing to all these properties, polypeptide materials have gained significant attention among all the researchers worldwide. The main purpose of this study was to develop synthetic polypeptides with controlled architecture and employ them for different biomaterial applications. The first chapter deals with the general introduction for the thesis and gives an insight over the polypeptide materials, their broad uses in the field of wound healing .d protein studies. And the latter part of this chapter explains the detailed research

objective of the thesis. The second chapter deals with the development of synthetic polypeptides and their employment in the formation of drug loaded micelle hydrogel composites. The drug release profiles of the composites were investigated in detail in this chapter with varying parameters. This chapter establishes the utility of the composites in wound healing study. The third chapter of this thesis deals with the *in vivo* study. For this study rat models were used to evaluate and examine the drug releasing efficacy of the drug loaded micelle-hydrogel composite prepared in the previous chapter for purpose of wound healing. This chapter also establishes the mechanical studies of the composites prepared. The fourth chapter of the thesis deals with a new arena of use of polypeptide material, using them to formulate gel microspheres for cell entrapment and release. This chapter also focuses of release of bioactive compounds with targeted delivery. The final and fifth chapter of this thesis presents the summary and scope of the thesis. It details the importance of this thesis and its contribution in the biomaterials field. The chapter also discusses the possible future impact of this thesis.

In conclusion, this thesis summaries the adaptability and the multifunctional nature of the polypeptide materials in this field.

CHAPTER 1

General Introduction

1.1 Synthetic polypeptides

Over the past several decades, synthetic polypeptides, poly- (amino acid)s, have received increasing attention in terms of controlled synthesis, structure–property relationships, and bio-related applications.[1] Polypeptide-based copolymers can self-assemble into miscellaneous aggregate structures, such as spherical micelles, cylindrical micelles, vesicles, and hierarchical structures in selective solvents.[2] Due to their decent biocompatibility, polypeptides and their assemblies are particularly promising candidates as delivery systems for various therapeutic payloads, for example, drugs and DNA.[3] The hydrophilic shell stabilizes the aggregates in blood circulation, and the hydrophobic core acts as a nano-reservoir for therapeutic agents. In addition, mimicking the role of mineral proteins, polypeptide aggregates have been applied as modifiers to mediate the internalization of inorganics in recent research.[4] For bio-related applications such as delivery vehicles and bio mineralization additives, it is essential to control the morphology, structure, and functionality of polypeptide self-assemblies. The molecular design is a basic factor determining the self-assembly behavior of copolymers in solution.[5] Copolymers with various topologies, including block, graft, and dendrimer-like, display diverse self-assembly behaviors in selective solvents. However, synthesis of copolymers with various topologies and defined chemical compositions is a daunting task. The cooperative self-assembly of copolymers with secondary components, such as homopolymers, copolymers, nanoparticles (NPs), and small molecules, has therefore emerged as an appealing strategy for constructing various aggregates.[6] In addition, copolymer self-assembly behavior is highly dependent on the preparation conditions such as the nature of the solvent and the polymer concentration. For the polypeptide based copolymers, the ordering of polypeptide rods and the rod–coil chain conformation transition induce distinct self-assembly behaviours.[7] Furthermore, because polypeptides are chiral polymers, chirality

should be another distinctive factor influencing the self-assembly behavior and function of the formed structures.[8] A high-performance delivery vehicle has various demands, such as stability during circulation, delivering payloads to specific sites, and releasing payloads in a desired manner.[9] Polypeptide assemblies are good candidates for ‘‘smart’’ delivery, responding to physical and chemical stimuli based on the following characteristics. (a) Ionic polypeptides such as poly (L-glutamic acid) (PLGA) and poly(L-lysine) (PLL) can be used to physically bind drugs bearing opposite charge. Changing the pH of the solution weakens the binding and releases the drugs. With the change of pH, the conformation of polypeptides may also change, facilitating the release of the drugs.[10] (b) Polypeptides contain various reactive groups, which could serve to chemically conjugate drugs with labile chemical bonds. The loaded drugs can be released by breaking the labile chemical bonds.[11] (c) Due to the physical or chemical stimuli, the structure of the deliveries can be disrupted, which induces a rapid release of payloads.[12] Bio minerals, generated under the mediation of natural proteins, have hierarchical organization and superior properties[13] Inspired by protein-controlled mineralization, the biomimetic mineralization of inorganics in the presence of synthetic polymers has attracted increasing attention.[14] Due to the resemblance in chemical composition to that of proteins, the synthetic hydrophilic polypeptides such as PLGA, polyaspartic acid (PAsp), PLL and their derivatives have been used to mediate the mineralization of inorganics.[15] Later, it was found that polymer self-assemblies are suitable additives mediating the bio mineralization of inorganics.[16] Because the polypeptide aggregates can mimic the folded structure of the mineral proteins, these polypeptide aggregates are more attractive for mediating the mineralization of inorganics.[17] An experimental understanding of both the self-assembly behavior of copolymers and the release behavior of deliveries usually suffers from difficulties related to limited experimental techniques. However, theory and simulation can somewhat

overcome the limitations because they provide more straightforward results and detailed information than pure experiments, including the chain distribution in the aggregates, the release process of the drugs, structural variation of delivery during drug release, and crystallization behaviour of biomineralization.[18]

Synthetic polypeptides (i.e. poly(amino acids)) are of pronounced importance because of their possible uses in biomedicine and biotechnology some of them being tissue engineering, drug delivery, and as therapeutics.[19] Based on the amino acid side chain they can take on definite well-organized conformations (e.g. helices, sheets and turns) and self-assemble into specifically distinct bio-mimetic configurations through non-covalent associations such as hydrogen bonding, van der Waals forces and π-π stacking.[20] Conventionally solid phase peptide synthesis (SPPS) has been actively used to make polypeptides with specifically precise amino acid arrangements on a laboratory scale.[21] While SPPS is extensively acknowledged as a routine and robust method, the effort demanding step-by-step amino acid coupling including de-protection/ coupling steps and the restriction of an attainable maximum chain length of around 50 amino acid residues can be limiting aspects.[22] On the other hand, the ring-opening polymerisation of amino acid N-carboxyanhydrides (NCA), while missing the ability to produce precise sequences, is a highly adaptable and multipurpose technique for the faster synthesis of higher molecular weight synthetic polypeptides.[23] Thanks to the constant development in NCA polymerisation in the last few years, synthetic polypeptides with manageable (high) molecular weight, narrow polydispersity, complex polymeric constructions and structures along with designated chirality can be prepared in great yield and huge amount.[24] The advancement in NCA polymerisation along with advanced orthogonal functionalization methods as well as the addition with other precise polymerisation techniques considerably broadens the possibility of polypeptide structure blocks in a range of

material designs strategy.[25] Directed applications for innovative and new polypeptide amalgam materials are often required in biomedicine and biotechnology containing tissue engineering, drug delivery and bio-diagnostics.

By design these materials can be engaged at the boundary of natural and synthetic polymeric materials. They associate the flexibility of contemporary synthetic procedures to attain improved characteristics along with natural building blocks (amino acids), which unlocks substantial prospects for a new biomaterials platform.

1.1.1 Ring-opening polymerization of α-amino acid N-carboxyanhydride (NCA)

The preparation and polymerisation of NCAs was first described by Hermann Leuchs in 1906.9,[8] After 1921, Curtius,[26] Wessely[27] and their coworkers utilized NCAs with various initiators such as water, alcohol or primary amines in the process of ring-opening polymerisation as the first report to prepare some polypeptides with high molecular weight. NCA can be prepared either by the combining N-alkyloxycarbonylamino acids with various halogenating agents (Leuchs method[26]) or by simply the action of a-amino acids on phosgene (Fuchs–Farthing method; [28] Scheme 1). Triphosgene, diphosgene and di-tertbutyltricarbonate and similar compounds have been used as phosgene alternatives, permitting phosgene to form progressively during NCA synthesis.[29] Typically recrystallization and/or also flash chromatography can be used for the obtaining purified NCAs and to eliminate any by-products produced during the course of synthesis including HCl, HCl–amino acid salts and 2-isocyanatoacyl chlorides as reaction can be adversely effected through inhibition and/or quenching of propagation of forming polymer chain by electrophilic by-products and thus affect the synthesis of polypeptides.[30] NCA ring-opening polymerisation can be initiated by a variety of nucleophiles and bases including but not confined

to amines and metal alkoxides (Scheme 1).[31] The two extensively acknowledged techniques for the polymerisation of NCAs are the ‘‘normal amine’’ (NAM) and the ‘‘activated monomer’’ (AMM) mechanisms.[32] Initiators for the latter characteristically comprise bases (i.e. tertiary amines) and alkoxides, which removes the proton from the NCA nitrogen (3-N) causing in the formation of an NCA anion. The deprotonated NCA anion then can initiate the NCA polymerisation and stimulate the propagation by attacking the 5-CO of additional NCA thereby creating a new anion by the discharge of CO_2. Polymerizations going through the AMM are usually fully uninhibited and thus less preferred in the preparation of well-defined polypeptides. The NAM approach is normally followed by reactions initiated by nonionic initiators for NCA polymerizations having at minimum one mobile hydrogen atom such as primary and secondary amines, alcohol and water. The origination step is established on the nucleophilic attack on the carbonyl (5-CO) of the NCA ring.[33] The ring opening happens and the unstable intermediate carbamic acid is formed for a short span by proton transfer. This carbamic acid then decarboxylates by the removal of CO_2 and the newly-formed primary amine stimulates the propagation of the polymerisation. The NAM provides better control above the molecular weight of the synthesized polypeptide along with end-group fidelity. Conversely, due to a chances of possible side reactions occurring such as the end group termination[34] or the formation of cyclic by-products[35] caused by contaminations in the NCAs or the solvent used in the reaction, or the presence of moisture, the reaction control can be significantly restricted. Deming and his group were the first to present the concept of ‘‘living’’ NCA polymerisation by means of transition metal catalysts.[36] He employed zero valent nickel and cobalt initiators[37] (i.e., $(PMe_3)_4Co$, and bpyNi(COD), bpy (2,20 –bipyridine) and synthesized block polypeptides with brilliant control on the molecular weight with a narrow polydispersity index (PDI). In this method, the synthesis of the chelating metallocyclic

intermediates is seen by the involvement of transition metal complex and NCA and is necessary for performing a living polymerisation of NCA for polypeptide synthesis. However, bringing together end-group functionality through the introduction of various initiator is wearisome process and has only been described in one literature instance using a bifunctional initiator comprising an activated bromide group for Atom Transfer Radical Polymerisation (ATRP) and a Ni amido amidate complex for NCA polymerisation.[38] Successive nickel initiated polymerisation of g-benzyl-L-glutamate (BLG) NCA and ATRP of methyl methacrylate produced a complex rod–coil block hybrid copolymer that was amalgam of polypeptide and methacrylate in form of poly(g-benzyl-L-glutamate-b-methyl methacrylate). Further, primary amine initiated NCA polymerisation is therefore still the most extensively used method and various experimental procedures have been examined and optimized to provide well-defined polypeptides. Hadjichristidis and co-workers demonstrated that by means of highly purified chemicals and high vacuum methods, homo- and block polypeptides with ultra-high and controlled molecular weight can be easily synthesied.[39] In this method, the extremely purified and distilled polymerisation solvent and initiator were used, along with the suppression of the carbamic acid–CO_2 equilibrium by the effective elimination of CO_2 from the reaction mixture as well as the controlling the side reactions among DMF and the terminal-groups of growing polymer chains were accounted for in the polymerisation mechanism. The rewards of the high vacuum system for the synthesis of precise polypeptides were also confirmed by Messman and coworkers.[40] By means of matrix-assisted laser desorption/ionization time-offlight mass spectrometry (MALDI-TOF MS), nano-assisted laser desorption/ionization time-of-flight mass spectrometry (NALDITOF MS), and ^{13}C NMR spectroscopy they confirmed that the method involving high vacuum polymerisation advanced entirely by the NAM with negligible termination. In 2004 alternative ground-breaking method to

remove side reactions in the NAM NCA polymerisation was described by Vayaboury and coworkers.[41] The group methodically examined the polymerization of Ne-trifluoroacetyl-L-lysine NCA initiated by hexylamine in DMF at various temperatures. The living amine chain-ends were investigated by size exclusion chromatography (SEC) and non-aqueous capillary electrophoresis (NACE) showed a dramatic increase from 22 % to 99 % when the polymerisation temperature was dropped from 20 to 0°C. The removal of the end reactions at low temperature was credited to greater activation energies requirements of the side reactions than that of the main chain propagation.[42] Conversely, an apparent disadvantage of the polymerisation at 0°C is the elongated reaction intervals. Very recently, Heise and Habraken studied NCA polymerisation of a variety of different NCAs to improve the NAM by combining together the goodness of the high-vacuum and the low-temperature techniques.[43]

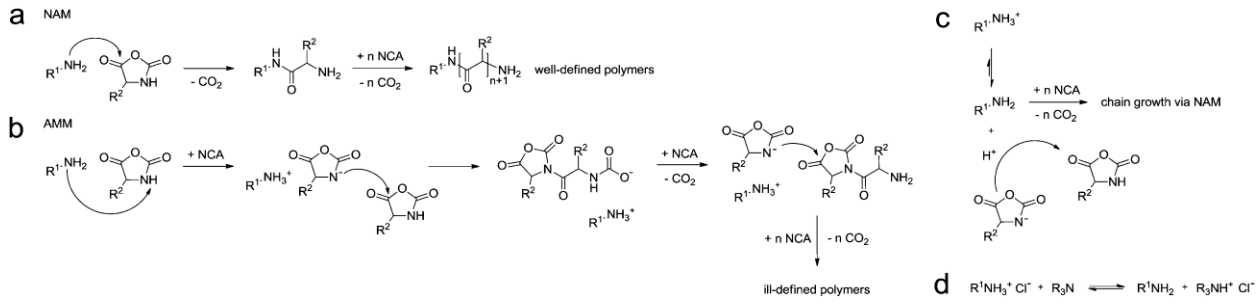

Figure 1.1 (a) Normal amine mechanism (NAM), (b) activated monomer mechanism (AMM), (c) proposed mechanism for the ammonium-mediated ring opening polymerisation13 and (d) primary/tertiary amine–ammonium equilibrium.[45]

The amalgamation of two dissimilar methods not only helped the NCA polymerisation in a controllable way but also considerably reduced the polymerisation time. A tetra block copolymer with narrow poly dispersity index and high control over structure was synthesized including poly(g-benzyl-L-glutamate), poly(L-alanine), poly(Ne-benzyloxycarbonyl-L-lysine) and poly(b-

benzyl-L-aspartate) blocks through the mixture of the ideal considerations of temperature and pressure. In 2007, a new organosilicon-meditated NCA polymerisation method was described by Cheng and coworkers.[46] Prominently, approximately measureable polymerisation with the controlled degree of polymerisation (DP) here 300 was accomplished in the time frame of 24 hours or even less at ambient conditions.[47] In 2011, a collection of rare earth complexes were presented as first report by Ling and coworkers as initiators for NCA polymerisation of g-benzyl-Lglutamate NCA and L-alanine NCA including rare earth isopropoxide ($RE(OiPr)_3$), tris(2,6-di-tert-butyl-4-methylphenolate) ($RE(OAr)_3$), tris(borohydride) ($RE(BH4)_3(THF)_3$), tris[bis(trimethylsilyl)amide] ($RE(NTMS)_3$) and trifluoromethanesulfonate etc.[48] Homo-, random and block copolymers were readily synthesized in great yield with predictable molecular weights and comparatively low PDIs (1.1–1.6), thereby displaying the living nature of the polymerization.

1.1.2 Nanostructures of polypeptide based self-assemblies

Polypeptide copolymers can self-assemble into diverse aggregate structures, including spherical micelles, cylindrical micelles, and vesicles. Moreover, hierarchical structures such as superhelices have also been observed in recent work.[49] The molecular architecture is a basic factor determining the self-assembly behaviour of polypeptide-based amphiphilic copolymers. With the development of polymer chemistry, copolymers with various topologies, including block, graft, brush-like, and dendrimerlike copolymers, have been synthesized. These copolymers display diverse self-assembly behaviours in selective solvents. In addition, cooperative self-assembly of polypeptide copolymers with secondary components has emerged as an appealing strategy to produce diverse aggregates with designed structures and functionalities.[50] A variety of guest components, including hydrophobic homopolymers,[51] amphiphilic copolymers,[52] nanoparticles (NPs),[53] and small molecules, have been applied to cooperatively self-assemble with polypeptide copolymers.

Compared with conventional polymers, a distinguishing characteristic of polypeptides is that they can adopt various conformations, including random coil, a-helix, and b-sheet.[54] The conformation of the polypeptide determines the properties of chains, such as rigidity and solubility in solution, which further influences the self-assembly behaviour of the polypeptide copolymers. For example, poly(g-benzyl L-glutamate) (PBLG) acts as a rigid rod in a-helix conformation; when adopting random coil conformation, PBLG becomes a flexible chain.[55] In aqueous solution, poly(L-glutamic acid) (PLGA) with a random coil conformation dissolves better than those with a-helix and b-sheet conformations.[56] Under certain conditions, the conformation of a polypeptide can transform from one to another, and the morphology and structure of the polypeptide assemblies can be varied by these transitions.[57] In addition, because polypeptides are chiral polymers, their chirality should be another important factor regulating the self-assembly behaviour of polypeptide copolymers. In this section, the self-assembly into various nanostructures of polypeptide copolymers and their corresponding mixtures are reviewed.

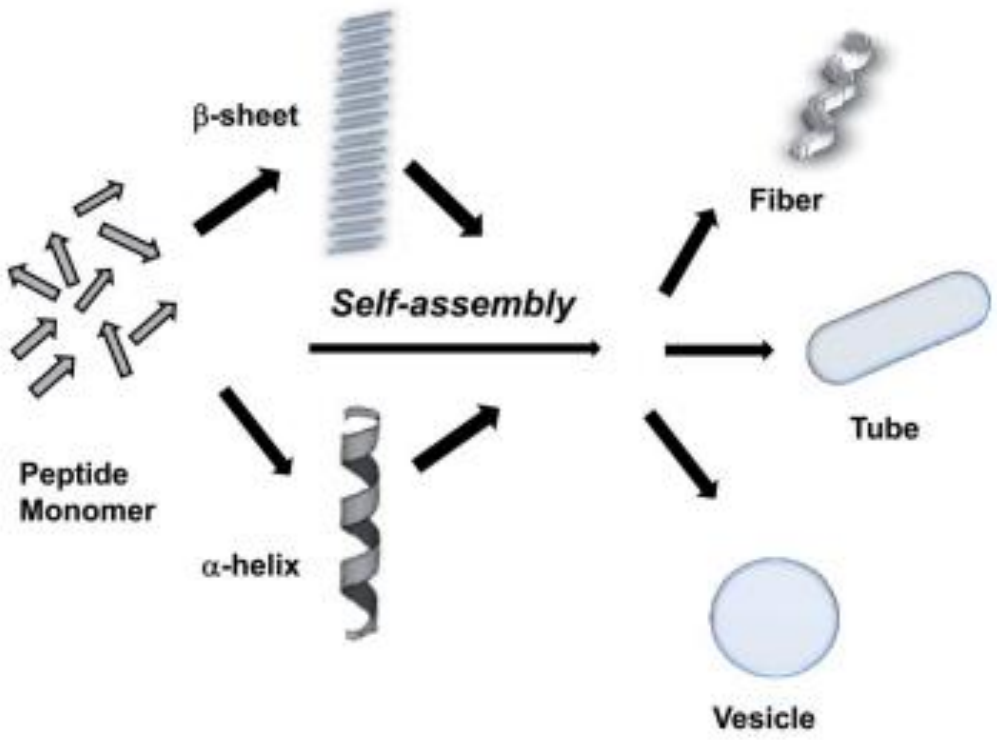

Figure 1.3 Self-assembly of peptides into different types of nanostructures.[58]

1.1.2.1 Aggregates self-assembled from single-component polypeptide copolymers

As elucidated by conventional block copolymer self-assembly systems, for example, polystyrene-b-poly(ethylene glycol) (PS-b-PEG), the morphology of the aggregates is mainly determined by the architecture and composition of the copolymers.[59] Preparation conditions such as the nature of the solvent and the polymer concentration also affect the aggregate morphology. For polypeptide copolymers, several distinct factors, including the ordering of rigid a-helical polypeptide chains, the variation of chain packing induced by conformation transitions, and the stimuli-induced solubility change of hydrophilic polypeptides, are applied to adjust the self-assembly behavior of polypeptide copolymers. In the following content, we discuss the self-assembly behavior of polypeptide copolymers with various macromolecular architectures.

1.1.2.2 Aggregates self-assembled from polypeptide block copolymers.

Block copolymers are the most studied building units in constructing self-assemblies, and they usually serve as models to study the principles of polymer self-assembly. In recent years, the self-assembly of polypeptide block copolymers has attracted increasing attention.[60] For polypeptide copolymers containing rigid hydrophobic polypeptide segments, the ordered packing of polypeptide rods causes the copolymer to display distinct self-assembly behaviours.[61] Block copolymers are widely studied in self-assembly research. For polypeptide-based block copolymers, making use of the characteristics of the polypeptide segments, including the rigidity of the chain and conformation transition under certain conditions, has led to diverse self-assembly structures. In addition to these simple diblock and triblock copolymers, there have been few studies on the self-assembly of polypeptide-based multi-block copolymers. Multi-block copolymers, typically (AB)n-type and A(BC)n-type, display unique self-assembly behaviours that have been illustrated through experiments and simulations.[62] Polypeptide-based multi-block copolymers could generate new assembly features. For example, due to the inherent structural features of the polypeptide segments, these multi-block polypeptide block copolymers are promising materials for the construction of hierarchical structures with multiple sensitivities to their surroundings

1.1.2.3 Aggregates self-assembled from polypeptide graft copolymers.

Graft copolymers are another important class of building polymers that lead to aggregates with multiple morphologies.[63] Compared with block copolymers, graft copolymers have received less attention but have obvious advantages in adjusting the self-assembly behaviours by changing the side chain properties, such as the grafting density, chain length, and environmental sensitivity. In polypeptide graft copolymers, the polypeptide segments can serve as either backbones or side

chains.[64] Kuo et al. used a combination of ATRP, ROP, and click chemistry to synthesize polystyrene-b-poly(g-propargyl-L-glutamateg-ethylene oxide) (PS-b-(PPLG-g-MEO_2)) block-graft copolymers. The conformation of the PPLG polypeptide segments was confirmed to be an a-helix. Their self-assembly behaviour was studied by adding water (selective solvent) to the polymer solution in DMF (common solvent).

1.1.3 Advantages of self-assembled peptide nanostructures for biomedical purposes

There are numerous uses in the biomedical arena where peptides that could readily form self-assembled nano-structures might have a significant part in various aspects such as of bio sensors and similar platforms, as effective drug-delivery and targeting systems, as contrast image means or as a hydrogels for tissue reparation and/or regeneration. This section presents the advantages that make this biomaterial such a promising candidate for such applications.

1.1.3.1 Synthesis

One of the more fascinating aspects of peptide structures that can self-assemble into confined and precise nanostructures is the point that their production happens in non-cruel circumstances. These kinds of biological supramolecular assemblies are usually made-up at temperatures close to room temperature, in the aqueous solvent settings and minus using any super specialized equipment. These factors make a enormous dissimilarities amongst these new biological nanomaterials and nanomaterials customarily utilized in nanotechnology such as currently employed ones like carbon nanotubes or silicon nanowires of which production involves higher temperatures, use of ultra-specialized apparatus and in some of the cases even involves use of clean-room facilities growing their manufacture cost. Moreover, the production of these self-assembled peptide nanostructures differs from a few seconds to few days of incubation.

Depending upon the type of the building block used, diverse shapes and architectures can be attained. An unusual case is the short aromatic dipeptide, diphenylalanine. By changing the production circumstances, nanotubes, nanofibers or nanoparticles can be easily produced . All these slight fabrication settings are replicated as low cost of the whole process.

1.1.3.2 Functionalization

In order to use these biological nanostructures as distinct imaging means or as part of a biosensing system they require to be adorned with suitable practical molecules rendering them with precise chemical and functional characteristics. Functional composites such as antibodies, magnetic or metallic particles, enzymes, quantum dots or fluorescent compounds have been combined into the assembly of self-assembled peptide.[65] Ryu and co-workers established photo luminescent peptide nanotubes by the in-situ combination of luminescent complexes containg photosensitizers such as salicylic acid.[66] Based on this notion, the same group later established an optical biosensor for the recognition of neurotoxins and compounds such as glucose and hydrogen peroxide

1.1.3.3 Biocompatibility

In spite of the increased levels of consideration provided to this type of biomaterial, an progressive research to assess the biocompatibility and immunogenicity of these nanostructures is still missing. Such an examination will convey vital evidence that will outline the opportunity to use this biomaterial in uses such as drug-delivery systems or tissue reparation in humans. The existing studies are inadequate to growth of cells and tissues in the presence of self-assembled peptide nanofibers or hydrogels and measured whether the tested cell or tissue development progress was affected by the presence of the biomaterial.

1.2 Wound healing

Wound dressings and covering devices comprise of a significant and wide reaching section of the health and pharmaceutical wound care market universally. Earlier, customary coverings such as natural or synthetic bandages, cotton wool, lint and gauzes all with changing grades of absorbency were utilized for the managing wounds and tissue damage. Their principal purpose being keeping the wound dry by letting free evaporation of wound exudates and inhibiting access to harmful bacteria and pathogens into the wound. Although it has now been revealed however, that having a warm humid wound surroundings attains more speedy and effective wound healing. Last two decades have slowly and steadily seen the upcoming of numerous dressings, with novel ones becoming presented each year. For instance, the total of newer dressings presented on the Drug Tariff in the UK increased from 4 in 1988 to 57 in May 1998 and by February 2007, the total number mounted at 262. These contemporary dressings are made on the notion of generating an optimum environment to permit epithelial cells to move and grow unhindered, for the optimal management and cure of wounds. These ideal conditions comprise a damp environment around the wound, unhindered oxygen flow to support renewing cells and tissues and a relatively low bacterial load. Other aspects which have added to the extensive variety of wound dressings comprise the diverse type of wounds (e.g. acute, chronic, exuding and dry wounds, etc.) and the point that no single kind of dressing is appropriate and applicable for the administration of all kinds of wounds. In addition, the wound healing course has numerous diverse stages that cannot be effectively targeted by any specific dressing.

Effective wound managing rely on considering a number of various aspects such as the type of wound being targeted, the healing course, patient situations in terms of health (e.g. diabetes),

environment and social setting, and the also physical and chemical nature of the offered dressings.[67] It is therefore significant, to evaluate and test the diverse dressings available in terms of their physical characteristics and clinical performance for any given type of wound and the also for the different stages of wound healing, before being taken for routine use.

1.2.1 Wounds

A wound can be explained as an imperfection or a disruption in the skin, consequence of a physical or thermal injury or damage or could be an outcome of the existence of an underlying medical or physiological condition. According to the Wound Healing Society, a wound is the outcome of 'disruption of normal anatomic structure and function'.[68] Based on the type of the healing course, wounds can be categorized as acute wounds and chronic wounds. Acute wounds are typically tissue damages that rebuild wholly, with almost negligible scarring, within the speculated time frame, typically 8–12 weeks.[69] The chief causes of acute wounds comprise mechanical damages caused due to external aspects such as scrapes, abrasions and/or tears which could be produced by frictional contact between the skin against a hard or sharp surface. Mechanical wounds also comprise piercing and penetrating wounds produced by sharp objects such as knives and or objects of high mechanical strength like gun shots, it also comprises surgical wounds caused by incisions made during a surgery or medical intervention (for example remove tumors). Additional class of acute wounds include wounds caused by high degree of heat such as burns and/or chemical injuries, which are caused from a various number of sources such as thermal, corrosive chemicals, exposure to radiation and/or a close contact with electricity. The hotness of the source and the exposure time of heat to the surface of skin governs the degree of a thermal burn.[70] Burns or thermal wounds will generally need dedicated care because of the accompanying trauma.

On the other hand, chronic wounds are generated from tissue damages that heal gradually, that is such injuries are often seen to have not been healed for beyond 12 weeks and often seen to reoccur. Such lesions fail to heal due to repetitive tissue abuses or core physiological conditions[71] such as disease like diabetes and presence of malignancies, persistent and/or reoccurring infections, deprived of essential primary treatment and other patient based factors. This result in a disorder of the arranged system of events during the wound healing process. Chronic wounds often contain decubitis ulcers (bedsores or pressure sores) and leg ulcers (venous, ischaemic or of traumatic origin).

Wounds can also be categorized based on the how many numbers of skin layers is injured and also based on area of skin affected. Wounds that disturbs the epidermal skin surface alone is denoted to as a superficial wound, whereas any wounds involving both the epidermis and the deeper dermis layers, injuring and/or involving the blood vessels, glandular region such as sweat glands and hair follicles is known as partial thickness wound. Full thickness wounds whereas happen when the subcutaneous fat underlying the dermis and/or even more deeper seated tissues are injured along with the epidermis and dermal layers.

1.2.2 Wound Healing

Wound healing is a precise biological series of processes related to the common phenomenon of growth and regeneration of new cells and subsequently tissue at the site of injury. This thesis does not primarily focuses on to review in detail the physiology of wound healing, but only to test the efficacy of devised materials which is relevant to wound management and the choice of wound dressings.[72] Wound healing advances through a sequence of codependent and overlying phases in which a range of cellular and matrix machineries act organized to reconstruct the integrity of damaged tissue and replace the lost tissue.[73] The wound healing procedure has been studied and

explained by Schultz[74] as comprising five intersecting stages that comprise multifaceted biochemical and cellular processes. These are defined as hemostasis, inflammation, migration, proliferation and maturation phases (Fig 1.3). In fact, Cooper[75] has claimed for expanding the understanding of wounds outside the cellular level to a molecular perspective as well. He emphasized the necessity to understand wound healing at numerous stages (cellular and molecular) to help advance wound handling and management. Wound healing preparations (dressings) and innovative technologies established to date emphasis on one or more of these features of the natural healing process that are summarized briefly below.

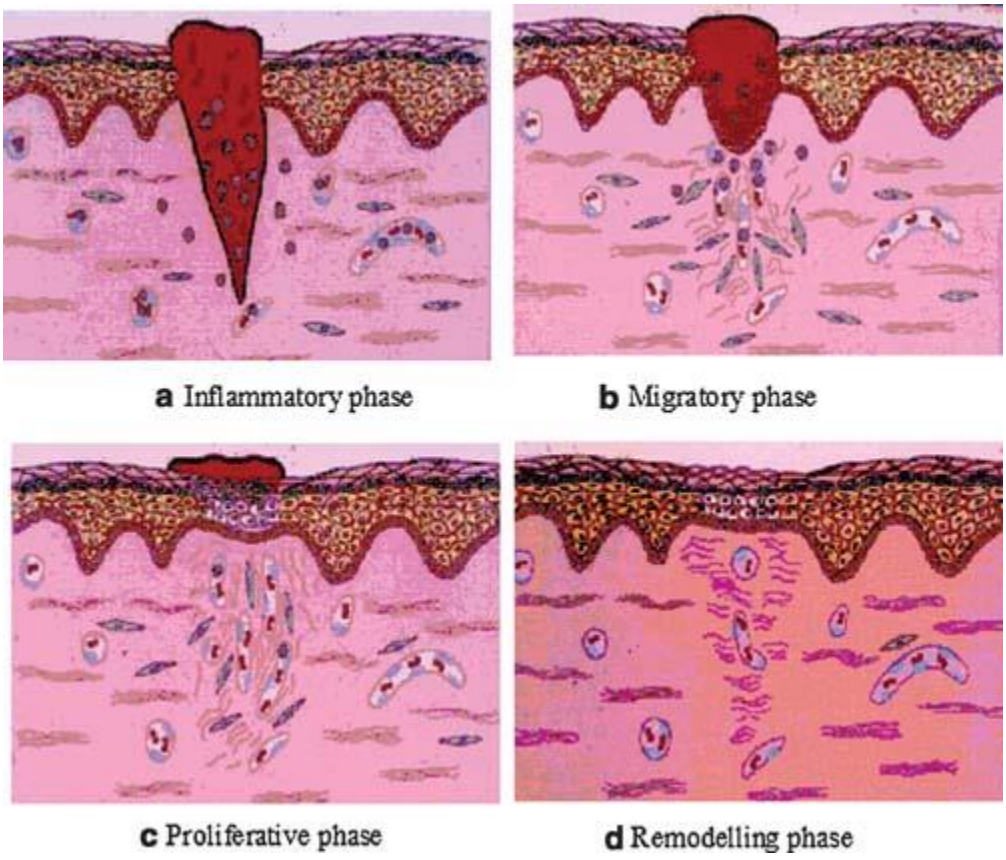

Figure 1.3 Schematic representation of the phases of wound healing (a) infiltration of neutrophils into the wound area (b) invasion of wound area by epithelial cells (c) epithelium completely covers the wound (d) many of the capillaries and fibroblasts, formed at early stages have all disappeared [76]

1.2.2.1 Haemostasis and Inflammation

Bleeding usually occurs when the skin is injured and serves to flush out bacteria and/or antigens from the wound. In addition, bleeding activates hemostasis which is initiated by exudate components such as clotting factors. Fibrinogen in the exudate elicits the clotting mechanism resulting in coagulation of the exudates (blood without cells and platelets) and, together with the formation of a fibrin network, produces a clot in the wound causing bleeding to stop. The clot dries to form a scab and provides strength and support to the injured tissue. Haemostasis therefore, plays a protective role as well as contributing to successful wound healing.[77]

The inflammatory phase occurs almost simultaneously with haemostasis, sometimes from within a few minutes of injury to 24 h and lasts for about 3 days. It involves both cellular and vascular responses. The release of protein-rich exudate into the wound causes vasodilation through release of histamine and serotonin, allows phagocytes to enter the wound and engulf dead cells (necrotic tissue). Necrotic tissue which is hard is liquefied by enzymatic action to produce a yellowish coloured mass described as sloughy. Platelets liberated from damaged blood vessels become activated as they come into contact with mature collagen and form aggregates as part of the clotting mechanism.

1.2.2.2 Migration

The migration phase involves the movement of epithelial cells and fibroblasts to the injured area to replace damaged and lost tissue. These cells regenerate from the margins, rapidly growing over the wound under the dried scab (clot) accompanied by epithelial thickening.

1.2.2.3 Proliferation

The proliferative phase occurs almost simultaneously or just after the migration phase (Day 3 onwards) and basal cell proliferation, which lasts for between 2 and 3 days. Granulation tissue is formed by the in-growth of capillaries and lymphatic vessels into the wound and collagen is synthesised by fibroblasts giving the skin strength and form. By the fifth day, maximum formation of blood vessels and granulation tissue has occurred. Further epithelial thickening takes place until collagen bridges the wound. The fibroblast proliferation and collagen synthesis continues for up to 2 weeks by which time blood vessels decrease and oedema recedes.

1.2.2.4 Maturation

This phase (also called the 'remodelling phase') involves the formation of cellular connective tissue and strengthening of the new epithelium which determines the nature of the final scar. Cellular granular tissue is changed to an acellular mass from several months up to about 2 years.

Table 1.1 describes the appearance of wounds in relation to the stages of wound healing. These descriptions relate not only to different types of wounds but also to the various stages through which a single wound may pass as it heals. [78]

Desirable Characteristics	Clinical Significance to Wound Healing
Debridement (wound cleansing)	Enhances migration of leucocytes into the wound bed and supports the accumulation of enzymes. Necrotic tissue, foreign bodies and particles prolong the inflammatory phase and serve as a medium for bacterial growth
Provide or maintain a moist wound environment	Prevents desiccation and cell death, enhances epidermal migration, promotes angiogenesis and connective tissue synthesis and supports autolysis by rehydration of desiccated tissue
Absorption. Removal of blood and excess exudate	In chronic wounds, there is excess exudate containing tissue degrading enzymes that block the proliferation and activity of cells and break down extracellular matrix materials and growth factors, thus delaying wound healing. Excess exudate can also macerate surrounding skin
Gaseous exchange (water vapour and air)	Permeability to water vapour controls the management of exudate. Low tissue oxygen levels stimulate angiogenesis. Raised tissue oxygen stimulates epithelialisation and fibroblasts
Prevent infection: Protect the wound from bacterial invasion	Infection prolongs the inflammatory phase and delays collagen synthesis, inhibits epidermal migration and induces additional tissue damage. Infected wounds can give an unpleasant odour
Provision of thermal insulation	Normal tissue temperature improves the blood flow to the wound bed and enhances epidermal migration
Low adherence. Protects the wound from trauma	Adherent dressings may be painful and difficult to remove and cause further tissue damage
Cost effective Low frequency of dressing change	Dressing comparisons based on treatment costs rather than unit or pack costs should be made (cost-benefit-ratio). Although many dressings are more expensive than traditional materials, the more rapid response to treatment may save considerably on total cost

1.3 Techniques of controlled wound healing drug delivery

1.3.1 Microspheres

Microencapsulation is a means of applying relatively thin coatings to small particles of solids or droplets of liquids and dispersions.[79] Due to their small size (1 -- 1000 µm) and other properties including ability to impart environment responsive characteristics, bioadhesion and swelling, microparticles are adaptable to a wide variety of dosage forms and product applications beneficial to wound healing preparations. This adaptability of microspheres, coupled with the ability to control drug release rate have been found to be highly advantageous in the treatment of chronic wounds.[80] Having particulate matters in the formulations, micro- and nano-particle systems also

offer an extra occlusive effect to the skin which is beneficial for wound healing.[81] Microspheres are also amendable to various instrumental methods of preparation such as spray drying techniques to produce microparticles with rough surface which is considered a promising approach to burn wounds healing because they adhere better to burned skin, thereby increasing the contact surface, allowing a better release of the formulation components in the injured area.[82]

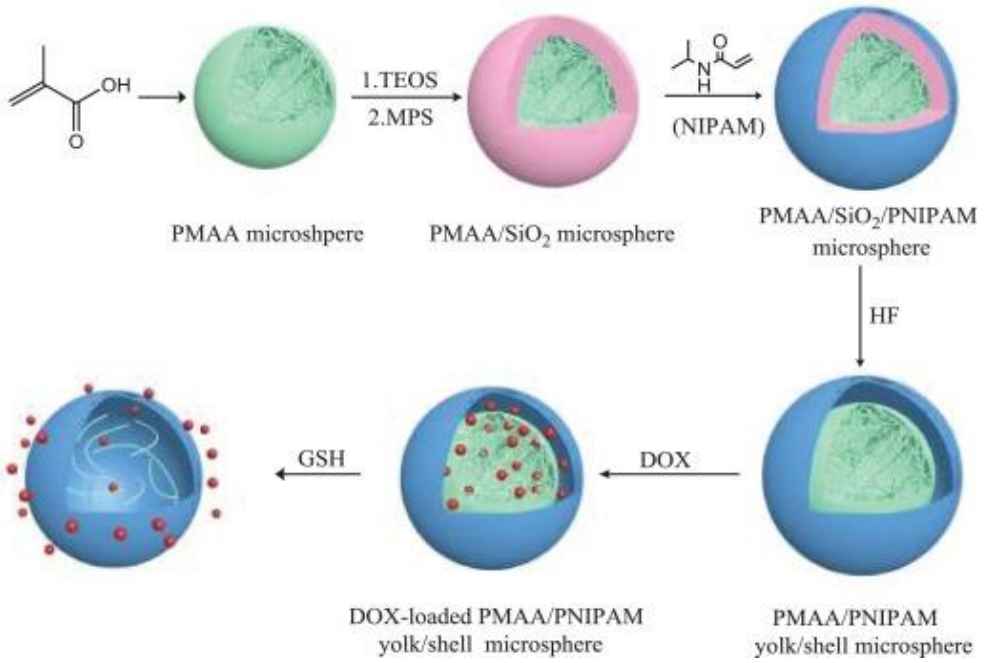

Figure 1.4 Schematic illustration of the fabrication process of the PMAA/PNIPAM yolk/shell microspheres, the DOX loading and the GSH-triggered disassembly of the drug carriers.[83]

1.3.2 Polymeric, gold and silver nanoparticles

Encapsulation of drugs into nanoparticles is an advantageous means to overcome the problems of free drugs such as poor aqueous solubility, limited biodistribution, quick degradation and clearance.[84] The small size and high surface-to-volume ratio of nanoparticles provide an ease of intracellular access and passage through the skin barrier which is ideal for topical drug delivery.[85] In fact, the use of nanoparticulate drug delivery vehicles for wound healing has been predicted to

revolutionize the future of diabetic therapy.[86] The slow and sustained release of the encapsulated drug from nanoparticle is also considered to reduce the toxicity and increase the safety of drugs for topical delivery as the whole amount of the encapsulated drug is never in direct contact with the skin at one time.[87]

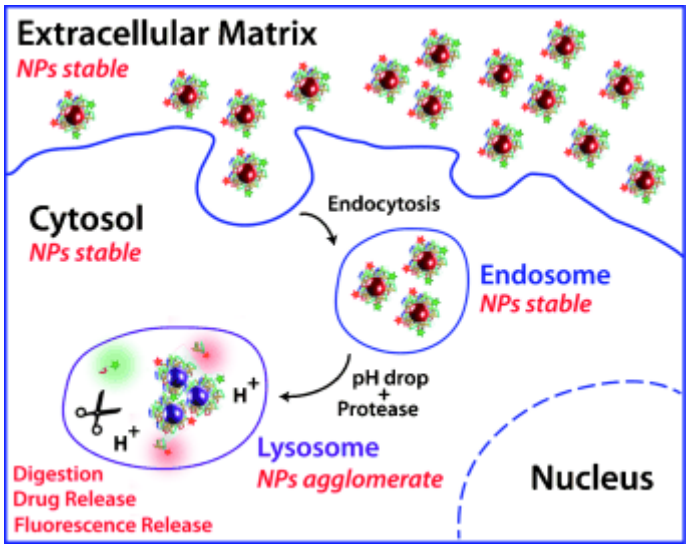

Figure 1.5 schematic represtations of nanoparticles mode of action for drug delivery[88]

1.3.3 Liposomes

Liposomes are vesicular structures consisting of hydrated lipid bilayers resembling the lipid cell membrane of the human body. Due to their unique phospholipid complex, vesicular carriers such as liposomes are being widely explored for use in topical drug delivery.[89] Such vesicular carriers can play a vital role in enhancing the solubility and bioavailability of both hydrophilic and lipophilic drugs as well as assisting in their sustained release,[90] as the lipophilic drugs can be incorporated into the lipid bilayer, whereas hydrophilic drugs can be incorporated into the aqueous interior. Liposomes are also reported to improve the membrane permeability of polar chemicals with large molecular weight apart from providing stability and sustaining the release of the drug.[91] Recently, several liposome-based formulations have been evaluated for controlled delivery of

wound healing drugs ranging from plant extracts[92] to growth factors.[93] Initial burst release as a result of the drug's presence on the liposomes surface followed by a sustained drug release over the next 24 h was observed in such liposomal formulations.

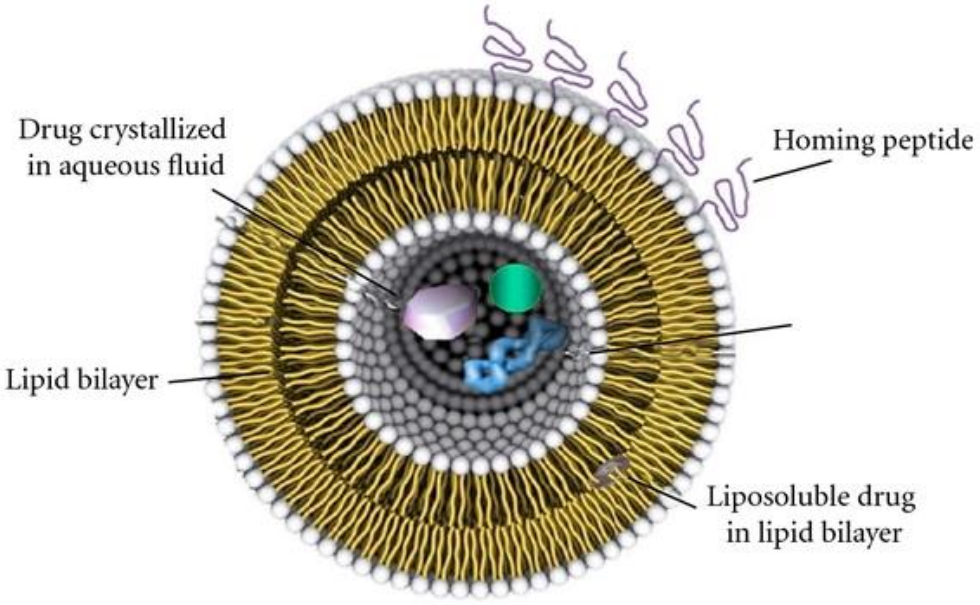

Figure 1.6 A schematic illustration of drug delivering liposome.[94]

1.3.4 Films

Free standing films has long been recognized as biomaterials in drug delivery, wound healing, tissue repair, and even in artificial-organ regeneration.[95] Such films prepared from hydrophilic bioadhesive polymers are also biodegradable and absorbable into the body fluids through the skin without any toxic effects, which is an ideal requirement for wound healing process.[96] Topical drug delivery as in wound healing films also offers advantages such as providing high and sustained concentration of medication at the site of injury.[97] In addition, modern dressings such as films, sponges, hydrocolloids, gels and pastes can also provide or maintain moist environment, allowing

gaseous exchange (water vapor, oxygen), and thermal insulation, remove blood and excess exudates while also easy to remove without causing trauma to facilitate wound healing.[98]

1.3.5 Hydrogels

In recent years, hydrogels have received considerable interest as specific absorbents in wound dressing materials. Polymeric hydrogels have the ability to absorb tissue exudates, prevent wound dehydration but allow oxygen to permeate which is required for efficient wound healing.[99] In addition, due to the porosity of the hydrogels and the moist environment it creates, the encapsulated therapeutic substances can be delivered into the wound in a sustained manner.[100]

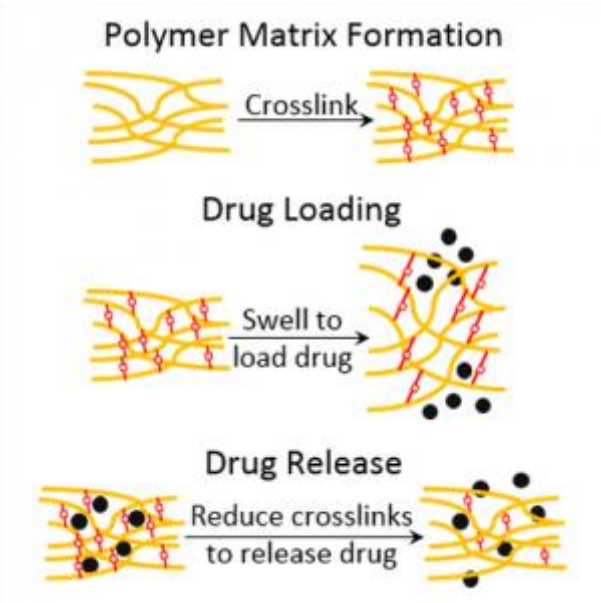

Figure 1.7 A schematic representation of hyrdogel for drug delivery purposes.[101]

The in situ gel-forming hydrogel, which were present as a sol state before application and converted into a gel system after administration and filling the wound sites are especially more desirable as a wound dressing.[102] A biodegradable in situ thermosensitive PEG-PCL-PEG gel-forming system incorporating curcumin-loaded micelles was prepared and applied to enhance the

cutaneous wound healing and repair. In the experimental incision model, the curcumin-loaded hydrogel treated group showed improved healing in terms of tensile strength and thicker epidermis whereas in the excision model, an enhancement wound closure was obtained.[103] A novel injectable chitosan and alginate-based hydrogel with particle size ~ 40 nm prepared by a nano-precipitation method was also developed and evaluated for its potential in enhancing the healing efficiency.[104] The hydrogel was shown to significantly enhance the re-epithelization of epidermis and deposition of collagen within the wound tissue.

Table 2 Some of the characteristics and advantages of different wound healing formulations[105]

Polymeric nanoparticles	Microspheres	Hydrogels	Liposomes
• Very small size (1 -- 1000 nm) • Enhance solubility of poorly aqueous soluble drugs • High surface-to-volume ratio • Sustained drug release • Enhance safety of some drugs administered topically • Enhance stability • Can be functionalized • Enhance antimicrobial properties by facilitating interaction with pathogen surfaces	• Small size (1 -- 1000 µm) • Biocompatible • Enhance stability • Ability to incorporate multiple drugs for simultaneous delivery • Sustained drug release • Adaptability • Occlusive effect to the skin Surface can be modified for better adherence to the skin • Amendable to different manufacturing methods • Bioadhesive type can be prepared	• Biocompatible and biodegradable • Absorb tissue exudates • Prevent wound dehydration • Allow oxygen to permeate • Create moist environment • Porous • Sustained drug release • High drug loading • Environment responsive	• Vesicular structures • Resemble lipid cell membrane of the body • Both hydrophilic and hydrophobic drugs can be encapsulated • Sustained drug release • Highly suitable for topical delivery Improve stability of drugs • Improve membrane permeability of polar drugs

1.4 Cell delivery through microencapsulation

Microsphere technology has been exploited in many emerging biomedical applications, including cell, drug, biomolecule, and gene delivery. Notably, cell-laden microspheres have been developed for two main classes of application: (i) *in vitro* cell culture for cell expansion and biomolecule manufacturing and (ii) *in vivo* cell delivery for cell replacement or therapy. Microspheres are relatively easy to fabricate and handle, and provide a large surface area:volume ratio for cell culture and *in vitro* applications. For *in vivo* applications, microspheres can provide minimally invasive, localized delivery and protection from the immune systems of patients. Cells delivered by microspheres may secrete (either naturally or through genetic modification) therapeutic factors in a sustained manner, circumventing the need for multiple administrations of drugs.

The paradigm of cell culture has switched from a conventional monolayer culture to utilizing biomimetic 3D platforms. It is well recognized that prolonged monolayer culture results in **dedifferentiation**.[106] However, macro-sized 3D platforms are not feasible for cell culture due to an oxygen diffusion constraint of a maximum 200 μm.[107] While some research groups focus on microvascularizing such macro-sized constructs, another scientific community aims to bypass the constraint via a bottom-up approach: creating micro-sized cellular constructs that may then be used as is, or put together to form macro-sized constructs. This has led to an increase in commercially available microspheres and microsphere generators, both of which are increasingly utilized by researchers.

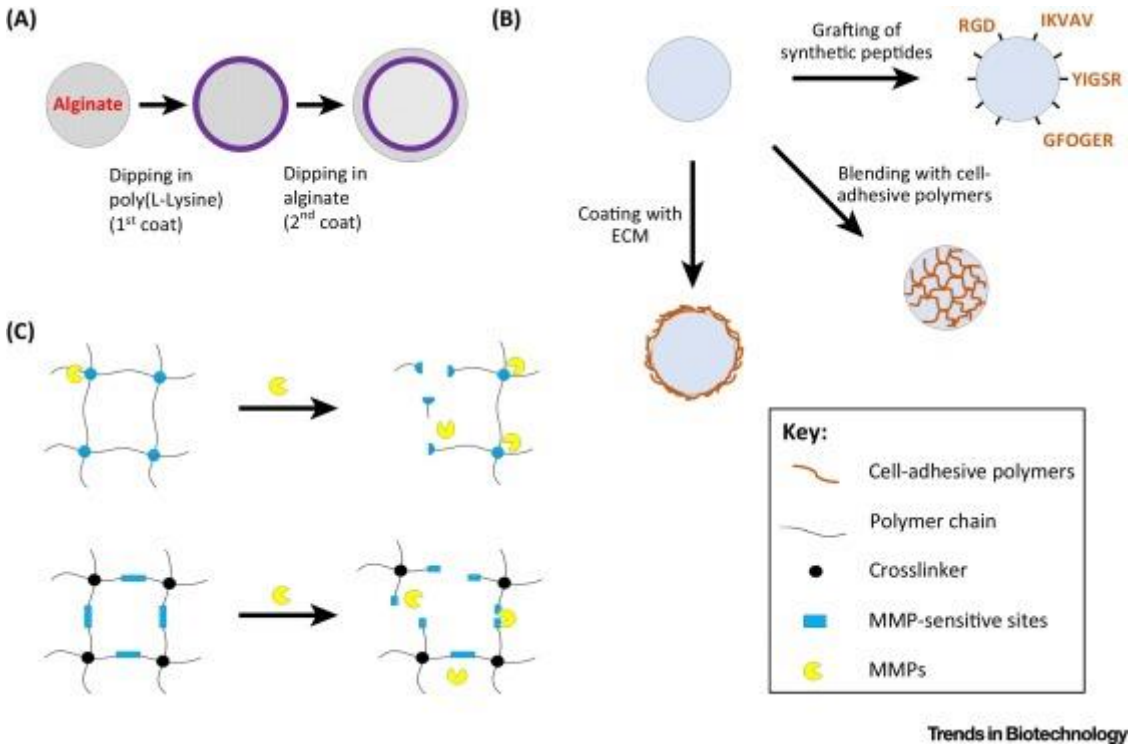

Figure 1.8 Pictorial Descriptions of Various Design Modifications to Aid Biomedical Applications.[108]

Microspheres designed for cell adhesion or encapsulation, categorized as **microcarriers** or **microcapsules**, are generally spherical polymerized networks with a diameter of 100–400 μm to maintain cells within the oxygen diffusion limits. Microcarriers are usually fabricated to have cell-adhesive moieties, which cells are then seeded on. By contrast, microcapsules are typically fabricated by crosslinking a polymer–cell suspension so as to entrap cells within the core of the microsphere. However, the seemingly simple product requires much thought in its design and optimization to provide the appropriate microenvironment in which cells can survive, reside, and maintain their desired function. Microsphere design also needs to take into consideration the cell type and polymer porosity, mechanical strength, cytotoxicity, **immunogenicity**, degradation products, and rates of their formation. Given the intricate interplay of design parameters required to successfully encapsulate cells within

microspheres and the quick pace of research advancement, here we this discuss the use of cell-laden microspheres in two main branches of therapeutic applications (*in vitro* culture and cell delivery) as well as important application-specific considerations to maximize efficacy and efficiency.

Microspheres are designed with the end function in mind: their application and cell type. Porosity, cell microenvironment, and degradability are some primary considerations. Customizability to fit applications is not based so much on the choice of fabrication technique but on the polymers, crosslinking parameters (e.g., polymer concentration, temperature, crosslinker type, and duration of crosslinking), and postfabrication modifications. The fabrication technique is generally chosen based on the desired simplicity, scalability, size, and size distribution. For example, if uniformly sized microspheres are required for ease of monitoring in vitro, microfluidics and extrusion techniques are preferred to emulsions, because the microspheres thus produced have a maximum 5 % variation in diameter.[109]

Biocompatibility, specific porosity, cell-adhesive properties, or controlled degradation are conferred via choice of polymer and their modifications, such as coatings and crosslinker choice. Both naturally derived and synthetic polymers have been used as cell-compatible materials, and each has unique advantages and disadvantages. Low-cost and biocompatible naturally derived polymers, such as alginate, suffer batch-to-batch variation and immunogenicity, whereas expensive and controllable synthetic polymers, such as poly(lactic-co-glycolic) acid (PLGA), have biocompatibility issues, especially with their degradation products. As such, naturally derived polymers require stringent and certified purification protocols to qualify as clinical-grade materials.

Porosity determines the diffusion and size of particles entering the microsphere. For immune isolation, the surface porosity of the microcapsule must prevent immunoglobulin, antibody, and immune cell intrusion without compromising the exchange of metabolites. Polycation poly(L-lysine) coating reduces the surface porosity, and is often masked by another alginate coating, because it can promote inflammation. Microcapsules of this kind are commonly known as alginate-poly-L-Lysine (PLL)-alginate (APA) microcapsules.[110] To date, there is no standardized porosity or molecular weight cut off (MWCO) for microcapsules, but scientists estimate a safe limit at approximately 150 kDa (corresponding to the MW of immunoglobulins). More in-depth studies must be performed to ascertain a safe MWCO for future clinically useable microcapsules. By contrast, for other applications that require infiltration of cells into microspheres, these may be fabricated with large pores either via double emulsion or stacked microfluidic devices. The microspheres thus prepared are used in various ways such as:

1.4.1 Cell Delivery for Tissue Regeneration

The ideology that lie behind the approach of using tissue engineering for regenerative medication is the usage of biological cells to formulate a macro-sized tissue which could then replace the function and configuration of the damaged or malfunctioning tissue. To check seepage, which reduces the effectiveness, cells are classically confined using a biomaterial. Though, as cells multiply and need more space, the scaffolding framework is estimated to degrade consequently. Thus, injectability and enhanced diffusion speeds also make microspheres a favored select over conventional macro-sized tissue formulates. They may also integrate different growth factors, which could be released or diffused from the microspheres according to the rate of degradation, to further aid and facilitate the differentiation of stem cells to be delivered.[111] Due to the difficulty,

various studies have constructed different microspheres rather than using commercially available and used micro carriers.

1.4.2 Localization and Tracking Techniques in-vivo

Microspheres laden with cells may be utilized as is, or employed as building blocks of a macro-sized constructs that can additionally concentrate microspheres to the chosen site. Making a macro-sized construct through a bottom-up method is simple: cell-loaded microspheres can undergo a secondary encapsulation in a polymer,[112] or fusion via sintering[113] or aggregation.[114] In the first occurrence, a secondary polymer encapsulation forms a macro-sized construct containing microspheres loaded with cells, which can mimic the model of a tissue *in vitro* or can be an injectable system that further confines and immune segregates the microspheres *in vivo*. This approach was applied to particularly immune isolate macrophages alongside a tumor mass with the objective of inhibiting leak, proliferation and escape of cells along with providing antitumor results.[115] A additional approach exploits perfusion bioreactors to compactly pack microspheres loaded with cells collected for a period of time; this method allows the growth of condensed ECM that helps in holding the microspheres together and thus results in formation of a macro-sized construct.[116] In another strategy, sintering utilizes solvent or heat treatment to fuse microspheres into an interconnected macro porous structure, onto which cells are seeded.

1.4.3 Cell Delivery

Cell-based therapy is progressively advancing and being promising, with numerous clinical trials already in place. Microspheres make a technique of brilliant cell delivery, since they are injectable and localizable to the preferred site (which is not the situation with a cell suspension) without hampering nutrient and waste diffusion in and out of it.

1.4.4 *In vitro* Cell Culture Applications

For clinical application of cell-based technology, cells must be cultured in large-scale systems competently and efficiently. Unlike non ADCs, ADCs require connection to a surface and cannot be grown in state of suspension; micro-carrier technology delivers an alternate to the incompetent and non-biomimetic monolayer culture. Ideally, micro-carriers should be of a fine size distribution for easiness of monitoring and sub-culturing; also, their density should be somewhat above 1.0 g/cm^3 for simple and easy collection from media by simple pouring or centrifugation and there should be nominal energy utilization for creating a stir in a bioreactor. Moreover, the anticipated porosity is also governed by the use: cell expansion can be preferentially performed on microporous micro-carriers (with cell attachment only on the outer surface) to permit effective detachment, whereas biomolecule manufacture may use **macroporous** microcarriers, because the added surface area in interior pores surges the cell density

1.4.5 Cell Expansion and Differentiation

Functional and rapidly dividing cells are requisite in huge numbers for therapeutic uses; for example, in scales of 10^7–10^8 cells per kg body weight in transplanting liver, [117] which thus in a way makes monolayer culture impractical. Micro carrier culture is able to deliver the answer to this situation by making the most of the commercial accessibility of large-scale bioreactors, high cell attachment efficiency (up to 10^8cells/ml),[118] ease of sample collection and fine-tuning of culture parameters, simplicity of sampling of microcarriers for confluency checks, and the prospect of lasting constant subculture by addition of empty beads.[119] Though, the absence or high price of xeno-free culture settings are still major holdups for any therapeutic cell expansion, which must resolute for commercialization to be conceivable.

1.4.6 Cell Delivery for Therapeutic Biomolecule Delivery

Cell-based therapeutics provide the benefits of the long-term, constant, and precise release of drugs or biomolecules, such as hormones and growth factors, circumventing repetitive, programmed dosages that produce a burst release upon administration. To arrest and immune segregate these therapeutic cells, which are commonly allogeneic or sometimes xenogeneic, alginate-based microcapsules are prevalent due to their mild crosslinking circumstances and their capability to preserve the viability of a range of cells. The microcapsule serves as a barricade amid the allogeneic cells and host immune system, and, hence, should be non-degradable and have little penetrability, so as to check interaction with immune-related cells and proteins. One easy way to decrease porosity is by creating APA microcapsules.[120] To enhance its biocompatibility, current studies substituted proinflammatory PLL with cationic coverings, such as poly-L-ornithine (PLO)[121] and chitosan.[122] An substitute method is to mask PLL with PEG-b-PLL copolymers.[123] Non-natural, non-degradable polymers have similarly been utilized for microencapsulation,[124] but their immune-isolation ability still requires better understanding and characterization.

1.5 References

1. a) Morgan DA. *Hosp Pharmacist* **2002** ,*9*: 261–266. b) Lazarus GS, Cooper DM, Knighton DR, Margolis DJ, Percoraro ER, Rodeheaver G, Robson MC. *Arch Dermatol* **1994**,130: 489–493. c) Percival JN. *Surgery*, **2002**, 20: 114–117.
2. a) Eming, S. A.; Martin, P.; Tomic-Canic, *Sci. Transl. Med*. **2014**, 6,265sr266– 265sr266, b) Pastar, I.; Stojadinovic, O.; Yin, N. C.; Ramirez, H.; Nusbaum, A. G.; Sawaya, A.; Patel, S. B.; Khalid, L.; Isseroff, R. R.; Tomic-Canic, *Adv. Wound Care* **2014**, 3, 445– 464.
3. a) Midwood, K. S.; Williams, L. V.; Schwarzbauer, J. E. *J. Biochem. Cell Biol*.**2004**, 36, 1031– 1037; b) Lindley, L. E.; Stojadinovic, O.; Pastar, I.; Tomic-Canic, M.Biology and *Plast. Reconstr. Surg.* **2016**, 138,18S– 28S.
4. a) Brem, H.; Tomic-Canic, *J. Clin. Invest.* **2007**, 117, 1219– 1222.
5. a) J. S. Lee, J. W. Bae, Y. K. Joung, S. J. Lee, D. K. Han, K. D. Park, *Int. J. Pharm.* **2008**, *346*, 57-63; b) L. Y. Qiu, Y. H. Bae, *Biomaterials* **2007**, *28*, 4132-4142; c) J. M. Davidson, K. N. Broadley, D. Quaglino, Jr., *Wound Repair Regen.* **1997**, *5*, 77-88.
6. a) X. Cheng, Y. Jin, T. Sun, R. Qi, H. Li, W. Fan, *Colloids Surf., B* **2016**, *141*, 44-52; b) J. A. Chikar, J. L. Hendricks, S. M. Richardson-Burns, Y. Raphael, B. E. Pfingst, D. C. Martin, *Biomaterials* **2012**, *33*, 1982-1990; c) W. Wang, E. Wat, P. C. Hui, B. Chan, F. S. Ng, C. W. Kan, X. Wang, H. Hu, E. C. Wong, C. B. Lau, P. C. Leung, *Sci. Rep.* **2016**, *6*, 241-255.
7. a) B. J. Lee, S. G. Ryu, J. H. Cui, *Int. J. Pharm.* **1999**, *188*, 71-80; b) L. Wei, C. Cai, J. Lin, T. Chen, *Biomaterials* **2009**, *30*, 2606-2613; c) Z. Wu, X. Zou, L. Yang, S. Lin, J. Fan, B. Yang, X. Sun, Q. Wan, Y. Chen, S. Fu, *Colloids Surf., B* **2014**, *122*, 90-98.
8. A. Wichterle, D. Lim, *Nature* **1960**, *185*, 117-118.

9. a) N. Roy, N. Saha, T. Kitano, P. Saha, *Carbohydr. Polym.* **2012**, *89*, 346-353; b) A. Gregorova, N. Saha, T. Kitano, P. Saha, *Carbohydr. Polym.* **2015**, *117*, 559-568.

10. a) E. G. Popa, M. E. Gomes, R. L. Reis, *Biomacromolecules* **2011**, *12*, 3952-3961; b) Z. Wang, Y. Zhang, J. Zhang, L. Huang, J. Liu, Y. Li, G. Zhang, S. C. Kundu, L. Wang, *Sci. Rep.* **2014**, *4*, 7064-7075.

11. a) S. Berski, J. van Bergeijk, D. Schwarzer, Y. Stark, C. Kasper, T. Scheper, C. Grothe, R. Gerardy-Schahn, A. Kirschning, G. Drager, *Biomacromolecules* **2008**, *9*, 2353-2359; b) F. Z. Cui, W. M. Tian, S. P. Hou, Q. Y. Xu, I. S. Lee, *J. Mater. Sci. Mater. Med.* **2006**, *17*, 1393-1401; c) K. M. Galler, J. D. Hartgerink, A. C. Cavender, G. Schmalz, R. N. D'Souza, *Tissue Eng. Part A* **2012**, *18*, 176-184.

12. a) N. Gajovic, G. Beinyamin, A. Warsinke, F. W. Scheller, A. Heller, *Anal. Chem.* **2000**, *72*, 2963-2968; b) F. Kivlehan, M. Paolucci, D. Brennan, I. Ragoussis, P. Galvin, *Anal. Biochem.* **2012**, *421*, 1-8.

13. a) Y. Akagawa, T. Kubo, K. Koretake, K. Hayashi, K. Doi, A. Matsuura, K. Morita, R. Takeshita, Q. Yuan, Y. Tabata, *J. Prosthodont. Res.* **2009**, *53*, 41-47; b) A. Ma, B. Zhao, A. J. Bentley, A. Brahma, S. MacNeil, F. L. Martin, S. Rimmer, N. J. Fullwood, *J. Mater. Sci. Mater. Med.* **2011**, *22*, 663-670;

14. a) B. Gao, T. Konno, K. Ishihara, *J. Biomater. Sci. Polym. Ed.* **2015**, *26*, 1372-1385; b) C. C. Karlgard, N. S. Wong, L. W. Jones, C. Moresoli, *Int. J. Pharm.* **2003**, *257*, 141-151.

15. a) C. Gong, S. Shi, L. Wu, M. Gou, Q. Yin, Q. Guo, P. Dong, F. Zhang, F. Luo, X. Zhao, Y. Wei, Z. Qian, *Acta. Biomater.* **2009**, 5, 3358-3370; b) B. Xue, V. Kozlovskaya, F. Liu, J. Chen, J. F. Williams, J. Campos-Gomez, M. Saeed, E. Kharlampieva, *ACS Appl. Mater. Interfaces* **2015**, 7, 13633-13644.

16. a) V. S. Ghorpade, A. V. Yadav, R. J. Dias, *Int. J. Biol. Macromolec.* **2016**, *93*, 75-86; b) G. P. Mishra, R. Kinser, I. H. Wierzbicki, R. G. Alany, A. W. Alani, *Eur. J. Pharm. Biopharm. e.V* **2014**, *88*, 397-405.

17. a) M. B. Charati, I. Lee, K. C. Hribar, J. A. Burdick, *Small* **2010**, *6*, 1608-1611; b) Y. N. Zhang, R. K. Avery, Q. Vallmajo-Martin, A. Assmann, A. Vegh, A. Memic, B. D. Olsen, N. Annabi, A. Khademhosseini, *Adv. Funct. Mater.* **2015**, *25*, 4814-4826.

18. a) C. M. Dong, Y. Chen, *J. Control. Release.* **2011**, *152 Suppl 1*, e13-14; b) C. Li, A. Faulkner-Jones, A. R. Dun, J. Jin, P. Chen, Y. Xing, Z. Yang, Z. Li, W. Shu, D. Liu, R. R. Duncan, *Angew. Chem.* **2015**, *54*, 3957-3961;

19. a) P. Markland, Y. Zhang, G. L. Amidon, V. C. Yang, *J. Biomed. Mater. Res.* **1999**, *47*, 595-602; b) K. Men, W. Liu, L. Li, X. Duan, P. Wang, M. Gou, X. Wei, X. Gao, B. Wang, Y. Du, M. Huang, L. Chen, Z. Qian, Y. Wei, *Nanoscale* **2012**, *4*, 6425-6433.

20. a) K. Peng, I. Tomatsu, A. Kros, *J. Control. Release.* **2011**, *152 Suppl 1*, e72-74; b) W. Li, L. Huang, X. Ying, Y. Jian, Y. Hong, F. Hu, Y. Du, *Angew. Chem.* **2015**, *54*, 3126-3131; b) F. Ye, H. Guo, H. Zhang, X. He, *Acta Biomater.* **2010**, *6*, 2212-2218.

21. a) C. Gong, Q. Wu, Y. Wang, D. Zhang, F. Luo, X. Zhao, Y. Wei and Z. Qian, *Biomaterials*, 2013, **34**, 6377-6387; X. Hu, H. Tan, P. Chen, X. Wang and J. Pang, *Journal of nanoscience and nanotechnology*, **2016**, *16*, 5480-5488; C. Lu, R. B. Yoganathan, M. Kociolek and C. Allen, *Journal of pharmaceutical sciences*, 2013, **102**, 627-637.

22. A. C. Farthing and R. J. Reynolds, *Nature*, **1950**, *165*, 647-659.

23. G. Vandermeulen, L. Rouxhet, A. Arien, M. E. Brewster and V. Preat, *International journal of pharmaceutics*, **2006**, *309*, 234-240.

24. a) T. J. Deming, *Nature* **1997**, *390*, 386-389; b) T. J. Deming, *Adv. Drug Deliv. Rev.* **2002**, *54*, 1145-1155.

25. T. Yang, W. Li, X. Duan, L. Zhu, L. Fan, Y. Qiao and H. Wu, *PloS one*, 2016, **11**, e0162607.

26. a) A. Acharya, B. Ramanujam, A. Mitra, C. P. Rao, *ACS nano* **2010**, *4*, 4061-4073; b) K. L. Copeland, J. A. Anderson, A. R. Farley, J. R. Cox, G. S. Tschumper, *J. Phys. Chem. B* **2008**, *112*, 14291-14295; c) K. Jitsukawa, A. Katoh, K. Funato, N. Ohata, Y. Funahashi, T. Ozawa, H. Masuda, *Inorg. Chem.* **2003**, *42*, 6163-6165; d) M. Yoshikawa, H. Iwasaki, H. Shinagawa, *J. Biol. Chem.* **2001**, *276*, 10432-10436.

27. A. M. Puertas, F. J. de las Nieves, *J. Colloid Interface Sci.* **1999**, *216*, 221-229.

28. D. T. Haynie, S. Balkundi, N. Palath, K. Chakravarthula, K. Dave, *Langmuir* **2004**, *20*, 4540-4547.

29. a) B. Cheppudira, M. Fowler, L. McGhee, A. Greer, A. Mares, L. Petz, D. Devore, D. R. Loyd, J. L. Clifford, *Expert Opin. Investig. Drugs* **2013**, *22*, 1295-1303; b) K. K. Chereddy, R. Coco, P. B. Memvanga, B. Ucakar, A. des Rieux, G. Vandermeulen, V. Preat, *J. Control. Release* **2013**, *171*, 208-215; c) M. Panchatcharam, S. Miriyala, V. S. Gayathri, L. Suguna, *Mol. Cell. Biochem.* **2006**, *290*, 87-96.

30. a) K. S. Akers, M. P. Rowan, K. L. Niece, J. C. Graybill, K. Mende, K. K. Chung, C. K. Murray, *BMC Infect. Dis.* **2015**, *15*, 184-196; b) D. A. Sanchez, D. Schairer, C. Tuckman-Vernon, J. Chouake, A. Kutner, J. Makdisi, J. M. Friedman, J. D. Nosanchuk, A. J. Friedman, *Nanomedicine* **2014**, *10*, 269-277; c) O. Tabbene, S. Azaiez, A. Di Grazia, I. Karkouch, I. Ben Slimene, S. Elkahoui, M. N. Alfeddy, B. Casciaro, V. Luca, F. Limam, M. L. Mangoni, *J. Appl. Microbiol.* **2016**, *120*, 289-300.

31. a) F. Gaudiere, S. Morin-Grognet, L. Bidault, P. Lembre, E. Pauthe, J. P. Vannier, H. Atmani, G. Ladam, B. Labat, *Biomacromolecules* **2014**, *15*, 1602-1611; b) B. Manickam, R. Sreedharan, M. Elumalai, *Curr Drug Deliv.* **2014**, *11*, 139-145; c) A. P. Mathew, K. Oksman, D. Pierron, M. F. Harmand, *Macromol. Biosci.* **2013**, *13*, 289-298;

32. a) R. Baumeister, G. Muller, B. Hecht, W. Hillen, *Proteins* **1992**, *14*, 168-177; b) J. M. Richardson, M. M. Lopez, G. I. Makhatadze, *Proc. Natl. Acad. Sci. U.S.A.* **2005**, *102*, 1413-1418.

33. a) J. S. Chiou, T. Tatara, S. Sawamura, Y. Kaminoh, H. Kamaya, A. Shibata, I. Ueda, *Biochim. Biophys. Acta* **1992**, *1119*, 211-217; b) K. Fukushima, T. Sakamoto, J. Tsuji, K. Kondo, R. Shimozawa, *Biochim. Biophys. Acta* **1994**, *1191*, 133-140.

34. a) J. Rao, Z. Luo, Z. Ge, H. Liu, S. Liu, *Biomacromolecules* **2007**, *8*, 3871-3878; b) J. Sun, C. Deng, X. Chen, H. Yu, H. Tian, J. Sun, X. Jing, *Biomacromolecules* **2007**, *8*, 1013-1017.

35. V. T. Huynh, G. Chen, P. d. Souza, M. H. Stenzel, *Biomacromolecules* **2011**, *12*, 1738-1751.

36. A. F. van Nostrum, *Soft Matter* **2011**, *7*, 3246-3259.

37. a) M. Koskela, F. Gaddnas, T. I. Ala-Kokko, J. J. Laurila, J. Saarnio, A. Oikarinen, V. Koivukangas, *Crit. Care* **2009**, *13*, 100-109.

38. R. M. Rico, R. Ripamonti, A. L. Burns, R. L. Gamelli, L. A. DiPietro, *J. Surg. Res.* **2002**, *102*, 193-197.

39. a) T. J. Nelson, A. Martinez-Fernandez, A. Terzic, *Nat Rev Cardiol* **2010**, *7*, 700-710; b) M. Mimeault, R. Hauke, S. K. Batra, *Clin Pharmacol Ther* **2007**, *82*, 252-264; c) G. Keller, *Gene Dev* **2005**, *19*, 1129-1155.

40. a) K. R. Boheler, J. Czyz, D. Tweedie, H. T. Yang, S. V. Anisimov, A. M. Wobus, *Circ Res* **2002**, 91. 189-201; b) J. Kramer, C. Hegert, K. Guan, A. M. Wobus, P. K. Muller, J. Rohwedel, *Mechanisms of development* **2000**, *92*, 193-205.

41. a) Y. S. Pek, A. C. A. Wan, J. Y. Ying, *Biomaterials* **2010**, *31*, 385-39; b) J. K. Choi, X. He, *PLoS One* **2013**, *8*, e56158.

42. a) D. T. Scadden, *Nature* **2006**, *441*, 1075-1079; b) E. Cukierman, R. Pankov, D. R. Stevens, K. M. Yamada, *Science* **2001**, *294*, 1708-1712; c) L. G. Griffith, M. A. Swartz, *Nat Rev Mol Cell Biol* **2006**, 7, 211-224.

43. B. S. Yoon, S. J. Yoo, J. E. Lee, S. You, H. T. Lee, H. S. Yoon, *Differentiation* **2006,** *74*, 49-159; b) D. E. Kehoe, D. H. Jing, L. T. Lock, E. S. Tzanakakis, *Tissue Eng Pt A* **2010**, *16*, 405-421.

44. A. Faulkner-Jones, S. Greenhough, J. A. King, J. Gardner, A. Courtney, W. M. Shu, *Biofabrication* **2013**, *5*, 279-286.

45. J. Park, C. H. Cho, N. Parashurama, Y. W. Li, F. Berthiaume, M. Toner, A. W. Tilles, M. L. Yarmush,, *Lab Chip* **2007**, *7*, 1018-1028.

46. a) A. M. Bratt-Leal, R. L. Carpenedo, T. C. McDevitt, *Biotechnol Prog* **2009**, *25*, 43-51; b) H. Kurosawa, *J Biosci Bioeng* **2007**, *103*, 389-98.

47. a) M. Shafa, B. Day, A. Yamashita, G. Meng, S. Liu, R. Krawetz, D. E. Rancourt, *Nat Methods* **2012**, *9*, 465-466.

48. D. A. Fluri, P. D. Tonge, H. Song, R. P. Baptista, N. Shakiba, S. Shukla, G. Clarke, A. Nagy, P. W. Zandstra, *Nat Methods* **2012**, *9*, 509-516.

49. Y. S. Hwang, B. G. Chung, D. Ortmann, N. Hattori, H. C. Moeller, A. Khademhosseini, *Proc Natl Acad Sci U S A* **2009**, *106*, 16978-16983.

50. a) N. S. Hwang, S. Varghese, Z. Zhang, J. Elisseeff, *Tissue Eng* **2006**, *12*, 2695-2706; b) H. Park, J. S. Temenoff, Y. Tabata, A. I. Caplan, A. G. Mikos, *Biomaterials* **2007**, *28*, 3217-3227.

51. G. Orive, R. M. Hernandez, A. R. Gascon, R. Calafiore, T. M. S. Chang, P. De Vos, G. Hortelano, D. Hunkeler, I. Lacik, A. M. J. Shapiro, J. L. Pedraz, *Nat Med* **2003**, *9*, 104-107.

52. H. Liu, J. Lin, K. Roy, *Biomaterials* **2006**, *27*, 5978-5989.

53. K. Y. Lee, D. J. Mooney, *Prog Polym Sci* **2012**, *37*, 106-126; b) A. D. Augst, H. J. Kong, D. J. Mooney, *Macromol Biosci* **2006**, *6*, 623-633; c)W. Zhang, X. He, *J Biomech Eng* **2009**, *131*, 515-527.

54. a) Y. H. Lee, F. Mei, M. Y. Bai, S. Zhao, D. R. Chen, *J Control Release* **2010**, *145*, 58-65; b) J. Kim, P. Sachdev, K. Sidhu, *Stem cell research* **2013**, *11*, 978-989.

55. F. Chen, Y. Zhan, T. Geng, H. Lian, P. Xu, C. Lu, *Anal Chem* **2011**, 8816-8820.

56. Y. Wu, I. C. Liao, S. J. Kennedy, J. Du, J. Wang, K. W. Leong, R. L. Clark, *Chem Commun (Camb)* **2010**, *46*, 4743-5.

57. L. Zhang, J. Huang, T. Si, R. X. Xu, *Expert Rev Med Devices* **2012**, *9*, 595-612.

58. D. B. Shenoy, A. A. Antipov, G. B. Sukhorukov, H. Mohwald, *Biomacromolecules* **2003**, *4*, 265-272.

59. T. Maguire, E. Novik, R. Schloss, M. Yarmush, *Biotechnol Bioeng* **2006**, *93*, 581-591.

60. W. Zhang, S. Zhao, W. Rao, J. Snyder, J. K. Choi, J. Wang, I. A. Khan, N. B. Saleh, P. J. Mohler, J. Yu, T. J. Hund, C. Tang, X. He, *J Mater Chem B Mater Biol Med* **2013**, *2013*, 1002-1009.

61. X. Wang, W. Wang, J. Ma, X. Guo, X. Yu, X. Ma, *Biotechnol Prog* **2006**, *22*, 791-800.

62. S. Sakai, I. Hashimoto, K. Kawakami, *Biotechnol Bioeng* **2008**, *99*, 235-243.

63. a) S. Sakai, S. Ito, K. Kawakami, *Acta Biomater* **2010**, *6*, 3132-3137; b) C. Kim, S. Chung, Y. E. Kim, K. S. Lee, S. H. Lee, K. W. Oh, J. Y. Kang, *Lab Chip* **2011**, *11*, 246-252.

64. a) P. Agarwal, S. Zhao, P. Bielecki, W. Rao, J. K. Choi, Y. Zhao, J. Yu, W. Zhang, X. He, *Lab Chip* **2013**, *13*, 4525-4533; b) Y. C. Tung, A. Y. Hsiao, S. G. Allen, Y. S. Torisawa, M. Ho, S. Takayama, *Analyst* **2011**, *136*, 473-478.

65. a) J. Choi, P. Agarwal, H. Huang, S. Zhao, X. He, *Biomaterials* **2014**, *35*, 5122-5128; b) D. R. Cole, M. Waterfall, M. McIntyre, J. D. Baird, *Diabetologia* **1992**, *35*, 231-237.

66. P. de Vos, C. G. van Hoogmoed, B. J. de Haan, H. J. Busscher, *J Biomed Mater Res* **2002**, *62*, 430-437.

67. W. Dou, D. Wei, H. Li, H. Li, M. M. Rahman, J. Shi, Z. Xu, Y. Ma, *Carbohydrate polymers* **2013**, *98*, 1476-1482.

68. J. C. Duarte, *Fems Microbiol Rev* **1994**, *13*, 121-121; b) D. M. Updegraf, Semimicro *Anal Biochem* **1969**, *32*, 420-427.

69. C. K. Griffith, C. Miller, R. C. A. Sainson, J. W. Calvert, N. L. Jeon, C. C. W. Hughes, S. C. George, *Tissue Eng* **2005**, *11*, 257-266; b) M. Zhang, D. Methot, V. Poppa, Y. Fujio, K. Walsh, C. E. Murry, *J Mol Cell Cardiol* **2001**, *33*, 907-921.

70. M. Amit, I. Laevsky, Y. Miropolsky, K. Shariki, M. Peri, J. Itskovitz-Eldor, *Nature protocols* **2011**, *6*, 572-579.

71. R. Zweigerdt, R. Olmer, H. Singh, A. Haverich, U. Martin, *Nature protocols* **2011**, *6*, 689-700; b) M. P. Storm, C. B. Orchard, H. K. Bone, J. B. Chaudhuri, M. J. Welham, *Biotechnol Bioeng* **2010**, *107*, 683-695.

72. P. W. Burridge, S. Thompson, M. A. Millrod, S. Weinberg, X. A. Yuan, A. Peters, V. Mahairaki, V. E. Koliatsos, L. Tung, E. T. Zambidis, *PLoS One* **2011**, *6*, e0175674.

73. S. J. Kattman, A. D. Witty, M. Gagliardi, N. C. Dubois, M. Niapour, A. Hotta, J. Ellis, G. Keller, *Cell Stem Cell* **2011**, *8*, 228-240.

74. a) S. S. Y. Wong, H. S. Bernstein, *Regen Med* **2010**, *5*, 763-775; b) P. B. Zhang, J. A. Li, Z. J. Tan, C. Y. Wang, T. Liu, L. Chen, J. Yong, W. Jiang, X. M. Sun, L. Y. Du, M. X. Ding, H. K. Deng, *Blood* **2008**, *111*, 1933-1941.

75. B. I. Jugdutt, *Circulation* **2003**, *108*, 1395-403; b) K. Song, Y. J. Nam, X. Luo, X. Qi, W. Tan, G. N. Huang, A. Acharya, C. L. Smith, M. D. Tallquist, E. G. Neilson, J. A. Hill, R. Bassel-Duby, E. N. Olson, *Nature* **2012**, *485*, 599-604.

76. a) R. G. Gourdie, N. J. Severs, C. R. Green, S. Rothery, P. Germroth, R. P. Thompson, *Journal of cell science* 1**993**, *105* (Pt 4). 985-991; b) L. F. Lemanski, *The Journal of cell biology* **1979**, *82*, 227-238.

77. Z. Ai, A. Fischer, D. C. Spray, A. M. Brown, G. I. Fishman, *The Journal of clinical investigation* **2000**, *105*, 161-171.

78. E. Gelinsky, Bruns' Beitrage zur klinischen Chirurgie **1957**, *194*, 51-73; b) V. Patrulea, V. Ostafe, G. Borchard, O. Jordan, European journal of pharmaceutics and biopharmaceutics : official journal of Arbeitsgemeinschaft fur Pharmazeutische Verfahrenstechnik e.V **2015**, *97*, 417-426; c) S. E. Wharram, X. Zhang, D. L. Kaplan, S. P. McCarthy, Macromolecular bioscience **2010**, *10*, 246-257.

79. a) R. Saraceno, A. Chiricozzi, S. P. Nistico, S. Tiberti, S. Chimenti, *The Journal of dermatological treatment* **2010**, *21*, 363-366; b) N. Yamamoto, T. Kiyosawa, *International wound journal* **2014**, *11*, 616-621; c) R. M. Zadeh Farahani, A. Shahidi, *Journal of tissue viability* **2009**, *18*, 57-58.

80. a) M. I. Khan, J. M. Islam, W. Kabir, A. Rahman, M. Mizan, M. F. Rahman, J. Amin, M. A. Khan, *Materials science & engineering. C, Materials for biological applications* **2016**, *69*, 609-615; b) S. Yanagibayashi, S. Kishimoto, M. Ishihara, K. Murakami, H. Aoki, M. Takikawa, M. Fujita, M. Sekido, T. Kiyosawa, *Bio-medical materials and engineering* **2012**, *22*, 301-310.

81. a) R. Rakhshaei, H. Namazi, Materials science & engineering. C, Materials for biological applications **2017**, *73*, 456-464; b) M. Rezvanian, N. Ahmad, M. C. Mohd Amin, S. F. Ng, International journal of biological macromolecules **2017**, *97*, 131-140.

82. a) N. Wathoni, K. Motoyama, T. Higashi, M. Okajima, T. Kaneko, H. Arima, International journal of biological macromolecules **2016**, *89*, 465-470; b) M. P. Brooks, Journal of the Mississippi State Medical Association **1973**, *14*, 385-390.

83. a) K. R. Kirker, G. A. James, APMIS : acta pathologica, microbiologica, et immunologica Scandinavica **2017**, *125*, 344-352; b) S. Tejada, A. Manayi, M. Daglia, S. F. Nabavi, A. Sureda, Z. Hajheydari, O. Gortzi, H. Pazoki-Toroudi, S. M. Nabavi, Current pharmaceutical biotechnology **2016**, *17*, 1002-1007.

84. a) B. S. Atiyeh, M. Costagliola, S. N. Hayek, S. A. Dibo, *Burns : journal of the International Society for Burn Injuries* **2007**, *33*, 139-148; b) H. Babavalian, A. M. Latifi, M. A. Shokrgozar, S. Bonakdar, S. Mohammadi, M. Moosazadeh Moghaddam,

Jundishapur journal of microbiology **2015**, *8*, e28320; c) J. Betts, *Evidence-based nursing* **2003**, *6*, 81-89.

85. a) M. J. Hudson-Peacock, C. M. Lawrence, *Journal of the American Academy of Dermatology* **1995**, *32*, 627-630; b) G. C. Jagetia, G. K. Rajanikant, *The Journal of surgical research* **2004**, *120*, 127-138; c) G. C. Jagetia, G. K. Rajanikant, *International wound journal* **2012**, *9*, 76-92.

86. A. F. Laplante, L. Germain, F. A. Auger, V. Moulin, FASEB journal : official publication of the Federation of American Societies for Experimental Biology **2001**, 15, 2377-2389.

87. a) D. L. Hunt, *ACP journal club* **2003**, *139*, 16-25; b) K. H. Kwan, X. Liu, M. K. To, K. W. Yeung, C. M. Ho, K. K. Wong, *Nanomedicine* **2011**, *7*, 497-504.

88. A. Mittal, R. Kumar, D. Parsad, N. Kumar, *Journal of tissue engineering and regenerative medicine* **2014**, *8*, 351-363; d) G. Stern, *Pflege Zeitschrift* **2007**, *60*, 201-202.

89. a) M. Boury-Jamot, J. Daraspe, F. Bonte, E. Perrier, S. Schnebert, M. Dumas, J. M. Verbavatz, *Handbook of experimental pharmacology* **2009**, 205-217; b) M. E. Posthauer, *Advances in skin & wound care* **2006**, *19*, 74-76; c) M. G. Rippon, K. Ousey, K. F. Cutting, *Journal of wound care* **2016**, *25*, 68, 70-65.

90. a) M. Ishihara, K. Ono, M. Sato, K. Nakanishi, Y. Saito, H. Yura, T. Matsui, H. Hattori, M. Fujita, M. Kikuchi, A. Kurita, *Wound repair and regeneration : official publication of the Wound Healing Society [and] the European Tissue Repair Society* **2001**, *9*, 513-521.

91. a) K. Lay-Flurrie, *Professional nurse* **2004**, *19*, 269-273; b) Y. Luo, H. Diao, S. Xia, L. Dong, J. Chen, J. Zhang, *Journal of biomedical materials research. Part A* **2010**, *94*, 193-204.

92. a) A. N. Begum, M. R. Jones, G. P. Lim, T. Morihara, P. Kim, D. D. Heath, C. L. Rock, M. A. Pruitt, F. Yang, B. Hudspeth, S. Hu, K. F. Faull, B. Teter, G. M. Cole, S. A. Frautschy, *The Journal of pharmacology and experimental therapeutics* **2008**, *326*, 196-208; b) F. Payton, P. Sandusky, W. L. Alworth, *Journal of natural products* **2007**, *70*, 143-146.

93. U. Singh, A. Barik, B. G. Singh, K. I. Priyadarsini, *Free radical research* **2011**, *45*, 317-325; b) X. H. Zheng, Y. X. Shao, Z. Li, M. Liu, X. Bu, H. B. Luo, X. Hu, *Journal of separation science* **2012**, *35*, 505-512.

94. a) R. De, P. Kundu, S. Swarnakar, T. Ramamurthy, A. Chowdhury, G. B. Nair, A. K. Mukhopadhyay, *Antimicrobial agents and chemotherapy* **2009**, *53*, 1592-1597; b) M. Roy, D. Sinha, S. Mukherjee, J. Biswas, *European journal of cancer prevention : the official journal of the European Cancer Prevention Organisation* **2011**, *20*, 123-131.

95. M. M. Hashem, A. H. Atta, M. S. Arbid, S. A. Nada, G. F. Asaad, Food and chemical toxicology : an international journal published for the British Industrial Biological Research Association **2010**, 48, 1581-1586.

96. A. Ukil, S. Maity, S. Karmakar, N. Datta, J. R. Vedasiromoni, P. K. Das, *British journal of pharmacology* **2003**, *139*, 209-218.

97. a) A. K. Choudhury, S. Raja, S. Mahapatra, K. Nagabhushanam, M. Majeed, *Antioxidants* **2015**, *4*, 750-767; b) W. M. Weber, L. A. Hunsaker, S. F. Abcouwer, L. M. Deck, D. L. Vander Jagt, *Bioorganic & medicinal chemistry* **2005**, *13*, 3811-3820; c) Y. X. Xu, K. R. Pindolia, N. Janakiraman, C. J. Noth, R. A. Chapman, S. C. Gautam, *Experimental hematology* **1997**, *25*, 413-422.

98. a) N. Chainani-Wu, *Journal of alternative and complementary medicine* **2003**, *9*, 161-168; b) V. P. Menon, A. R. Sudheer, *Advances in experimental medicine and biology* **2007**, *595*,

105-125; c) S. Wessler, P. Muenzner, T. F. Meyer, M. Naumann, *Biological chemistry* **2005**, *386*, 481-490.

99. a) G. Liang, S. Yang, L. Jiang, Y. Zhao, L. Shao, J. Xiao, F. Ye, Y. Li, X. Li, *Chemical & pharmaceutical bulletin* **2008**, *56*, 162-167; b) M. Xie, D. Fan, Z. Zhao, Z. Li, G. Li, Y. Chen, X. He, A. Chen, J. Li, X. Lin, M. Zhi, Y. Li, P. Lan, *International journal of pharmaceutics* **2015**, *496*, 732-740.

100. G. Chauhan, G. Rath, A. K. Goyal, *Artificial cells, nanomedicine, and biotechnology* **2013**, *41*, 276-281; b) S. Umar, M. A. Shah, M. T. Munir, M. Yaqoob, M. Fiaz, S. Anjum, K. Kaboudi, M. Bouzouaia, M. Younus, Q. Nisa, M. Iqbal, W. Umar, *Poultry science* **2016**, *95*, 1513-1520.

101. a) P. Lu, Q. Tong, F. Jiang, L. Zheng, F. Chen, F. Zeng, J. Dong, Y. Du, Journal of Huazhong University of Science and Technology. Medical sciences **2005**, *25*, 668-670; b) W. Zhang, T. Cui, L. Liu, Q. Wu, L. Sun, L. Li, N. Wang, C. Gong, Journal of biomedical nanotechnology **2015**, *11*, 1173-1182.

102. a) R. Freeman, B. King, Journal of clinical pathology **1972**, 25, 912-914; b) R. Marion, Canadian journal of medical technology **1973**, *35*, 30-31.

103. H. D. Landahl, Proceedings of the Society for Experimental Biology and Medicine. Society for Experimental Biology and Medicine **1953**, *84*, 74-79.

104. C. Stein, S. Kuchler, *Trends in pharmacological sciences* **2013**, *34*, 303-312.

105. a) M. Kiernan, *Community nurse* **1999**, *5*, 47-48; b) H. M. Mori, H. Kawanami, H. Kawahata, M. Aoki, *BMC complementary and alternative medicine* **2016**, *16*, 144.

106. a) V. Moulin, F. A. Auger, D. Garrel, L. Germain, *Burns : journal of the International Society for Burn Injuries* **2000**, *26*, 3-12; b) Raja, K. Sivamani, M. S. Garcia, R. R. Isseroff, *Frontiers in bioscience : a journal and virtual library* **2007**, *12*, 2849-2868.

107. D. F. King, L. A. King, The American Journal of dermatopathology **1986**, 8, 168-176.

108. a) J. L. Oschman, G. Chevalier, R. Brown, *Journal of inflammation research* **2015**, *8*, 83-96; b) M. Resan, M. Vukosavljevic, D. Vojvodic, B. Pajic-Eggspuehler, B. Pajic, *Clinical ophthalmology* **2016**, *10*, 993-1000.

109. W. Suh, K. L. Kim, J. M. Kim, I. S. Shin, Y. S. Lee, J. Y. Lee, H. S. Jang, J. S. Lee, J. Byun, J. H. Choi, E. S. Jeon, D. K. Kim, *Stem cells* **2005**, *23*, 1571-1578.

110. a) X. Y. Gu, S. E. Shen, C. F. Huang, Y. N. Liu, Y. C. Chen, L. Luo, Y. Zeng, A. P. Wang, *Diabetes research and clinical practice* **2013**, *102*, 53-59; b) S. Okizaki, Y. Ito, K. Hosono, K. Oba, H. Ohkubo, K. Kojo, N. Nishizawa, M. Shibuya, M. Shichiri, M. Majima, *The American journal of pathology* **2016**, *186*, 1481-1498.

111. Y. Wang, X. Fu, N. Ma, Zhonghua zheng xing shao shang wai ke za zhi = Zhonghua zheng xing shao shang waikf [i.e. waike] zazhi = Chinese journal of plastic surgery and burns **1996**, 12, 45-47.

112. a) S. R. Doctrow, A. Lopez, A. M. Schock, N. E. Duncan, M. M. Jourdan, E. B. Olasz, J. E. Moulder, B. L. Fish, M. Mader, J. Lazar, Z. Lazarova, *The Journal of investigative dermatology* **2013**, *133*, 1088-1096; b) R. Monteil, G. Biron, *Therapie* **1971**, *26*, 535-544.

113. a) D. M. Douglas, J. C. Forester, R. R. Ogilvie, *The British journal of surgery* **1969**, *56*, 219-222; b) I. Grabska-Liberek, R. Galus, W. Owczarek, K. Wlodarsk, S. Zabielski, J. Malejczyk, D. Sladowski, *Polski merkuriusz lekarski : organ Polskiego Towarzystwa Lekarskiego* **2013**, *35*, 51-54.

114. C. S. Kamma-Lorger, C. Boote, S. Hayes, J. Albon, M. E. Boulton, K. M. Meek, *Experimental eye research* **2009**, *88*, 953-959; d) E. Mussini, J. J. Hutton, Jr., S. Udenfriend, *Science* **1967**, *157*, 927-929.

115. a) F. Arnold, D. C. West, *Pharmacology & therapeutics* **1991**, *52*, 407-422; b) S. Yoshida, H. Yoshimoto, A. Hirano, S. Akita, *Plastic and reconstructive surgery* **2016**, *137*, 1486-1497.

116. M. Grunewald, I. Avraham, Y. Dor, E. Bachar-Lustig, A. Itin, S. Jung, S. Chimenti, L. Landsman, R. Abramovitch, E. Keshet, *Cell* **2006**, *124*, 175-189.

117. C. Urbich, S. Dimmeler, *Circulation research* **2004**, *95*, 343-353.

118. a) H. F. Lu, J. S. Yang, K. C. Lai, S. C. Hsu, S. C. Hsueh, Y. L. Chen, J. H. Chiang, C. C. Lu, C. Lo, M. D. Yang, J. G. Chung, *Neurochemical research* **2009**, *34*, 1491-1497; b) H. S. Shang, C. H. Chang, Y. R. Chou, M. Y. Yeh, M. K. Au, H. F. Lu, Y. L. Chu, H. M. Chou, H. C. Chou, Y. L. Shih, J. G. Chung, *Oncology reports* **2016**, *36*, 2207-2215.

119. P. Urbina-Cano, L. Bobadilla-Morales, M. A. Ramirez-Herrera, J. R. Corona-Rivera, M. L. Mendoza-Magana, R. Troyo-Sanroman, A. Corona-Rivera, *Journal of applied genetics* **2006**, *47*, 377-382.

120. a) Stojadinovic, O.; Pastar, I.; Nusbaum, A. G.; Vukelic, S.; Krzyzanowska, A.; Tomic-Canic, M. *Wound Repair Regen.* **2014**, *22*, 220– 227; b) Liang, L.; Stone, R. C.; Stojadinovic, O.; Ramirez, H.; Pastar, I.; Maione, A. G.; Smith, A.; Yanez, V.; Veves, A.; Kirsner, R. S.; Garlick, J. A.; Tomic-Canic, M. *Wound Repair Regen*. **2016**, *24*, 943– 953.

121. a) Loesche, M.; Gardner, S. E.; Kalan, L.; Horwinski, J.; Zheng, Q.; Hodkinson, B. P.; Tyldsley, A. S.; Franciscus, C. L.; Hillis, S. L.; Mehta, S.; Margolis, D. J.; Grice, E. *J.*

Invest. Dermatol. **2017**,*137*, 237– 244; b) Veves, A.; Falanga, V.; Armstrong, D. G.; Sabolinski, M. L.Graftskin, *Diabetes Care* **2001**, *24*, 290– 295.

122. a) Marston, W. A.; Hanft, J.; Norwood, P.; Pollak, R. *Diabetes Care* **2003**, *26*, 1701–1705; b) Driver, V. R.; Lavery, L. A.; Reyzelman, A. M.; Dutra, T. G.; Dove, C. R.; Kotsis, S. V.; Kim, H. M.; Chung, K. *Wound Repair Regen.* **2015**, *23*, 891– 900; c) Smiell, J. M.; Wieman, T. J.; Steed, D. L.; Perry, B. H.; Sampson, A. R.; Schwab, B. H. *Wound Repair Regen*. **1999**, *7*, 335– 346.

123. a) Wei, E. X.; Kirsner, R. S.; Eaglstein, W. H. *J. Am. Acad. Dermatol*. **2016**, *75*,203; b) Barrientos, S.; Brem, H.; Stojadinovic, O.; Tomic-Canic, M *Wound Repair Regen.* **2014**, *22*, 569– 578.

124. a) Richmond, N. A.; Vivas, A. C.; Kirsner, R. S. *Med. Clin. North Am.* **2013**, *97*, 883–898; b) Fonder, M. A.; Lazarus, G. S.; Cowan, D. A.; Aronson-Cook, B.; Kohli, A. R.; Mamelak, A. *J. Am. Acad. Dermatol.* **2008**, *58*, 185– 206; c) Kalashnikova, I.; Das, S.; Seal, S *Nanomedicine* **2015**, *10*, 2593– 2612.

CHAPTER 2

Facile amphiphilic polypeptide based micelle-hydrogel composites for controlled dual drug delivery

2.1 Introduction

Complications in the treatment of advanced disease have highlighted the requirement for drug co-administration in a dose-controlled manner. Conventional forms of drug administration often necessitate higher dose or recurrent administration to yield desired therapeutic effects, potentially resulting in lower efficacy and patient compliance as well as adverse effects and induced toxicity.[1] Conversely, combination therapies utilizing multiple drugs concurrently may enhance the progression of treatment as well as tissue regeneration in cases of injury or trauma.[2] To improve these effects, different drug formulations should be administered at their optimal dose and treatment exposure periods. However, simple drug delivery systems only partly fulfill these needs independently; thus, controlled dual drug release systems are required. Although a few studies have addressed the fabrication of dual drug delivery systems (DDS),[3] controllability over the release of the second drug has remained an issue,[4] limiting the purpose of dual delivery and potentially yielding adverse effects from drug overexposure.

The majority of reported dual DDS contain hydrogel as a primary component of drug encapsulation. Since the first synthetic hydrogels were formulated,[5] the use of hydrogel technology has been broadened to many fields including food additives,[6] regenerative medicine,[7] tissue engineering,[8] diagnostics,[9] biomedical implants,[10] as well as pharmaceuticals[11] and drug delivery.[12] Hydrogels comprise three-dimensional network structures possessing unique properties such as porosity, strength, and swelling in aqueous environments that can be tuned over a wide range of parameters, making them ideal for use in DDS.[13] However, for biological and drug delivery purposes, the range of natural as well as synthetic hydrophilic polymers is restricted based on their biocompatibility and biodegradability. Notably, hydrogels based on poly amino acids (homo-, di-, or multi-block polymers)[14] have recently emerged as promising physical candidates

especially suitable for controlled drug delivery owing to their ready formation, assembly, and stimuli responsiveness.[15] However, these hydrogels also exhibit limitations like the slow and inefficient uptake of drugs by sorption and limited loading potential especially for hydrophobic drugs.[16] Furthermore, the crosslinking reaction may conjoin the drug to the hydrogel or compromise its chemical integrity, restricting drug delivery, whereas the hydrogel itself may exhibit non-biodegradability and composition problems

As an alternative, polymeric micelle-based DDS[17] offer the ease of self-assembly, exhibit distinct stability in soluble states, and contain well-defined hydrophobic and hydrophilic domains that markedly improve hydrophobic drug solubility, allowing high drug loading capability. Conversely, limitations include overall micelle stability, dose control, long-term release, and site specific drug delivery. However, recent advances in establishing complex DDS suggest the potential for developing a delivery formulation providing simultaneous gelation and a better degree of drug loading in an aqueous environment.

Accordingly, we aimed to design a system capable of sustaining hydrogel integrity as well as providing better controllability over drug release through drug encapsulation in micellar nano-reservoirs. The amphiphilic di-block polypeptide-based micelle-hydrogel[18] composite described here integrates these two strategies (micelles and hydrogels) in a single entity for controlled and switchable drug co-delivery.

2.2 Materials and methods

2.2.1 Materials

ε-Benzyloxycarbonyl-L-lysine (H-Lys (Z)-OH), γ-benzyl-L-glutamic acid (H-Glu (OBzl)-OH), phenylalanine (H-phe-OH), trifluoroacetic acid, and 30 % hydrogen bromide (HBr) in acetic acid were purchased from Watanabe Chemical IND., Ltd. (Hiroshima, Japan). N, N-dimethylformamide (DMF) anhydrous, hexane (anhydrous), and tetrahydrofuran (THF) were acquired from Kanto Chemical Co., Inc. (Tokyo, Japan). Diethyl ether and dimethyl sulfoxide (DMSO) were bought from Nacalai Tesuque (Kyoto, Japan). Triphosgene and curcumin (Cur) were purchased from Tokyo Chemical Industry Co., Ltd. (Tokyo, Japan). Amphotericin B (AmpB) and genipin were purchased from Wako Pure Chemical Industries, Ltd. (Osaka, Japan) and Amatek Chemical Co., Ltd. (Hong Kong,) respectively. Phosphotungstic acid was bought from Sigma Aldrich (Tokyo, Japan). All chemicals were used as received.

2.2.2 Synthesis of N-carboxyanhydrides of Amino Acids.

Synthesis of N-carboxyanhydrides (NCA) of L-lysine (Lys (Z)-NCA), L-glutamic acid (Glu (OBzl)-NCA), and L-phenylalanine (Phe-NCA) was performed using the protocol reported by Farthing and Reynolds[19] using triphosgene. Briefly, for the preparation of Lys (Z)-NCA, Lys (Z)-OH (3 g, 10.71 mmol) was suspended in a two-neck flask in tetrahydrofuran (THF) (30 mL). Triphosgene (3.17 g, 10 mmol) in THF (20 mL) was added to the suspension with stirring at 50 °C under reflux for 3 h until the solution turned clear. After 3 h, the excess phosgene was removed from the solution under reduced pressure. The crude product thus obtained was re-suspended in THF and was poured in n-hexane to yield a white precipitate that was recrystallized twice in a mixture of THF/n-hexane. Yield: 2.3 g; 7.5 mmol; 75 %. ^{1}H-NMR (400 MHz, dimethylsulfoxide (DMSO)-d_6, 25 °C): 1.29–1.44 (m, 4H, J=7.2 Hz), 1.56–1.82 (m, 2H, J=6.7 Hz), 3.01 (q, 2H, J=5.3

Hz), 4.43 (t, 1H, J=6.2), 5.03 (s, 1H), 7.37 (m, 5H, J= 7.1 Hz), 9.011 (s, 1H). ^{13}C-NMR (400 MHz, DMSO-d_6): 21.66 (s), 28.82 (s), 30.69 (s), 40.3 (s; masked by DMSO multiplet), 57.07 (s), 65.19 (s), 127.78 (s), 127.83 (s), 128.40 (s), 137.31 (s), 152.04 (s), 156.16 (s), 171.72 (s).

Glu(OBzl)-NCA and Phe-NCA were also prepared following a similar protocol.

Glu(OBzl)-NCA Yield: 2.12 g; 8.01 mmol; 64 %. ^{1}H-NMR (400 MHz, DMSO-d_6, 25 °C, TMS): 1.07–1.25 (m, 2H, J= 5.4 Hz), 1.68 (t, 2H, J= 6.1 Hz), 3.63 (t, 1H, J= 7.8 Hz), 4.24 (s, 2H), 6.52 (m, 5H, J= 5.9 Hz), 8.25 (m, 1H, J=7.4 Hz). ^{13}C-NMR (400 MHz, DMSO-d_6): 26.45 (s), 29.11 (s), 56.24 (s), 65.75 (s), 125.03 (s), 128.10 (s), 128.49 (s), 136.05 (s), 151.91 (s), 171.38 (s), 171.75 (s).

Phe-NCA Yield: 2.43 g; 12 mmol; 82 %. ^{1}H-NMR (400 MHz, DMSO-d_6, 25 °C): 3.04–3.23 (m, 2H, J= 6.9 Hz), 4.82 (t, 1H, J= 8.3 Hz), 7.37 (m, 5H, J=5.1 Hz), 9.62 (s, 1H). ^{13}C-NMR (400 MHz, DMSO-d_6): 35.64 (s), 66.08 (s), 128.29 (s), 128.53 (s), 128.98 (s), 136.91 (s), 154.01 (s), 170.72 (s).

2.2.3 Synthesis of PLL-PPA and PGA-PPA Di-block Copolymers.

The block copolymers PZLL-b-PPA and P(OBzl)GA-b-PPA were synthesized in a two-step process: firstly, the hydrophilic block (of either glutamic acid or lysine) was synthesized by ring-opening polymerization of the respective NCA. For this, 7 mmol Lys (Z)-NCA (2 g)/Glu (OBzl)-NCA (1.8 g) was dissolved in 5 mL dimethylformamide with n-hexylamine (9.5 μL, 0.07 mmol) used as the initiator and stirred for 48 h at room temperature. Upon complete utilization of the first block monomer, Phe-NCA (0.67 g, 0.35 mmol) was added as the second hydrophilic block and stirred for another 36 h, and then precipitated with an excess of diethyl ether under vigorous stirring. Then, the viscous polymer was again dissolved in dimethylformamide and re-precipitated with

diethyl ether to give a white solid of PZLL-PPA or P(OBzl)GA-PPA. The polymers were dried under vacuum at room temperature. De-protection was performed by dissolving the polymers in trifluoroacetic acid and 33 % HBr/CH_3COOH followed by stirring for 10 h at room temperature. The de-protected polymers were precipitated with an excess of diethyl ether to obtain white solids that were dried in vacuum at room temperature for 48 h to yield PLL-PPA and PGA-PPA.

2.2.4 Characterization.

^{1}H and ^{13}C NMR spectra were obtained at 25 °C on a Bruker AVANCE III 400 spectrometer (Bruker BioSpin Inc., Fällanden, Switzerland) in DMSO-d_6. Gel permeation chromatography (GPC) measurements were performed before de-protection of the polypeptides using a Shodex GPC101 (Yokohama, Japan) with a connection column system of 803 and 807 and equipped with Jasco 830 RI and Jasco UV-2075 plus detectors using pullulan as a molecular weight standard. Transmission Electron Microscopy (TEM) was performed using a Hitachi H-7100 TEM (Tokyo, Japan). Samples were prepared by adding the micellar solution onto a copper mesh and allowing it to dry. The dried sample was stained with phosphotungstic acid and observed.

2.2.5 Formation of Micelles.

For the preparation of micelles (empty), a 2 % (w/v) solution of amphiphilic polypeptide was prepared separately in DMSO and stirred for 2 h to ensure complete dissolution. This solution was then dropped into distilled water under continuous stirring. The resulting solution was transferred into a dialysis bag (MWCO 3500) and dialyzed against distilled water with a change in solvent 2–3 times a day for 2 days.

2.2.6 Critical Micellar Concentration (CMC) Determination.

Pyrene was used as a hydrophobic probe for the determination of CMC values of the PLL-*b*-PPA and PGA-*b*-PPA micelles. Pyrene solution in acetone (100 µL, 6×10^{-6} mol L^{-1}) was added into

two sets of aliquots and the acetone was allowed to evaporate. Then, 1.0-mL micellar (PLL-PPA or PGA-PPA) solutions at various concentrations were added to the aliquots and incubated overnight with continuous shaking. Pyrene was excited at 334 nm using a Jasco FP-8600 spectrofluorometer (Oklahoma City, OK, USA). A red shift in the excitation peak was observed upon varying the concentration of the polymer. The ratio of fluorescence intensity as a function of log of concentration of polymer was plotted to determine the CMC value.

2.2.7 Stability.

Micelle size was measured on a Malvern Zetasizer Nano ZS (Malvern, UK). For stability testing, the micelle solutions were prepared and micelle size was measured in a polystyrene cuvette over 7 days. For drug loaded micelles, the loaded micelles were suspended in phosphate buffered saline (PBS) buffer and size was recorded over 2 weeks. All samples had a concentration of approximately 1 mg mL^{-1} and were filtered through an 0.8-μm Millex GP filter (Merck Millipore Ltd., Billerica, MA, USA) prior to measurement.

2.2.8 Loading of AmpB and Cur in Micelles.

For drug loading, 20 mg AmpB/Cur were dissolved in 2 mL DMSO. Then, 100 mg polymer solution was added to the prepared drug solution and stirred for 2 h. The polymer and drug solution was next added to 10 mL distilled water dropwise with continuous stirring. The obtained solution was lyophilized using the freeze dry method for storage and further use.

2.2.9 Drug loading Efficiency.

To determine loading efficiency, 10 mg drug-loaded micelles were weighed into a mini centrifuge tube and reconstituted in 500 μL DMSO for complete dissolution of micelles into free polymers. After filtration, the concentration was recorded using a UV-Vis spectrophotometer. AmpB

concentration was measured by spectroscopy at 368 nm and Cur was measured at 426 nm against a standard calibration curve.[20] The following formula was used for calculation:

$$\%\ \text{Loading efficiency} = \frac{\text{amount of drug in micelles}}{\text{amount of total drug loaded}} \times 100 \qquad (1)$$

2.2.10 Preparation of Hydrogels.

The hydrogels were prepared by cross-linking between genipin and the amino group in PLL-b-PPA polymers. The freeze-dried drug-loaded micelles were dissolved in deionized water (2% w/v of each) and the resultant solutions were stirred for at least 2 h to ensure that the polypeptides were dissolved in completely. Genipin (0.5–2.5 % w/v) was mixed with the polypeptide solution and was allowed to stand for 20 h to form dark blue hydrogels. The gelation and time of gelation of the cross-linked polypeptide hydrogels were investigated using the vial tilting method.

2.2.11 Drug Release.

A standard shape (circular disc with height of 5 mm) of micelle-hydrogel was cut using a punch of 10 mm diameter and was immersed in 50 mL PBS. The PBS was subsequently changed every 4 h and the collected PBS was used to measure the amount of drug at fixed time points using spectroscopy. The standard sample was prepared by dissolving both Amp B and Cur and recording standard curves at different λ_{max} for both Cur and Amp B to account for the interference arising from the action of one drug on another during the recording of absorbance in the dual drug release studies.

2.2.12 Swelling Study.

The swelling ratios of genipin cross linked micelle-hydrogels composites were measured at 37 °C. Equal size (circular disc of diameter 10 mm and height 5 mm) hydrogel samples were punched from fresh made composites and were weighed and immersed in PBS at pH 7.4 for 24 h. Then, the

samples were gently removed from the buffer and gently wiped with filter paper to remove the excess buffer on the surface. These composites were then weighed. The swelling percentage was calculated as follows:

$$\text{Swelling Percentage} = \frac{Wt - Wo}{Wo} \times 100 \qquad (2)$$

Here, Wo denotes the weight of the composite before swelling and Wt is weight of composite after 24 h swelling in the buffer

2.2.13 Circular Dichorism.

The secondary structure changes of the synthesized polypeptides were studies by far-UV circular dichroism (CD) spectra before and after pH treatment. The concentration of polypeptide was prepared 20 μM and the spectrum was recorded in a cuvette of path length 0.5 cm, using a JASCO-820 spectropolarimeter. Each spectrum was baselinecorrected and was collected as an average of three scans at a scan rate of 200 nm min^{-1} and a response time of 2 second.

2.3 Results and discussion

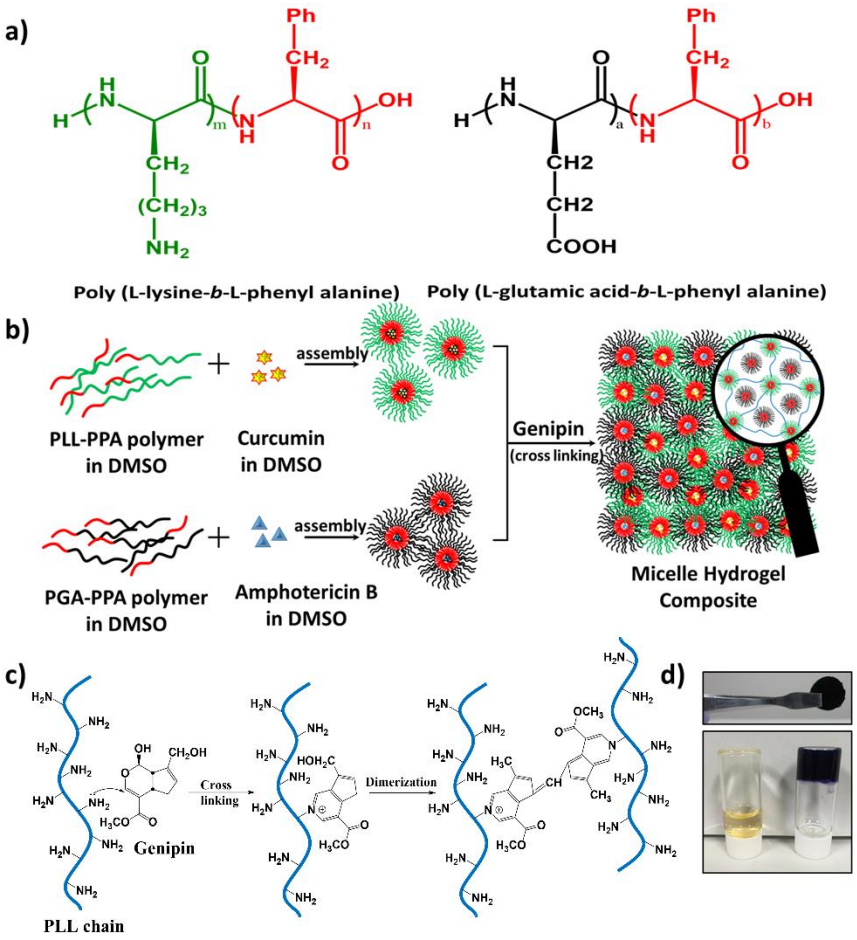

Figure 2.1 Preparation of micelle hydrogel composite. (a) Schematic structure of prepared copolymers. (b) Schematic representation of composite preparation based on genipin crosslinking. (c) Schematic representation of crosslinking by genipin and (d) photograph of the genipin crosslinked micelle-hydrogel composite before and after gelation and as a self-standing gel.

We successfully employed the highly condensed ampholytic micelles and demonstrated controlled dual drug release from their core. As shown in Figure 2.1, the proposed micelle-hydrogel composite constitutes two distinct drug-loaded nano-reservoirs (differently charged in differing crosslinking environments), providing mutually exclusive drug release profiles beneficial for synergistic wound healing. The drug-loaded composites were characterized for drug release profile

switching ability in vitro under various pH, composition, and cross linking conditions to provide sufficient groundwork for clinical trials.

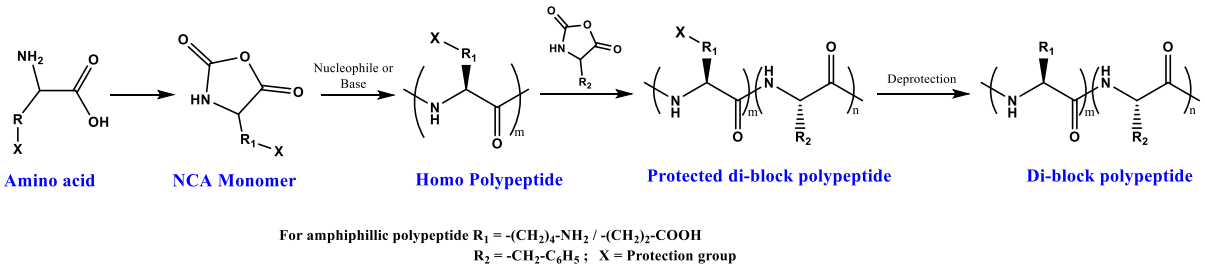

Scheme 2.1 Representation of the preparation of polypeptides by ring opening polymerization of NCA and subsequent de-protection.

A facile fabrication strategy was followed to develop micelle-hydrogel composite development. Briefly, two different amphiphilic di-block polypeptides were synthesized (Figure 1a) in N,N-dimethylformamide by ring opening polymerization[21] using Nε-benzyloxycarbonyl-L-lysine-Nα-carboxy anhydride (Lys (Z)-NCA) and L-phenylalanine NCA (Phe-NCA) to yield the cationic amphiphile poly (L-lysine-*b*-L-phenyl alanine) (PLL-PPA), and with γ-benzyl-L-glutamate NCA (Glu (OBzl)-NCA) and Phe-NCA yielding poly (L-glutamic acid-*b*-L-phenylalanine) (PGA-PPA) as the anionic amphiphile (after subsequent de-protection) at ambient temperature as shown in Scheme 2.1. The synthesized NCA monomers were characterized using ^{1}H-NMR and ^{13}C NMR and di-block polypeptides were characterized by ^{1}H-NMR and GPC (Table 2.1). The polypeptide molecular weight was controlled by the initiator to monomer molar ratio and examined using a time course study showing well-controlled polymer molecular weights with narrow polydispersity index (Figure 2.2).

Table 2.1 Overview of polypeptides synthesized using NCA amino acid polymerization.

Polymer	DP		M_n X 10^3	PDI[b]	CMC (mg mL^{-1})	Micelle size[c] (nm)
	Block a (PLL / PGA)	Block b (PPA)				
PLL_{200}-PPA_5	187	4.1	51.13	1.17	0.67	472
*PLL_{100}-PPA_5	91	4.7	28.93	1.23	0.22	196
PGA_{200}-PPA_5	193	3.9	35.80	1.32	0.43	368
*PGA_{100}-PPA_5	88	4.3	18.33	1.15	0.15	173

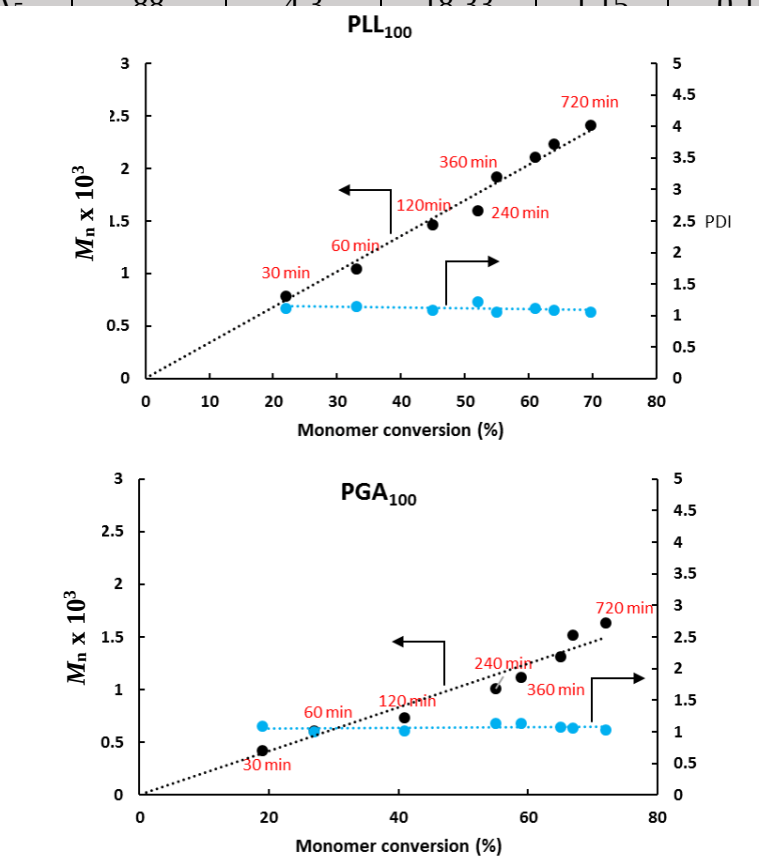

Figure 2.2 Molecular weight (M_n) and the PDI as a function of monomer conversion showing the controllability of the polymerization reaction; a. PLL block and b. PGA block

Among all the synthesized polypeptides, the polypeptides with hydrophilic to hydrophobic block ratio of 100:5 were used for preparing micelle-hydrogel composites and investigating in-vitro dual drug release. This ratio of hydrophilic to hydrophobic group was optimized studying the solubility of the synthesized polymers in water, as the polymers with higher than 5 mole percent of PPA tend to be less soluble in water and showed considerably higher CMC. These di-block polypeptides readily self-assembled into micelles in aqueous solution (Figure 2.1b); micelle morphology was studied using TEM and dynamic light scattering (DLS), revealing a spherical shape for both (Figure 2.3). Average hydrodynamic diameters were 170 and 195 nm for PGA-PPA and PLL-PPA, respectively, at physiological pH (Figure 2.4) vs. 10–15 nm in TEM, wherein the charged shell (PLL/PGA) block was dehydrated and thus packed in tightly coiled helices, which on interaction with water swelled considerably (10–15 times their original diameter). [22]

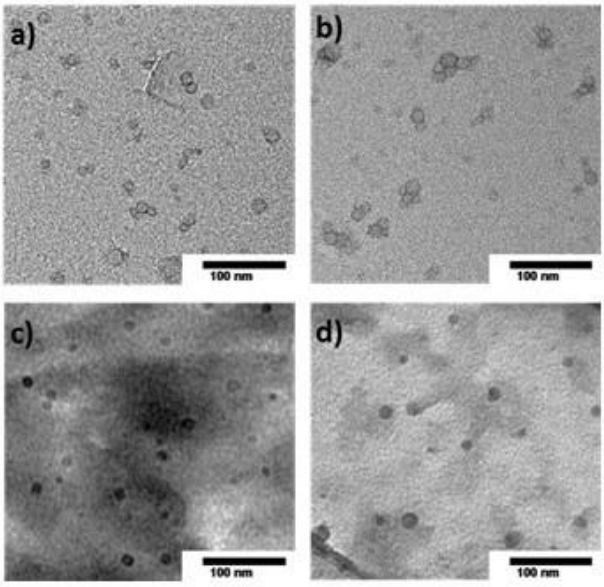

Figure 2.3 Particle size characterization of prepared micelles by transmission electron microscopy. (a) and (c) show PGA-PPA micelles before and after Amphotericin B loading and (b) and (d) show PLL-PPA micelles before and after loading of curcumin.

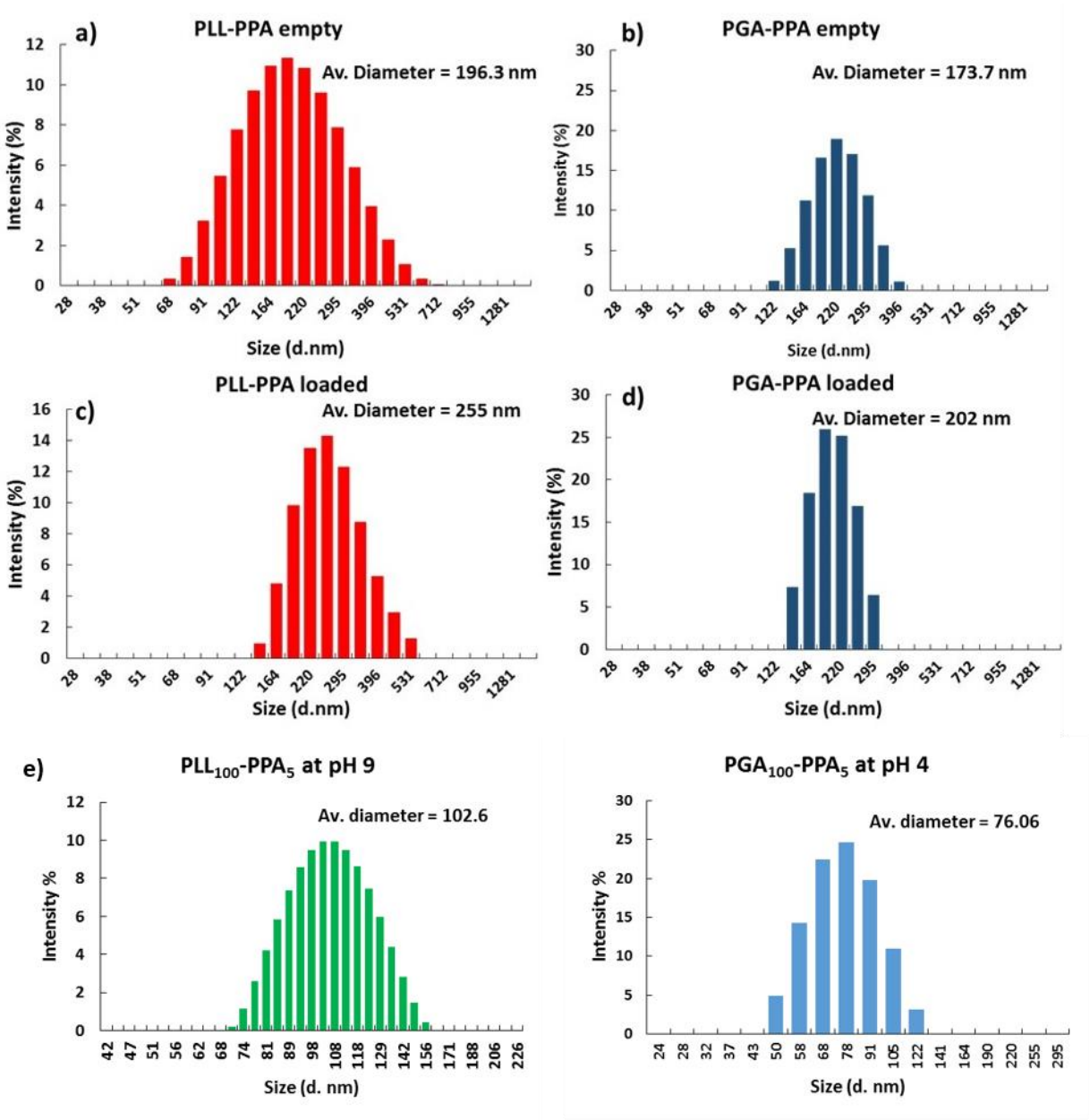

Figure 2.4 Dynamic Light Scattering (DLS) results (a) and (c) show PLL-PPA micelles before and after curcumin loading; (b) and (d) show PGA-PPA micelles before and after loading of amphotericin B; (e) and (f) showing the change in hydrodynamic diameter of PLL_{100}-PPA_5 and PGA_{100}-PPA_5 at pH 9.0 and 4.0 respectively.

To confirm this swelling behavior, micelle size was studied at various pH, with substantial size decrease upon transition from charged to uncharged states (e.g., PLL-PPA hydrodynamic diameter of 102 nm at pH 9.0 and PGA-PPA diameter of 76 nm at pH 4.0 (Figure 2.4 e and f). A critical

micelle concentration (CMC) value of 0.15 and 0.22 mg mL-1 was seen for PGA_{100}-PPA_5 and PLL_{100}-PPA_5 (subscripts indicating the block ratio at feed) respectively (Figure 2.5).

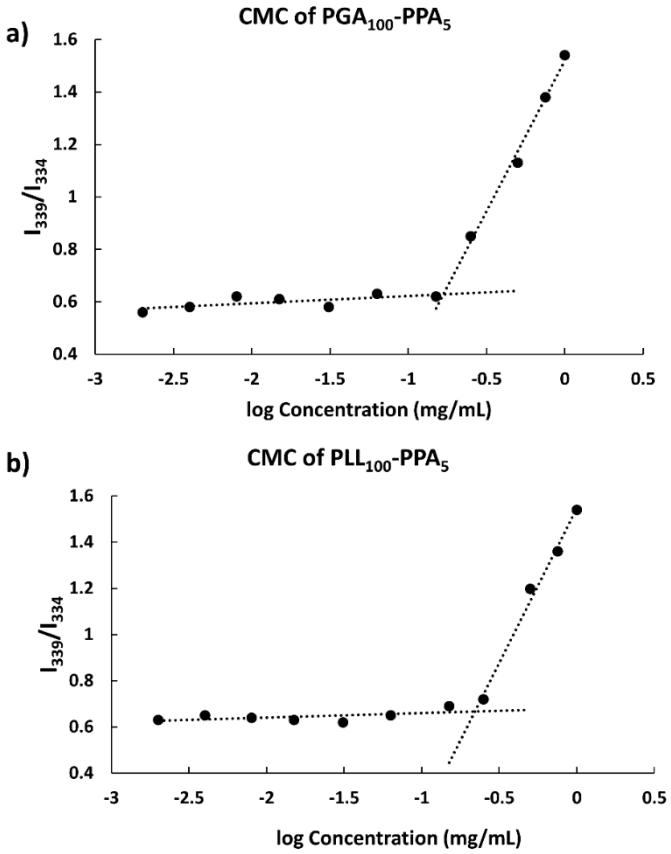

Figure 2.5 CMC determination of (a) PGA-PPA and (b) PLL-PPA. Intensity ratio (339/334) of pyrene vs. logarithm concentration of polypeptide.

However, although block copolymers with smaller block sizes, especially the hydrophobic block (as herein) may show a higher CMC in water, the PLL-PPA and PGA-PPA di-blocks showed a low formed micelle CMC value, indicating high polypeptide micellization efficiency through π-π stacking[23] of the benzyl groups of the phenyl alanine block in the core, and also leading to high stability. In colloidal systems, the ζ-potential predicts stability in terms of suspension aggregation,

with a stable system exhibiting a ζ -potential magnitude > ±30 mV.[24] Here, DLS also showed micelle stability as a function of size, with fair stability in aqueous solution over 14 days with minimal degradation or aggregation (Figure 2.6). This may be attributed to the highly charged shells, arising from ionizable side chain groups in the hydrophilic part of the polypeptides yielding a ζ-potential of 68 and −63 mV at physiological pH for PLL_{100}-PPA_5 and PGA_{100}-PPA_5, respectively, repelling any between-micelle ionic interactions.[25]

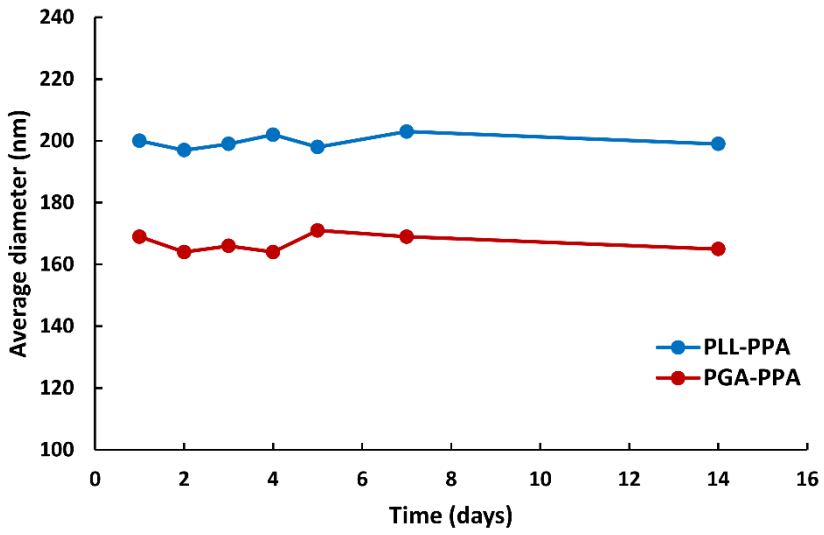

Figure 2.6 Stability of micelles over time. Diameter as observed by DLS shows fair stability of micelles with almost no aggregation.

To assess the potential of the DDS for delivery of wound healing agents, the prepared micelle cores were used as nano-reservoirs for the model drugs curcumin (Cur) and amphotericin B (AmpB) to generate the drug-loaded micelle-hydrogel composites, with high loading efficiency (76.5 % and 87.4 %) in PLL-PPA and PGA-PPA, respectively. Cur has been shown to have efficacy toward wound healing[26] and AmpB was used as a model fungicidal drug, critical for preventing topical wound sepsis.[27] These core-loaded nano-reservoirs were then crosslinked using the free $-NH_2$ (Figure 2.1c) groups in the PLL-PPA micelle shell via the water soluble

biocompatible cross linker genipin[28] to form a hydrogel network of characteristic dark blue color with free PGA-PPA micelles trapped inside the network. The sol to gel transition was confirmed by the tube inversion method and stable self-standing gels were observed (Figure 2.1d).

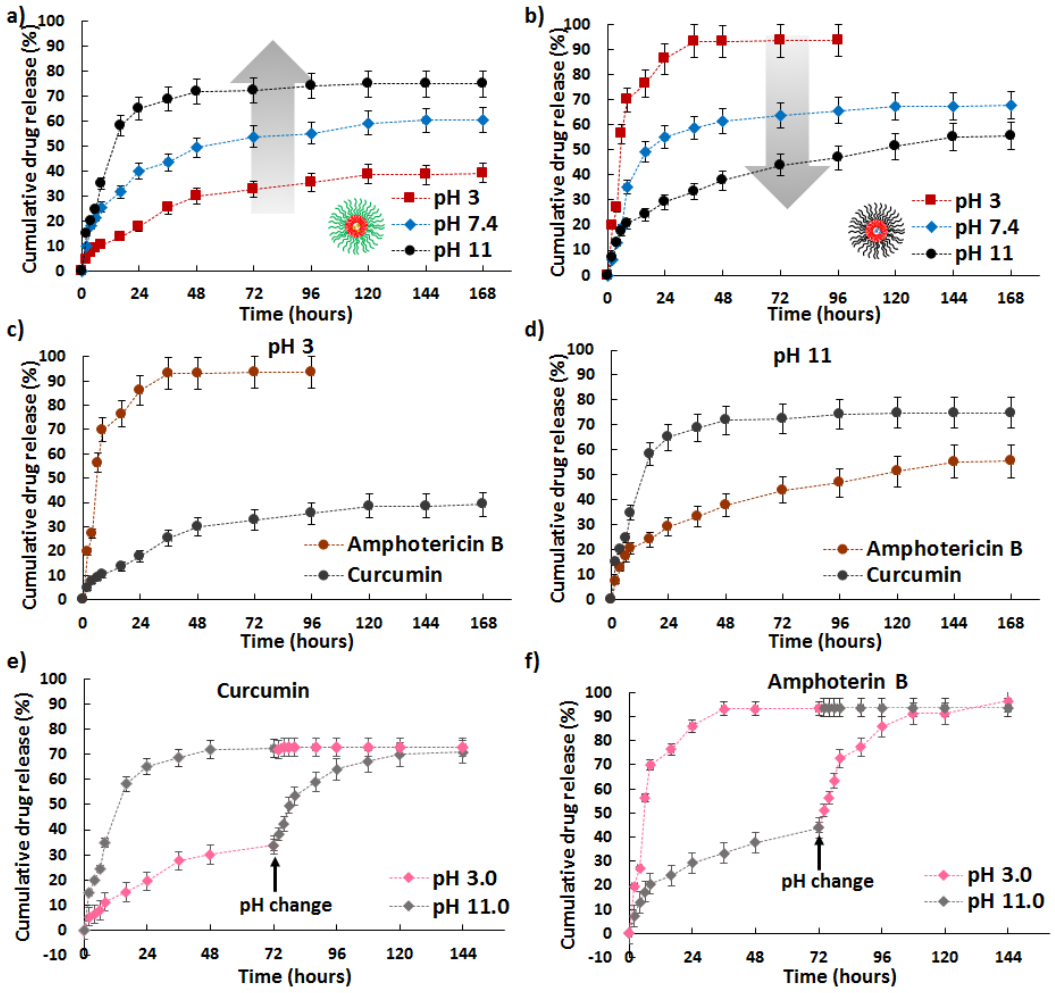

Figure 2.7 In vitro drug release profiles of the polymer micelles at different pH and crosslinking values (pH 3.0, 7.4, and 11) at constant cross linker concentration (1 % of genipin). (a) Curcumin; (b) amphotericin B; and (c) and (d) switchability of drug release profiles at pH 3 and 11, respectively. (e) and (f) show the biphasic release of drugs from composites, when the surrounding buffer was switched from one pH to another.

Because of the ionizable properties of the micelle-hydrogel composites, we next investigated their pH responsiveness. A 4 % w/v (2 % each of PLL-PPA and PGA-PPA) micellar mixture was gelled using 1.0 % genipin; this gelation condition was used throughout study unless stated otherwise,

and was then subjected to drug release assessment in different pH environments (pH 3, 7, and 11) (Figure 2.7 a and b). The drug release profile clearly indicated that the drug loaded composite was susceptible to change in pH. The cationic PLL-PPA micelles showed a rushed release of Cur at pH 11, with a slower release at lower pH. In contrast, PGA-PPA micelles showed an opposite trend with burst release at pH 3 and an extended release profile at higher pH. As the PLL and PGA blocks surpassed their respective pKa (8.2 and 4.3) and moved to a relatively uncharged state, both lysine and glutamic acids, which are known for their helix forming ability in an uncharged state,[29] attained a helix conformation. Change in pH from 3 to 11 caused rapid deprotonation of L-lysine side chains in micelles; a similar transition was seen for PGA upon pH change from 11 to 3, whereupon the carboxylic groups of glutamic acid side chains gained a proton to become neutral. Advancement from charged to uncharged states changed the micelle hydrophilic chain conformations. The random coil states tended to form a highly ordered helix conformation causing shrinking of the hydrophilic segment with marked decrease in the water solubility.[30] This transition can be clearly seen in the change in the CD spectra of the polypeptides at different pH (Figure 2.8). This, thus generates a strain on the micellar core, resulting in rapid drug leakage from the micelles. As both micelles showed this transition going toward the opposite end of the pH scale, a reverse trend in micellar behavior was recorded that could be switched by changing the pH (Figure 2.7 c and d). To further confirm our assumptions regarding the switchability in terms of drug release profile, we subjected the composites to a sudden change in pH and studied the cumulative release rate. As seen in Figure 2.7 e and f, a biphasic release curve was observed with a sudden jump in release rate when subjected to drastic pH changes, which supported our claim. Although this outcome is not closely related to the biological environment as such drastic pH difference is rarely observed in vivo, the switchable profile of the prepared composite through environmental changes

including pH is notable. Therefore, the feature of environmentally responsive switchability allows drug delivery systems to be dramatically controlled with respect to their swelling behavior, drug permeability, and release profile in response to variations in the pH or ionic strength of the surrounding fluid, which may be useful for modulated drug delivery.

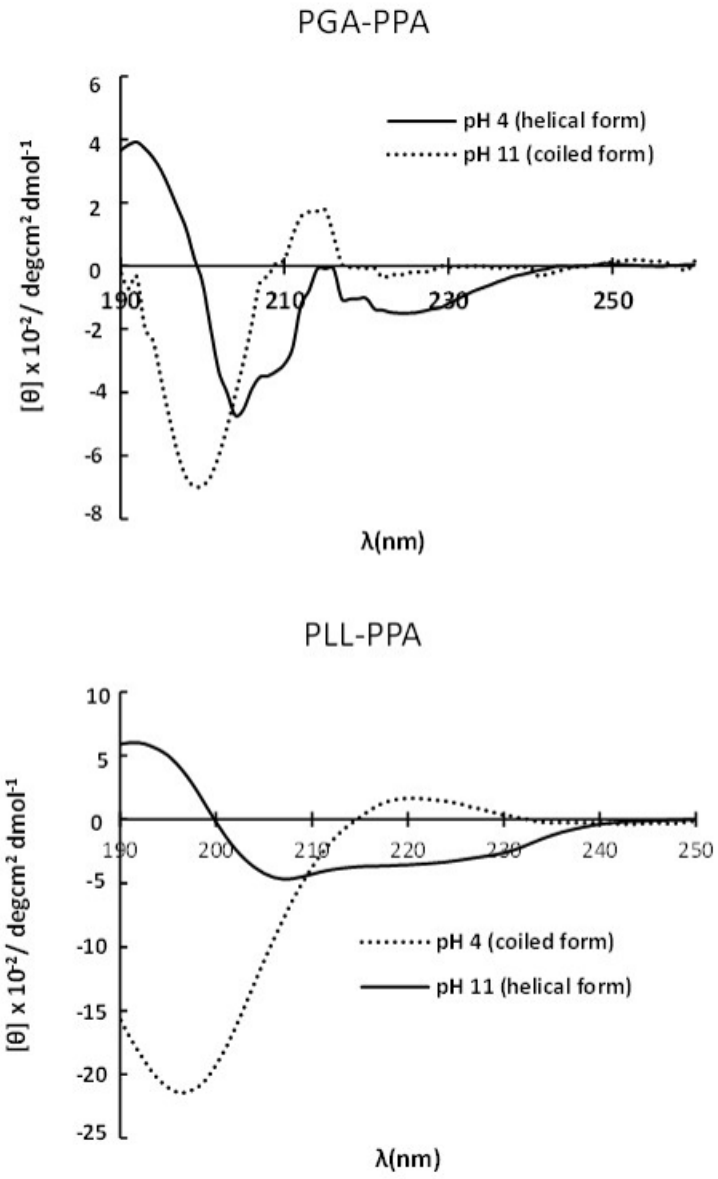

Figure 2.8 CD spectra of PGA-PPA (top) and PLL-PPA (bottom) at pH showing their respective transitions from random coil to α-helix at change in pH.

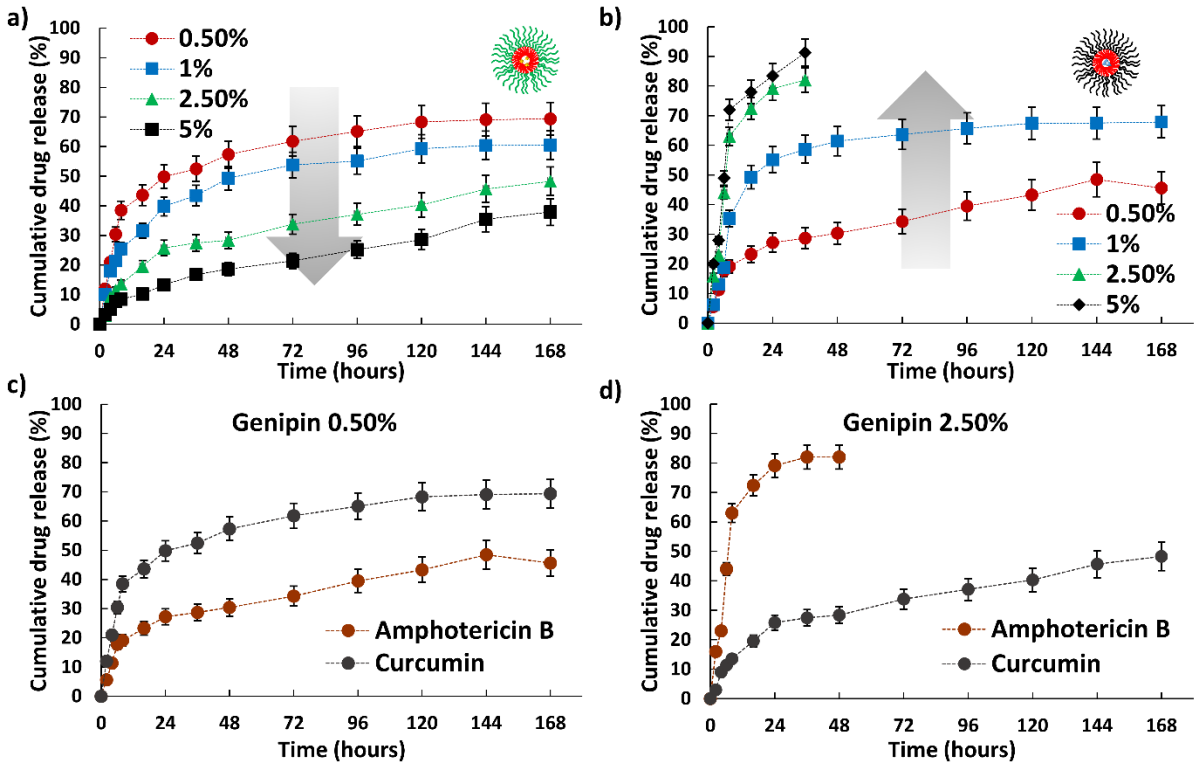

Figure 2.9 In vitro drug release profiles of the polymer micelles at different crosslinking values at pH 7.4. (a) Curcumin; (b) amphotericin B; and (c) and (d) release profile switching at different cross linker concentrations

To better understand the switching ability of the formed composites for drug release, we investigated their drug release profiles over various crosslinking densities by using cross linker concentrations at 0.5, 1, 2.5, and 5 %. This yielded opposite trends in drug release pattern at pH 7.4 for both micelle groups. Cur loaded in PLL-PPA micelles showed marked drug release rate decrease from 70 to 38 % with increased cross linker concentration from 0.5 to 5 % (Figure 2.9a) whereas Amp B loaded in PGA-PPA micelles showed a positive trend from 45 to 91 % with increased genipin concentration, showing burst release in higher gel concentrations (2.5 and 5 %) (Figure 2.9b). With increased genipin concentration, more $-NH_2$ PLL side groups are involved in inter- and intra-micelle crosslinking. And as the crosslinking density increases, the micelle shells are more stabilized to firmly hold the core. And this leads to a more stable hydrophobic core of

the PLL-PGA micelles and the leaching of the drug from the core is slowed down sustainably, leading to slower drug release (figure 2.9c). Oppositely as the cross linker concentration increases the PGA-PPA micelles which are trapped among the PLL-PPA crosslinked systems become extensively constrained due to lack of proper space, as the interlinking among PLL-PPA micelles increases and PGA-PPA experience a higher distorting stress as they are held in a tightly packed situation, stressing the unbound AmpB-loaded PGA-PPA micelles.[31] In turn, PGA-PPA micelles succumb to the stress[32] and core structure disruption leads to a burst release of Amp B from the micelles (Figure 2.9d). Thus, two differing pharmacokinetic drug profiles occurred by changing the cross linker concentration, which may be conducive to tailoring micelle-hydrogel composites for optimum drug release over a sustained period without causing unnecessary drug leakage and thus instigating toxicity.

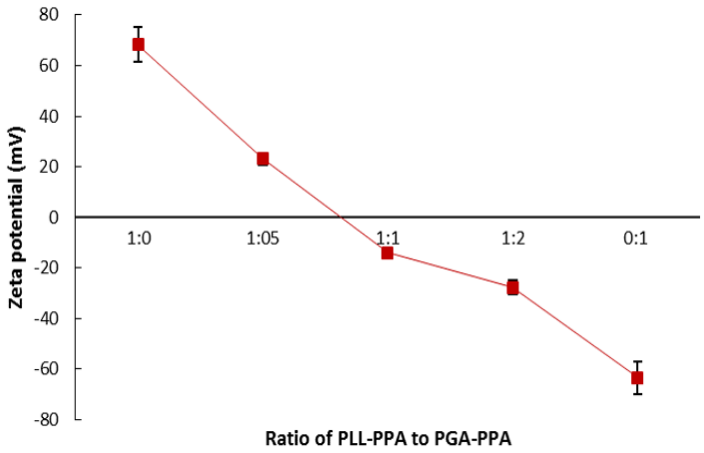

Figure 22.10 Variations in zeta potential of various ratios of PLL-PPA: PGA-PPA micelles.

Finally, we examined the role of surface charges resulting from the interplay of charges in the block polypeptide shells on the composite drug release profiles. The PLL-PPA and PGA-PPA micelle composition (% w/w) was systematically varied to achieve mixed micellar solutions (1:0,

1:0.5, 1:1, 1:2, and 0:1) with charges from 68 to −63 mV (Figure 2.10). The first four systems were also crosslinked to form composites (as no $–NH_2$ groups were available for crosslinking in the 0:1 ratio) and their drug release profiles assessed at pH 7.4 (Figure 2.11). PLL-PPA micelle crosslinking provided considerable stability toward swelling upon higher positive surface charge, yielding faster drug release in 68 and 23 mV composites with no burst release; at negative surface charge, the crosslinked micelle remained unaffected by the swelling, exhibiting sustained drug release. Conversely, micelle hydrogel composites with high surface charge (both positive and negative) showed rapid AmpB release whereas those with low net charge showed sustained release. This could be due to differential composite swelling rates based on surface charge (Figure 2.12).

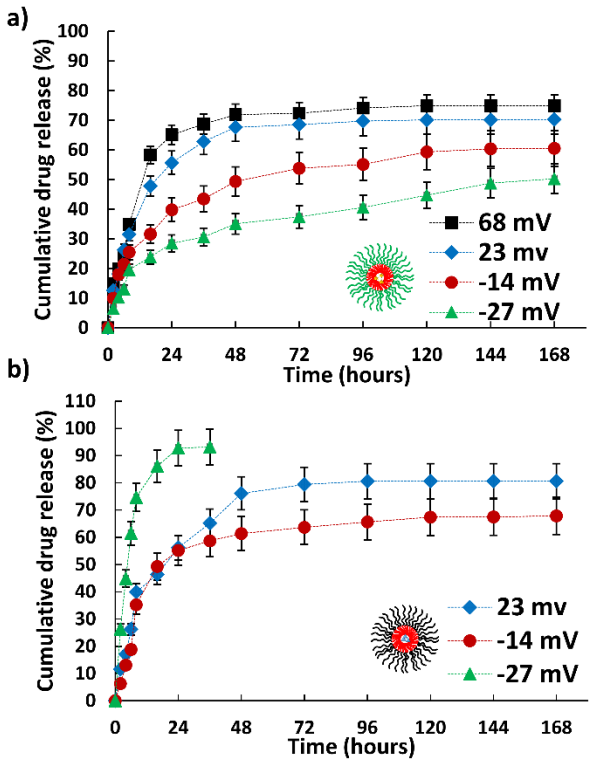

Figure 2.11 Percent drug release against time from (a) curcumin release from loaded PLL-PPA micelles and (b) amphotericin B release from loaded PGA-PPA micelles, at different ζ-potentials.

This kinetic trend of faster PGA-PPA drug release with higher surface charge may act as an efficient tool for dual drug delivery at wound sites to accelerate healing; as initial sepsis may delay the wound healing process.[33] A burst release of antibiotic and/or antifungal drugs in the first phase may be beneficial for avoiding sepsis in the exposed wound, whereas sustained release may aid wound closure.

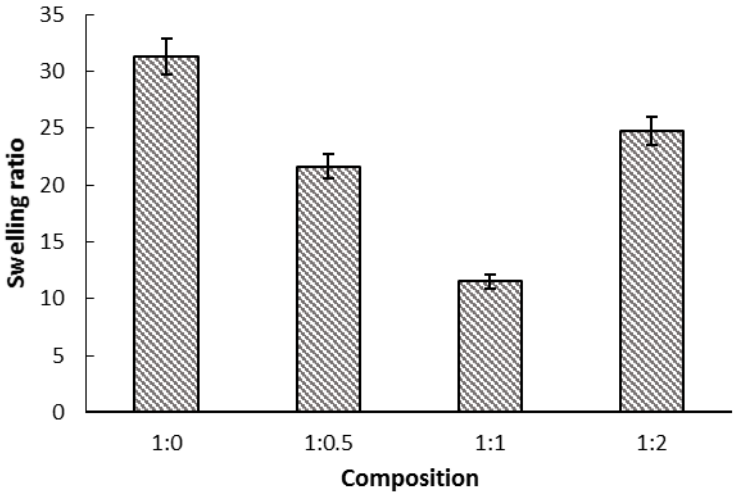

Figure 2.12 The equilibrium swelling ratios of the composites with varying ratios of PLL-PPA: PGA-PPA. (n=3)

Further, the effect of temperature on the drug release profile of the micelles-hydrogel composite was also studied and optimized. As seen in Figure 2.13, the higher temperatures like 50 °C and 60 °C show a relative short-term release behavior compared to that at lower temperatures. However, the release behavior of Curcumin from the PLL-PPA micelles shows a better and sustained long-term release in comparison to Amphotericin loaded micelles and is markedly dependent on environmental temperature. As perceived in the figure, both micelles being of similar chemical nature (polypeptides) behave similarly to temperature changes i.e. the increase in temperature evidently increases the amount of drug release from the micelles. This could be due to the fact that

as temperature rises the polypeptides chains attain a high entropy confirmation with least stabilizing interactions among themselves, which causes the micelles to lose its structure and thus the retardation of the molecule diffusion from its core tends to be weak. As a result, the release rates of both Amp and Cur are accelerated with increasing temperatures.

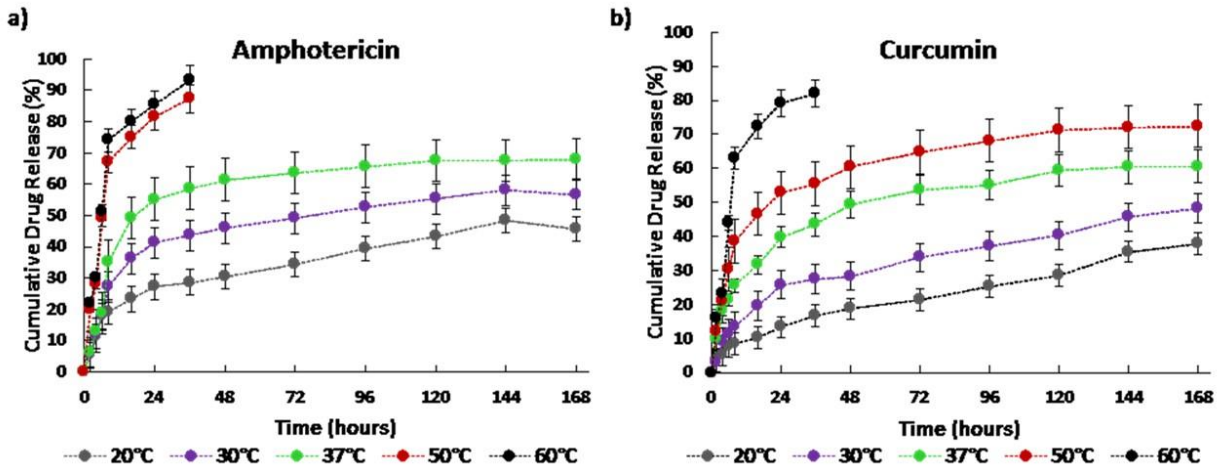

Figure 2.11 Percent drug release against time from (a) curcumin release from loaded PLL-PPA micelles and (b) amphotericin B release from loaded PGA-PPA micelles, at different temperatures.

This proves that prepared system is thus tunable to highest degree of needs not just to show switchability and opposite release profile but also works well at optimum biological conditions giving similar drug release profiles of two different drugs and making it suitable for wide range of applications.

2.4 Conclusion

These results indicate that our micelle-hydrogel composite, with excellent tunable properties and controllable multidrug release, may serve as a potential dual drug release system. This polypeptide-based delivery system displays distinctive advantages for clinical application, such as

1) Combinational drug delivery: the dual DDS can solve the problem of substandard therapeutic effects of single DDS;

2) Independent drug release: each drug can be released from the micelle-hydrogel composite system independently without affecting the release of the other;

3) Tunability: our composite contains two oppositely charged polypeptide micelles that differentially interact with various environments and present distinctive, well-controlled pharmacokinetic drug release profiles; and

4) Ease of handling: the micelle hydrogel composite is simple to prepare and the drug release behaviors can be easily tailored by varying composite preparation parameters.

We expect that the amphiphilic polypeptide based micelle-hydrogel composite system may provide a promising solution as a dual-drug carrier with controlled release behavior of each drug for combined therapy applications.

2.5 References

1. a) T. R. Hoare, D. S. Kohane, *Polymer* **2008**, *49*, 1993-2007; b) R. Langer, *Nature* **1998**, *392*, 5-10; c) W. B. Liechty, D. R. Kryscio, B. V. Slaughter, N. A. Peppas, *Annu. Rev. Chem. Biomol. Eng.* **2010**, *1*, 149-173.
2. a) J. S. Lee, J. W. Bae, Y. K. Joung, S. J. Lee, D. K. Han, K. D. Park, *Int. J. Pharm.* **2008**, *346*, 57-63; b) L. Y. Qiu, Y. H. Bae, *Biomaterials* **2007**, *28*, 4132-4142; c) J. M. Davidson, K. N. Broadley, D. Quaglino, Jr., *Wound Repair Regen.* **1997**, *5*, 77-88.
3. a) X. Cheng, Y. Jin, T. Sun, R. Qi, H. Li, W. Fan, *Colloids Surf., B* **2016**, *141*, 44-52; b) J. A. Chikar, J. L. Hendricks, S. M. Richardson-Burns, Y. Raphael, B. E. Pfingst, D. C. Martin, *Biomaterials* **2012**, *33*, 1982-1990; c) W. Wang, E. Wat, P. C. Hui, B. Chan, F. S. Ng, C. W. Kan, X. Wang, H. Hu, E. C. Wong, C. B. Lau, P. C. Leung, *Sci. Rep.* **2016**, *6*, 24112.
4. a) B. J. Lee, S. G. Ryu, J. H. Cui, *Int. J. Pharm.* **1999**, *188*, 71-80; b) L. Wei, C. Cai, J. Lin, T. Chen, *Biomaterials* **2009**, *30*, 2606-2613; c) Z. Wu, X. Zou, L. Yang, S. Lin, J. Fan, B. Yang, X. Sun, Q. Wan, Y. Chen, S. Fu, *Colloids Surf., B* **2014**, *122*, 90-98.
5. A. Wichterle, D. Lim, *Nature* **1960**, *185*, 117-118.
6. a) N. Roy, N. Saha, T. Kitano, P. Saha, *Carbohydr. Polym.* **2012**, *89*, 346-353; b) A. Gregorova, N. Saha, T. Kitano, P. Saha, *Carbohydr. Polym.* **2015**, *117*, 559-568.
7. a) E. G. Popa, M. E. Gomes, R. L. Reis, *Biomacromolecules* **2011**, *12*, 3952-3961; b) Z. Wang, Y. Zhang, J. Zhang, L. Huang, J. Liu, Y. Li, G. Zhang, S. C. Kundu, L. Wang, *Sci. Rep.* **2014**, *4*, 7064.
8. a) S. Berski, J. van Bergeijk, D. Schwarzer, Y. Stark, C. Kasper, T. Scheper, C. Grothe, R. Gerardy-Schahn, A. Kirschning, G. Drager, *Biomacromolecules* **2008**, *9*, 2353-2359; b) F.

Z. Cui, W. M. Tian, S. P. Hou, Q. Y. Xu, I. S. Lee, *J. Mater. Sci. Mater. Med.* **2006**, *17*, 1393-1401; c) K. M. Galler, J. D. Hartgerink, A. C. Cavender, G. Schmalz, R. N. D'Souza, *Tissue Eng. Part A* **2012**, *18*, 176-184.

9. a) N. Gajovic, G. Beinyamin, A. Warsinke, F. W. Scheller, A. Heller, *Anal. Chem.* **2000**, *72*, 2963-2968; b) F. Kivlehan, M. Paolucci, D. Brennan, I. Ragoussis, P. Galvin, *Anal. Biochem.* **2012**, *421*, 1-8.
10. a) Y. Akagawa, T. Kubo, K. Koretake, K. Hayashi, K. Doi, A. Matsuura, K. Morita, R. Takeshita, Q. Yuan, Y. Tabata, *J. Prosthodont. Res.* **2009**, *53*, 41-47; b) A. Ma, B. Zhao, A. J. Bentley, A. Brahma, S. MacNeil, F. L. Martin, S. Rimmer, N. J. Fullwood, *J. Mater. Sci. Mater. Med.* **2011**, *22*, 663-670;
11. a) B. Gao, T. Konno, K. Ishihara, *J. Biomater. Sci. Polym. Ed.* **2015**, *26*, 1372-1385; b) C. C. Karlgard, N. S. Wong, L. W. Jones, C. Moresoli, *Int. J. Pharm.* **2003**, *257*, 141-151.
12. a) C. Gong, S. Shi, L. Wu, M. Gou, Q. Yin, Q. Guo, P. Dong, F. Zhang, F. Luo, X. Zhao, Y. Wei, Z. Qian, *Acta. Biomater.* **2009**, 5, 3358-3370; b) B. Xue, V. Kozlovskaya, F. Liu, J. Chen, J. F. Williams, J. Campos-Gomez, M. Saeed, E. Kharlampieva, *ACS Appl. Mater. Interfaces* **2015**, 7, 13633-13644.
13. a) V. S. Ghorpade, A. V. Yadav, R. J. Dias, *Int. J. Biol. Macromolec.* **2016**, *93*, 75-86; b) G. P. Mishra, R. Kinser, I. H. Wierzbicki, R. G. Alany, A. W. Alani, *Eur. J. Pharm. Biopharm. e.V* **2014**, *88*, 397-405.
14. a) M. B. Charati, I. Lee, K. C. Hribar, J. A. Burdick, *Small* **2010**, *6*, 1608-1611; b) Y. N. Zhang, R. K. Avery, Q. Vallmajo-Martin, A. Assmann, A. Vegh, A. Memic, B. D. Olsen, N. Annabi, A. Khademhosseini, *Adv. Funct. Mater.* **2015**, *25*, 4814-4826;

15. a) C. M. Dong, Y. Chen, *J. Control. Release.* **2011**, *152 Suppl 1*, e13-14; b) C. Li, A. Faulkner-Jones, A. R. Dun, J. Jin, P. Chen, Y. Xing, Z. Yang, Z. Li, W. Shu, D. Liu, R. R. Duncan, *Angew. Chem.* **2015**, *54*, 3957-3961;
16. a) P. Markland, Y. Zhang, G. L. Amidon, V. C. Yang, *J. Biomed. Mater. Res.* **1999**, *47*, 595-602; b) K. Men, W. Liu, L. Li, X. Duan, P. Wang, M. Gou, X. Wei, X. Gao, B. Wang, Y. Du, M. Huang, L. Chen, Z. Qian, Y. Wei, *Nanoscale* **2012**, *4*, 6425-6433.
17. a) K. Peng, I. Tomatsu, A. Kros, *J. Control. Release.* **2011**, *152 Suppl 1*, e72-74; b) W. Li, L. Huang, X. Ying, Y. Jian, Y. Hong, F. Hu, Y. Du, *Angew. Chem.* **2015**, *54*, 3126-3131; b) F. Ye, H. Guo, H. Zhang, X. He, *Acta Biomater.* **2010**, *6*, 2212-2218.
18. a) C. Gong, Q. Wu, Y. Wang, D. Zhang, F. Luo, X. Zhao, Y. Wei and Z. Qian, *Biomaterials*, 2013, **34**, 6377-6387; X. Hu, H. Tan, P. Chen, X. Wang and J. Pang, *Journal of nanoscience and nanotechnology*, 2016, **16**, 5480-5488; C. Lu, R. B. Yoganathan, M. Kociolek and C. Allen, *Journal of pharmaceutical sciences*, 2013, **102**, 627-637.
19. A. C. Farthing and R. J. Reynolds, *Nature*, 1950, **165**, 647.
20. G. Vandermeulen, L. Rouxhet, A. Arien, M. E. Brewster and V. Preat, *International journal of pharmaceutics*, 2006, **309**, 234-240.
21. a) T. J. Deming, *Nature* **1997**, *390*, 386-389; b) T. J. Deming, *Adv. Drug Deliv. Rev.* **2002**, *54*, 1145-1155.
22. T. Yang, W. Li, X. Duan, L. Zhu, L. Fan, Y. Qiao and H. Wu, *PloS one*, 2016, **11**, e0162607.
23. a) A. Acharya, B. Ramanujam, A. Mitra, C. P. Rao, *ACS nano* **2010**, *4*, 4061-4073; b) K. L. Copeland, J. A. Anderson, A. R. Farley, J. R. Cox, G. S. Tschumper, *J. Phys. Chem. B* **2008**, *112*, 14291-14295; c) K. Jitsukawa, A. Katoh, K. Funato, N. Ohata, Y. Funahashi,

T. Ozawa, H. Masuda, *Inorg. Chem.* **2003**, *42*, 6163-6165; d) M. Yoshikawa, H. Iwasaki, H. Shinagawa, *J. Biol. Chem.* **2001**, *276*, 10432-10436.

24. A. M. Puertas, F. J. de las Nieves, *J. Colloid Interface Sci.* **1999**, *216*, 221-229.
25. D. T. Haynie, S. Balkundi, N. Palath, K. Chakravarthula, K. Dave, *Langmuir* **2004**, *20*, 4540-4547.
26. a) B. Cheppudira, M. Fowler, L. McGhee, A. Greer, A. Mares, L. Petz, D. Devore, D. R. Loyd, J. L. Clifford, *Expert Opin. Investig. Drugs* **2013**, *22*, 1295-1303; b) K. K. Chereddy, R. Coco, P. B. Memvanga, B. Ucakar, A. des Rieux, G. Vandermeulen, V. Preat, *J. Control. Release* **2013**, *171*, 208-215; c) M. Panchatcharam, S. Miriyala, V. S. Gayathri, L. Suguna, *Mol. Cell. Biochem.* **2006**, *290*, 87-96.
27. a) K. S. Akers, M. P. Rowan, K. L. Niece, J. C. Graybill, K. Mende, K. K. Chung, C. K. Murray, *BMC Infect. Dis.* **2015**, *15*, 184; b) D. A. Sanchez, D. Schairer, C. Tuckman-Vernon, J. Chouake, A. Kutner, J. Makdisi, J. M. Friedman, J. D. Nosanchuk, A. J. Friedman, *Nanomedicine* **2014**, *10*, 269-277; c) O. Tabbene, S. Azaiez, A. Di Grazia, I. Karkouch, I. Ben Slimene, S. Elkahoui, M. N. Alfeddy, B. Casciaro, V. Luca, F. Limam, M. L. Mangoni, *J. Appl. Microbiol.* **2016**, *120*, 289-300.
28. a) F. Gaudiere, S. Morin-Grognet, L. Bidault, P. Lembre, E. Pauthe, J. P. Vannier, H. Atmani, G. Ladam, B. Labat, *Biomacromolecules* **2014**, *15*, 1602-1611; b) B. Manickam, R. Sreedharan, M. Elumalai, *Curr Drug Deliv.* **2014**, *11*, 139-145; c) A. P. Mathew, K. Oksman, D. Pierron, M. F. Harmand, *Macromol. Biosci.* **2013**, *13*, 289-298;
29. a) R. Baumeister, G. Muller, B. Hecht, W. Hillen, *Proteins* **1992**, *14*, 168-177; b) J. M. Richardson, M. M. Lopez, G. I. Makhatadze, *Proc. Natl. Acad. Sci. U.S.A.* **2005**, *102*, 1413-1418.

30. a) J. S. Chiou, T. Tatara, S. Sawamura, Y. Kaminoh, H. Kamaya, A. Shibata, I. Ueda, *Biochim. Biophys. Acta* **1992**, *1119*, 211-217; b) K. Fukushima, T. Sakamoto, J. Tsuji, K. Kondo, R. Shimozawa, *Biochim. Biophys. Acta* **1994**, *1191*, 133-140; c) J. Rao, Z. Luo, Z. Ge, H. Liu, S. Liu, *Biomacromolecules* **2007**, *8*, 3871-3878; d) J. Sun, C. Deng, X. Chen, H. Yu, H. Tian, J. Sun, X. Jing, *Biomacromolecules* **2007**, *8*, 1013-1017.
31. V. T. Huynh, G. Chen, P. d. Souza, M. H. Stenzel, *Biomacromolecules* **2011**, *12*, 1738-1751.
32. A. F. van Nostrum, *Soft Matter* **2011**, *7*, 3246-3259.
33. a) M. Koskela, F. Gaddnas, T. I. Ala-Kokko, J. J. Laurila, J. Saarnio, A. Oikarinen, V. Koivukangas, *Crit. Care* **2009**, *13*, R100; b) R. M. Rico, R. Ripamonti, A. L. Burns, R. L. Gamelli, L. A. DiPietro, *J. Surg. Res.* **2002**, *102*, 193-197.

CHAPTER 3

In-vivo testing and measurement of efficacy of composites in wound healing

3.1 Introduction

Through the last few decades, greater attention has been given towards the development of new dressing materials to help wound healing.[1] Although conventional (non-occlusive) wound dressings, that provide dry wound healing conditions, still acquire the largest section of the dressing materials, but in present days the use of occlusive dressings,[2] hydrocolloid,[3] and hydrogel dressings,[4] which offer hydrated wound healing conditions, has improved considerably. The next vital phase in the development of new dressing materials is the development of dressing materials capable of delivering active molecules/ drugs at the wound site. The easiest example of which can be growth factor/drug loaded dressings, because of the well-known fact that topical or exogenous application of active substances directly at the wound site improves healing.

Wound healing is a series of complex and well-orchestrated events occurring after an injury or physical trauma to the skin,[5] with an aim of complete restoration of the integrity of damage tissue and reinstatement of this functional barrier.[6] However in some extreme situations (i.e. traumas with large full-depth skin damages)[7], complete re-epithelialization takes longer.[8] Therefore, extensive studies are being concentrated on wound dressing systems to promote better wound healing and to reduce scar formation.[9]

But the process of healing is disturbed by dehydration of wound[10] which compromises the ideal atmosphere to help the healing process. Therefore, keeping the moisture of the wound is of prime

importance for effective and fast wound healing. In such cases hydrogels are a promising candidates, with ability to absorb wound exudates,[11] check wound dehydration, and allow inflow of oxygen. Furthermore, along with the hydrated environment that hydrogels provide. They can serve an additional purpose of delivering bioactive substances directly to the wound in a sustained behavior.

Curcumin,[12] is the principle curcuminoid and active component of *Curcuma longa*. Chemically, it is known as diferuloylmethane or 1,7-bis(4-hydroxy-3-methoxyphenyl)-1,6-heptadiene-3,5-dione, is a naturally occurring low molecular weight polyphenolic phytoconstituent. Curcumin in the form of turmeric (powder of dried rhizome of *Curcuma longa*, and has been widely and predominantly used in Asian countries especially India[13], China in the form dyeing material,[14] flavoring agent,[15] and in many forms of customary medical practices to treat a range of inflammatory and chronic ailments. Various studies on curcumin have shown to exhibit evidences in support of its numerous pharmacological benefits, such as anti-oxidant,[16] anti-inflammatory,[17] anti-bacterial,[18] anti-viral,[19] anti-tumor,[20] as well as hyperlipidemic activities. It has been described that administration of curcumin both topically and orally is effective in rapid wound healing. Yet, the therapeutic efficacy of curcumin is restricted because of its poor solubility in aqueous media, reduced oral bioavailability, and high fist pass metabolism. Another disadvantage that curcumin faces is the means of application, as it being a polyphenol can result in toxic reaction if applied in

a highly concentrated dose. Hence, a water soluble formulation with controlled release property would be preferred for clinical application of curcumin.

So, the purpose of this study was to evaluate the in vivo biocompatibility and efficacy of a new micelle-hydrogel composite system prepared (discussed in chapter 2) for wound dressing, and serving as reservoir capacities for the sustained delivery of curcumin. This new hydrogel consists of polypeptide micelles cross-linked with genipin, both of which are biocompatible and are frequently used for medical purposes. Furthermore, this chapter discusses the evaluation of the prepared composites for *in vivo* wound healing activity test in full-thickness excision wound model. Besides, biomechanical tests, biochemical analysis, and histopathological examinations were conducted to investigate the therapeutic effects of curcumin loaded micelle hydrogel composites on rat cutaneous wound models.

3.2 Materials and Methods

3.2.1 Wound creation

A standard full thickness excision wound was created for the study purpose. At day 0, mice were anaesthetized (chloroform and air) and the dorsum shaved and cleaned (saline-soaked gauze, then swabbed with 70% IMS). A single full-thickness wound (20 mm x 20 mm) created in the left dorsal flank skin of each rat to the depth of loose subcutaneous tissues and the wounds were left open. Animals were divided into four groups (6 rats per group), wounds were topically treated with a single application of blank hydrogels (without drug), Low conc. hydrogels (hydrogels loaded with low concentration of curcumin 0.5 mg), or High conc. hydrogels Cur–M–H ((hydrogels loaded with low concentration of curcumin 1.5 mg), respectively the last group was dressed in medical gauge and termed as control. On top of all wounds, a piece of Tegaderm (3M, USA) was applied to prevent the rats from removing the treatments. On experimental wounding, animals were housed in individual cages, maintained at an ambient temperature of 23°C, with 12-hour light/dark cycles. Mice were provided with food and water *ad libitum.*

For biochemical studies, histopathological examinations, and antioxidant analysis (3 rats per group), all animals were scarified under anesthesia at day 4 and day 8 after surgery, because the maximal changes occur during the first week after wounding. Wound collagen content, granulation

tissue formation, wound maturity, and SOD and catalase activity were investigated in detail according to the methods mentioned below.

3.2.2 Histopathologic examination

The removed skin specimens along with wounded area from each rat group were collected to evaluate the histopathological alterations. The collected specimens were fixed in 10% buffered formalin, processed, embedded in paraffin, and then sectioned perpendicular to the wound surface into thin sections following standard protocols. Sections were stained with hematoxylin–eosin (H&E) and DAPI (4', 6-diamidino-2-phenylindole) and Iba 1. All sections were analyzed using light microscopy (Biozero keyence bz 8000).

3.2.3 Wound healing and wound closure evaluation

Immediately following wounding; and subsequently after dressing removal and cleansing with sterile saline at days 4 and 8 (following re-anaesthetisation, as above); wounds were digitally photographed together with an identity plate and calibration bar. Scaled, digital images of each wound were used to measure wound closure, using Image J image analysis software. Wound closure measurements were calculated, by measuring the open wound area in each digital image, at each time point. Open wound areas were then expressed as a % of their original area, immediately upon wounding at day 0 by the formula give as:

$$\%\, Wound\ closure = \frac{[wound\ area\ at\ day\ 0 - wound\ area\ at\ day\ X]}{Wound\ area\ at\ day\ 0} \times 100$$

3.2.4 Evaluation of granulation

The level of granulation tissue deposition within wounds was semi-quantitatively scored from panoramic photomicrographs of H&E stained sections; taken from the center of each wound. These were scored by two experienced observers, who were unaware of the treatment group allocation, using a 5-point visual scoring scale.

3.2.5 Evaluation of cranio-caudal wound contraction or re-epithelialization

Percentage cranio-caudal contraction (a histological measure of central wound contraction, in a cranio-caudal direction) was determined using H&E stained sections through the center of wounds. Histological wound width calculations were expressed as a percentage of the original central wound width, from wound images taken at day 0.

3.2.6 Inflammation study

The extent of inflammation in the wounds was detected in each group of animals through DAPI and Iba 1 antibody staining of their tissue samples.

3.2.7 Evaluation of super oxide dismutase (SOD)

Tissue sample from rats was perfused with PBS to remove any adhering red blood cells. Homogenize tissue or lyse cells in ice cold 0.1M Tris/HCl, pH 7.4 containing 0.5 % Triton X-100, 5mM β-mercapto ethanol. The crude mixture thus obtained was centrifuged for 5 minutes at 4°C and the pellet contain the cell debris was discarded. The supernatant contains total enzyme activity from cytosolic and mitochondria. The supernatant was then tested for total SOD content through reduction of Nitro blue tetrazolium whose absorbance was measured at 560 nm.[21]

3.2.8 Estimation of catalase

The above specified supernatant as contains net enzymatic activity of the tissue system was tested for catalase as well. For catalase estimation the supernatant was mixed with H2O2 and decrease in the absorbance of H2O2 was recorded at 240 nm.[22]

3.2.9 Estimation of collagen content

The wounded tissue samples were frozen in liquid nitrogen and were freeze dried with subsequent lyophilization. The lyophilized samples were then incubated overnight in 0.5 M acetic acid and then followed by homogenization. The homogenate thus obtained was centrifuged and tested for total collagen content using Biovision total collagen assay kit (BVN K218-100).

3.2.10 Measurement of the mechanical properties of hydrogels

The mechanical properties of the gel were measured using a strain-controlled rheometer (TA Instruments Model TA AR2000ex). A parallel geometry with plate diameter of 25 mm was employed. Hydrogels for the rheological studies were prepared in the same fashion as those for previous studies.

3.3 Results and Discussions

Wound healing is distinct timeline of physical aspects (phases) consisting of the post-trauma repair process in case of an injury. In intact skin, the epidermis (upper layer) and dermis (deeper layer) form a defensive blockade against the external environment for our body. When the barrier is broken, i.e. the skin is injured a coordinated cascade of biochemical actions are brought into motion to heal the damage (figure 3.1). This includes various steps in order of:

- Hemostasis (blood clotting): In the initial moments of injury, platelets in the blood begin to accumulate at the site of injury. This causes activation of platelets, and they release chemical signals to promote clotting. This results in the activation of fibrin, through a chain of well-designed events which forms a webbing and acts as "glue" to bind platelets to each other. This makes a clot that aids to close the opening in the blood vessel, preventing further bleeding.
- Inflammation: This is an important phase in the process of wound healing. The cells damaged and dead during the injury are cleared out of the site. It also aids removal of bacteria and other infection causing pathogens. Phagocytic cells such as macrophages play a key role in this process. And simultaneously the platelets release growth factors to mature the wound into proliferative phase.
- Proliferation: This phase marks the growth of new tissue at the injury site. This phase is onset with the starting of granulation, where the new cells migrate to the site of injury and proliferate. Angiogenesis, connective tissue deposition, re-epithelialization and wound contraction are key phenomenon occurring.

- Maturation (remodeling): Complete repair is done in this phase when, the remodeling and maturation of the cells occur. Connective tissues are rearranged along tension lines, and cells that have finished serving their purpose are strategically removed by programmed cell death, or apoptosis.

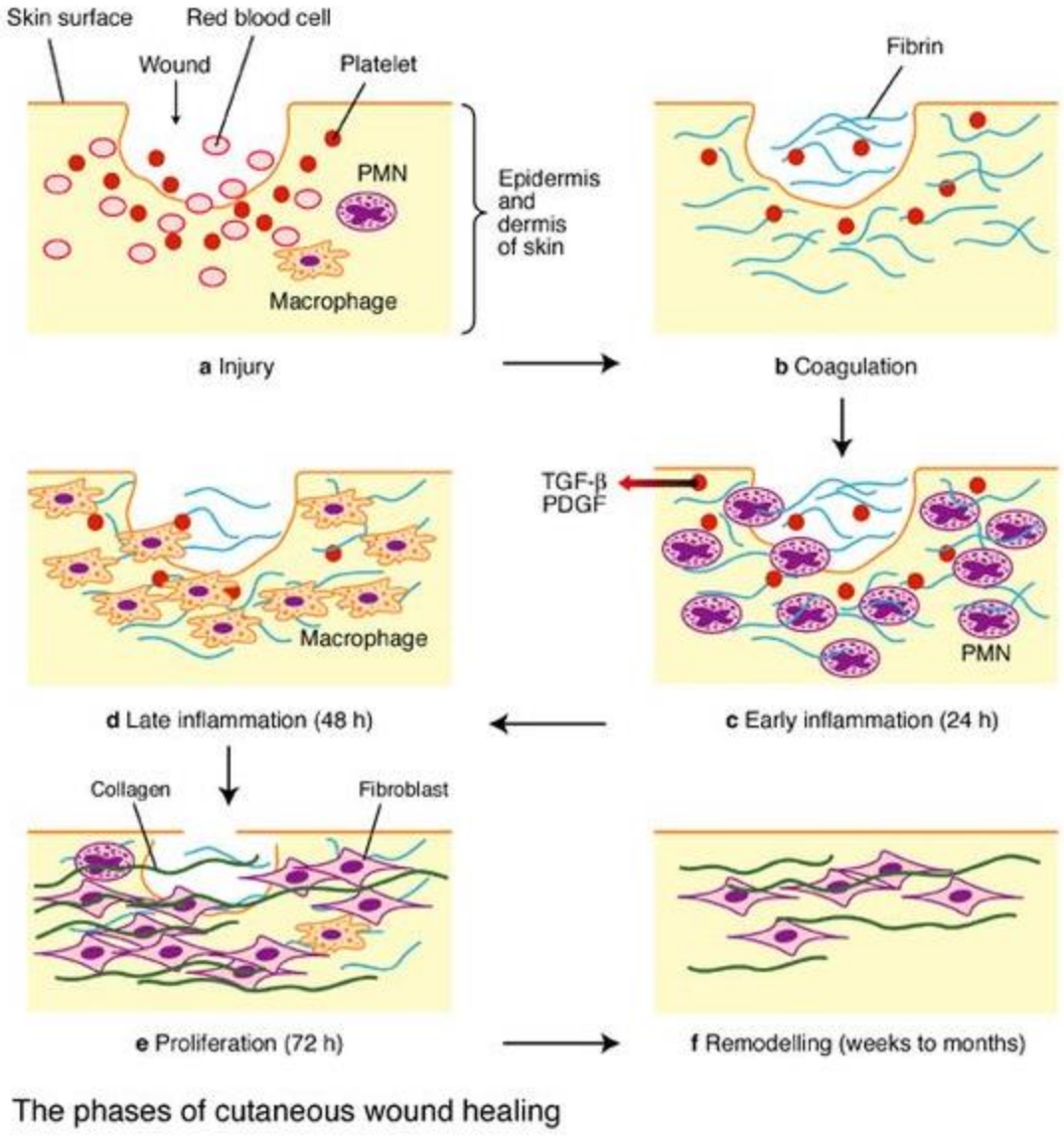

Figure 3.1 The stages of wound healing.[23]

The bio efficacy of a newly formulated micelle-hydrogel composite as a wound dressing was evaluated in vivo by subcutaneous implantation studies in rat models. For this rats were

anesthetized and shaved. A template was marked at their dorsum and incision was made to yield a 20 x 20 mm^2 full depth excision wound. These wounds were subsequently dressed with hydrogels or gauge according to the experimental need followed by tegaderm, and were evaluated for various parameters over the period of 8 days.

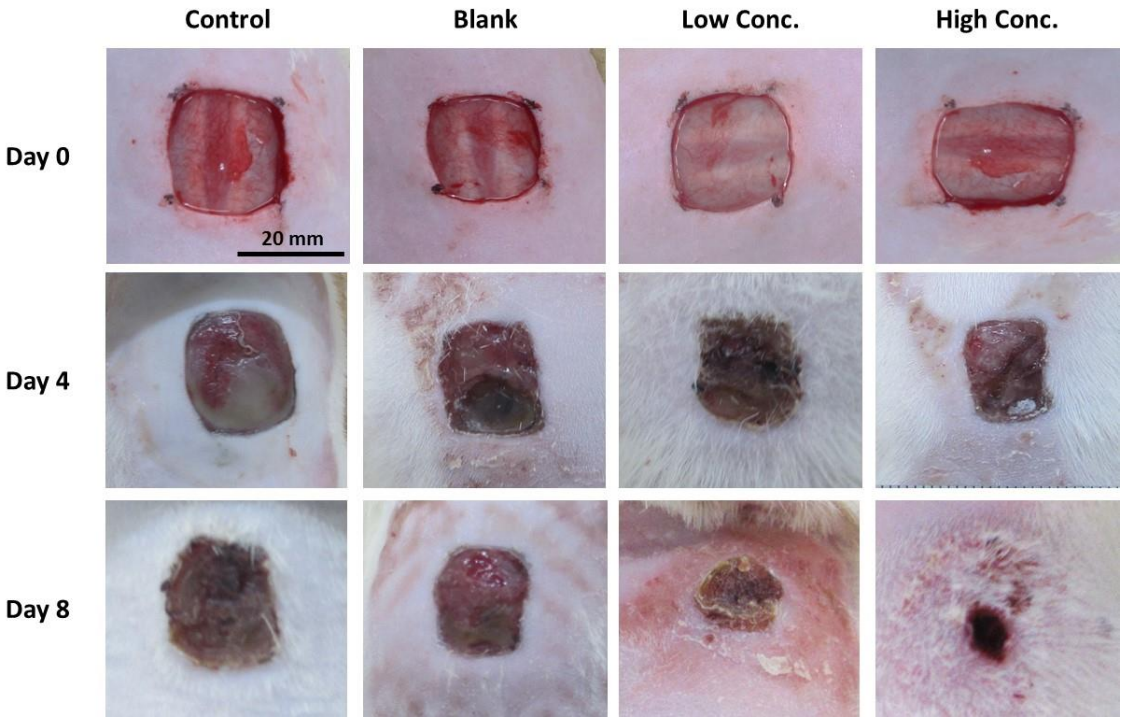

Figure 3.2 Macroscopic appearance of wound in the mice at day 0, 4 and 8 under different experimental groups.

Evaluation of wound healing progress induced in rat models, by control, blank, LC and HC groups in the excision wound model is shown in Figure 3.2. Wounds treated with LC and HC group of micelle hydrogel composites showed noticeable dryness and any indication of any pathological fluid oozing out from the wounds was missing. In addition to that, there was no visible sign of occurrence of inflammation or infection in the wounds as compared to control or blank groups. Wound closure was analyzed in each group as a percentage of the reduction in wounded area at

day 4 and day 8 (Figure 3.3 a). Animals treated with high concentration of curcumin containing micelles (53.04 ± 4.26% at day 4; 87.32 ± 3.11% at day 8) showed more substantial wound closure than gels loaded with lower concentration of curcumin (22.23 ± 3.86% at day 4, 73.39 ± 4.03% at day 8), blank (15.12 ± 2.92% at day 4, 32.67 ± 3.81 % at day 8), and control groups (7.31 ± 3.64% at day 4, 18.73 ± 6.21% at day 8). As the image shows the wound started to close in 4 days in treated groups, and an appreciable wound closure was seen in the HC in comparison to other groups. In addition the treated wound (LC and HC) decreased in size without oozing or any visible signs of infection.

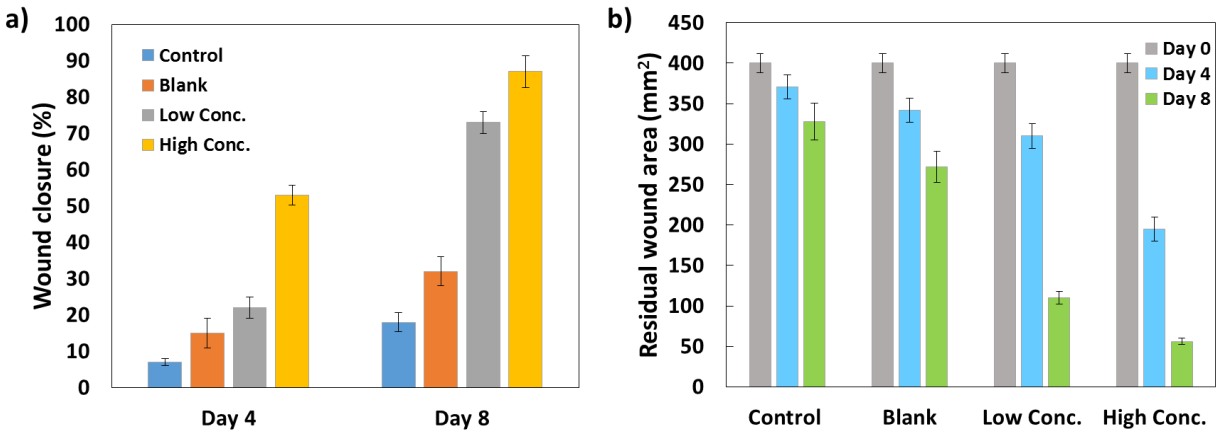

Figure 3.3 a) wound closure % of different rat groups at day 4 and 8, b) residual wound size of the treated rats in comparison to day 0.

The residual wound area was also determined in each rat group by measuring the open wound area after day 4 and 8 subsequently. Wound began to close since day 4 and residual wound sizes were seen to decrease in all rat groups by the end of day 8. A drastic reduction was seen in the residual wound area after 8 days of treatment with the HC gels (Figure 3.3 b) as they show the smallest wound size. In contrast the control group showed the largest residual wound area confirming the slow healing of wound. The decrease in surface area is an important parameter in wound healing

as to reduce the occurrence of infection and inflammation. Thus the results support the fact that the micelle hydrogel composite were able to accelerate wound healing. The other two groups blank and LC shows an intermediate response between control groups and HC. Overall, at day 4 and day 8, wound contractions in HC group were significantly higher than those in other groups.

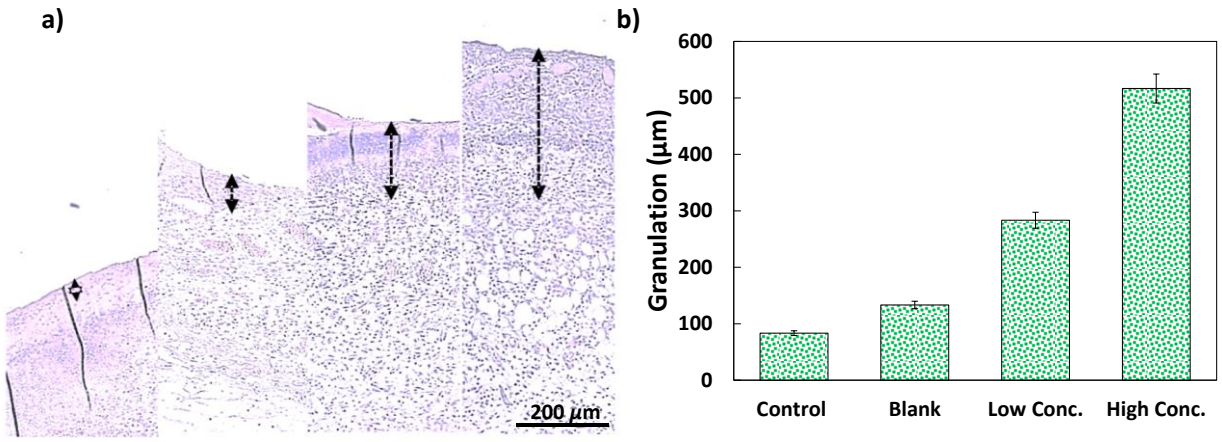

Figure 3.4 The thickness of granulation in the tested animals a) Histological observation of the newly formed granulated tissue after day 8 and b) Graph showing the granulation thickness in the samples.

Further to better evaluate the wound closure and microscopic level the effect of provided treatment on the process of granulation[24] and re-epithelialization[25] was studied. The hematoxylin and eosin stained tissue samples were studied for thickness of granulation tissue and extend of re-epithelization. As seen in (Figure 3.4) there was a significant enhancement in the granulation of the samples treated with HC at day 8. However no significant improvement is seen in the granulation of control samples which show minimum or almost no granulation. The granulation in the LC was also improved owing to the regular supply of curcumin from the implanted gels. The blank samples showed moderated granulation better than that of control samples but significantly less than the treated samples.

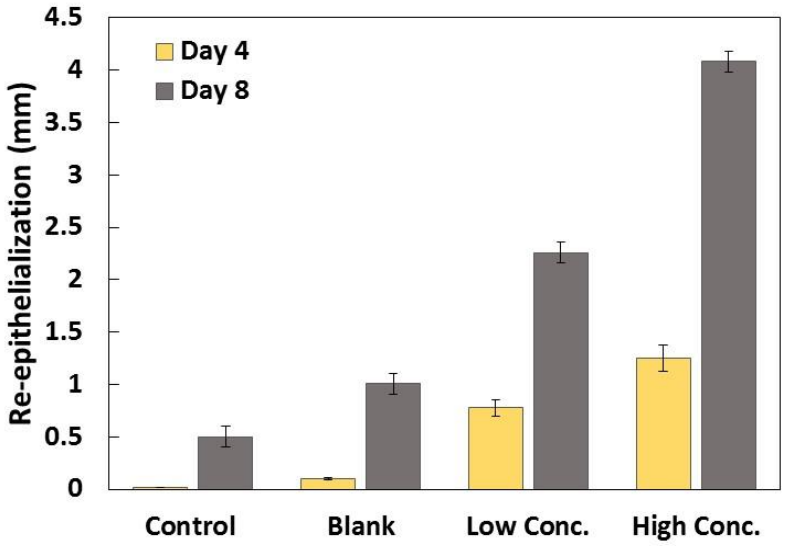

Figure 3.5 The length of re-epithelialization in the different rat groups at day 4 and day 8.

For re-epithelialization analysis, re-epithelialization was observed in all the test groups group at day 4 and day 8. As observed in figure 3.5, there was no significant epithelial regeneration in blank and control groups after day 4 of the surgery. Conversely the LC and HC groups shows an enhanced formation of epithelial lining as early as 4 days after wounding. However, the re-epithelialization was improved in all samples by day 8. These results were consistent with those of residual wound area. As seen in the figure 3.6 wound treated with HC shows a well-defined regenerated and differentiated epidermal layer in day 8 of the study, showcasing a fairly higher cell number and a relatively thick dermis than those of other samples. LC also showed an enhanced re-epithelialization but less than HC. On the other hand other samples showed an early on-going epithelial layer formation with poor granulation and traces of edema.

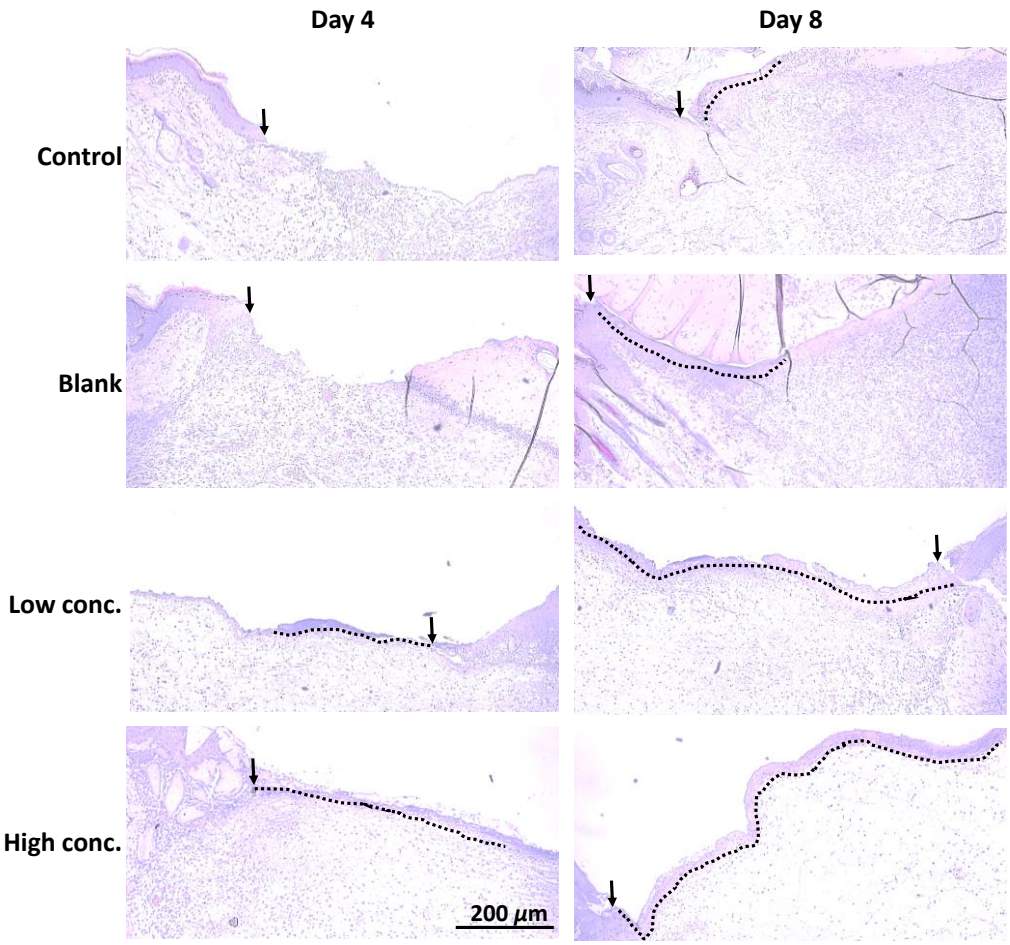

Figure 3.6 Histological observation of the regeneration of epithelial tissue in the wounds in different rat groups. The arrow indicate the point of wound edge and the dotted line gives the path of re-epithelialization.

The hematoxylin and eosin staining[26] has supported the enhanced wound healing in the rat groups treated with HC and LC. However to better understand the situation of the implanted gels we need to evaluate the inflammatory[27] response at the site of implant to access the gel's efficacy towards would healing gels. Several previous studies have discovered purposeful consequences of the innate immune response of the resident cells as well as the employed inflammatory cells (such as macrophages) during skin wound repair. They not only fight invading microbes, contribute to scavenging of dead and decaying cells, but also crucially support the repair process by releasing a

spectrum of growth factors. However, due to the release of pro-inflammatory and cytotoxic mediators, uncontrolled activity of macrophages may also be detrimental to tissue repair. Indeed, imbalanced inflammation characterized by increased numbers of macrophages is a hallmark of an attenuated repair response in human diseases encompassing diabetes mellitus,[28] vascular disease, and aging. So to evaluate this, we performed DAPI and Iba 1^{+} staining of the wounded tissue sections from different mice groups and studied the inflammatory response at day 4 and day 8 of wounding.

And as seen clearly in figure 3.7, at day 4 of the wounding the control group showed an extremely high inflammatory response. As seen in the image, the day 4 in control group showed a massive accumulation of macrophages at the wound site marked with green dot (cytosol of macrophages stained with Iba 1^{+} antibodies). The accumulation of macrophages in control group showed a decrease toward the day 8 of wounding but still had significantly high deposition of macrophages in comparison to other groups. The blank showed second highest inflammatory response at day 4 which showed a significant decline by day 8, showing that the wound has moved from inflammation phase towards proliferation phase with the onset of granulation as seen previously in figure 3.3. The other two samples (LC and HC) on the other hand showed least to no accumulation of macrophages at day 4, showing an enhanced wound healing with their proliferation phase has already started, this could also be seen by the large number of accumulated cells in LC and HC samples (blue dot) as marked by DAPI staining (which stains all nuclei in general). At day 4 a clear granulation is seen in HC samples through accumulation of non-inflammatory cells, which by day 8 turns into a well-defined regeneration of epithelia. Similarly the LC samples also, show no visible sign of enhanced inflammation at day 4 and showing a clear

onset of re-epithelialization by day 8, supporting the claims of improved wound healing in our hydrogels treated groups.

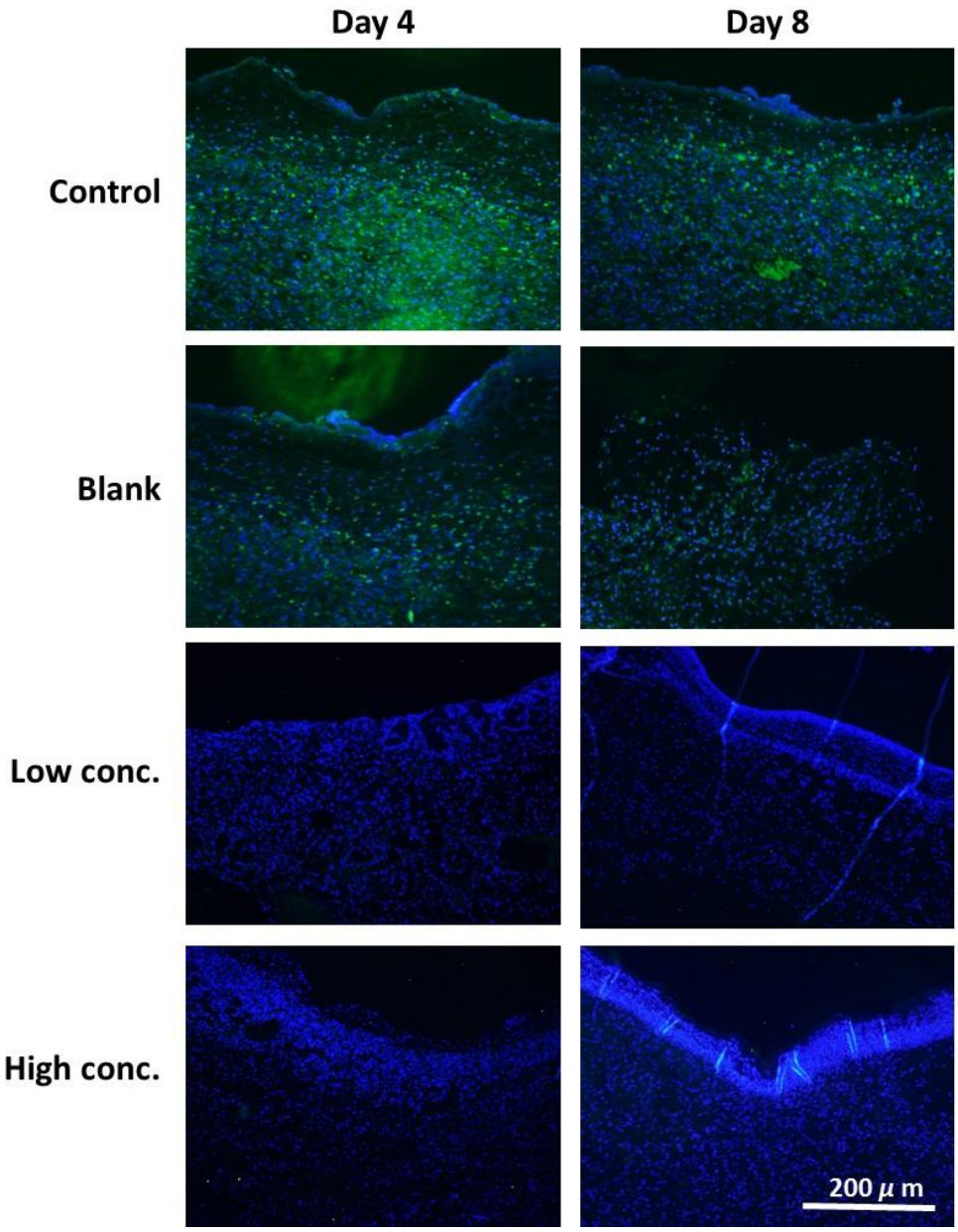

Figure 3.7 Evaluation of inflammatory response through DAPI and Iba1^{+} staining of tissue samples of different rat groups. Blue dots are nucleii of all cells stained by DAPI and green dots represent the macrophage cytosol stained by Iba1^{+} antibodies.

Also, apart from histological studies there other biochemical parameters to evaluate the efficiency of wound healing. For instance, few previous studies have clearly suggested that wounding induces

an increase of oxidative stress in the injured tissue which induces gene expression of SOD.[29] But as we are using curcumin as our model drug, and attributed to the antioxidant activity of curcumin, oxidative stress of wounds should show a decreasing trend over the period of wound healing by scavenging superoxide radical created at the site of injury. And confirming our assumption, when the SOD content of the injured tissues were estimated a clear decrease in the net SOD content of the wound was seen. This not only indicated towards the better wound healing conditions but also supports our claim of a controlled release of curcumin from our micelle-hydrogel composite, slowly over a period of time to keep the oxidative stress under check. As seen in the figure 3.8, SOD level in the HC and LC groups showed a decline in both day 4 and 8 in comparison to blank and control groups which showed an increment in the level of SOD at day 8.

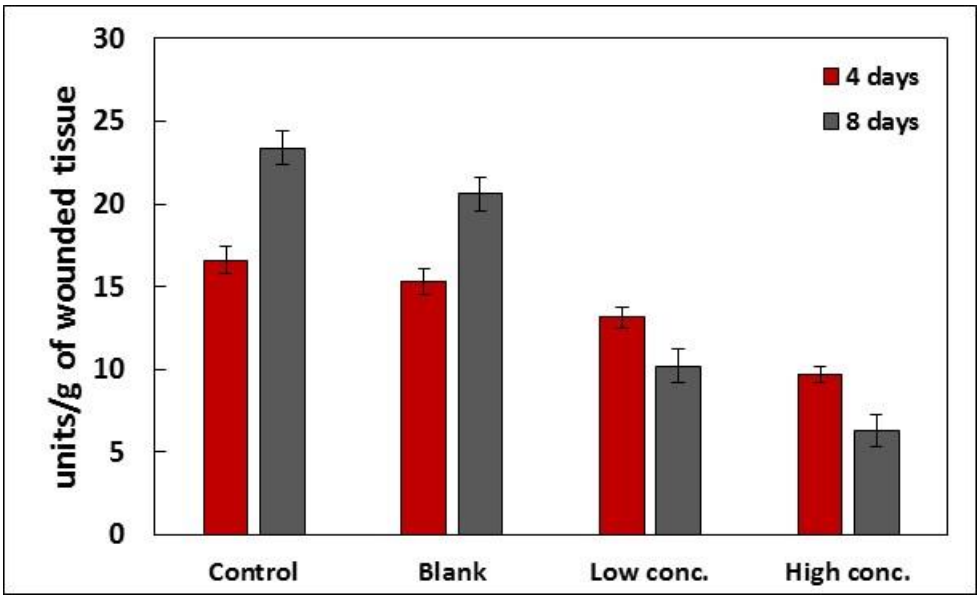

Figure 3.8 The level of Super oxide dismutase (SOD) in the wounded tissue of different rat groups after day 4 and 8 of the surgery.

But subsequently, as the expression of SOD in low the superoxide radicals in tissue are were being converted to hydrogen peroxide. This hydrogen peroxide is also toxic for cells as well as hampers the wound healing process again by causing a different kind of oxidative stress which is milder

than that caused by superoxide radicals. And this in turn stimulates the expression of peroxide scavenging enzyme catalase. Therefore it is evident that lower the SOD activity, higher will be generation of peroxide and in turn higher will be the catalase[30] activity. And as clearly evident by the results seen in figure 3.9.

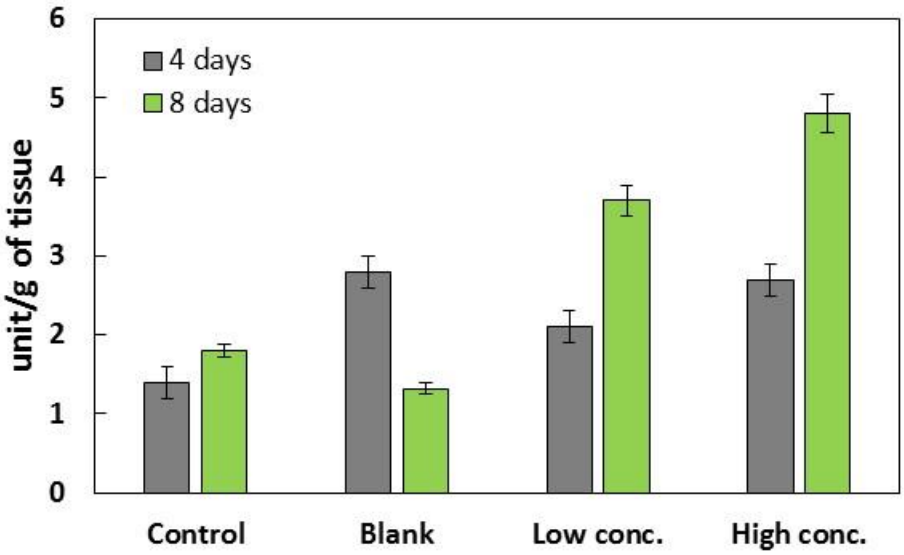

Figure 3.9 The level of catalase in the wounded tissue of different rat groups after day 4 and 8 of the surgery.

Thus, as seen above in LC and HC groups, SOD contents were low, and therein the content of catalase were high in both models. SOD level was radically low in HC treated group than that in blank or control groups. However the catalase was slightly higher in HC than that of LC, but still showed significant gap with blank and control groups. . It is clear, that with low SOD and high catalase content in the granulation tissues of group HC shows the highest wound healing efficacy in comparison to other groups.

As it seen above, histopathologic results of the wounds that were treated under HC, LC blank and control groups on day 4 and day 8 of surgery show them in different stages of wound healing. And

as discussed earlier proliferative and maturation phases are the ones marking the better healing of wound and comprise of phenomenon like angiogenesis and connective tissue (collagen) deposition. So to strengthen our hypothesis towards the fact that our drug loaded micelle-hydrogel composites aid the process of wound healing, we estimated the net collagen content of the wounded tissues. Figure 3.10 depicts the net collagen content of the wounded tissues at 4 and 8 days of surgery.

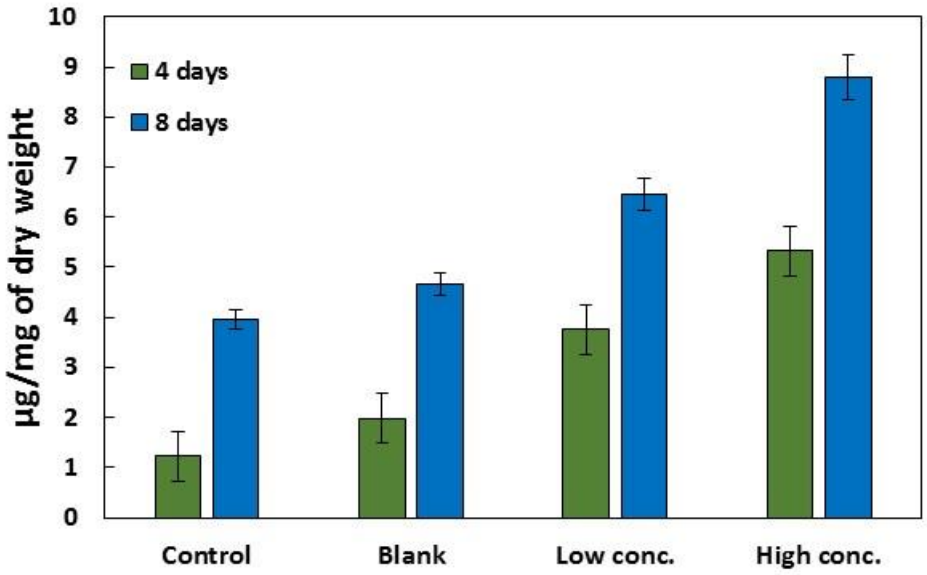

Figure 3.10 The total amount of collagen in the wounded tissue of different rat groups after day 4 and 8 of the surgery.

As seen in the image, the results of total collagen[31] content clearly acknowledges the previous results. The HC showed highest amount of collagen content among all the samples at day 4 as well as at day 8 strongly indicating an enhanced wound healing in comparison to other samples. This is in the agreement of the high granulation, re-epithelialization and lower inflammation stating that sample treated with HC has attained the late proliferative phase where the increased accumulation of the collagen fibers in the extra-cellular matrix region is occurring. In contrast, to other groups

LC has also showed a better total collagen content than blank and control showing a better wound healing.

Further, a crucial parameter in wound healing process, is angiogenesis. As the pre-existing vascular network around the created wound is not sufficient to provide ample nutrients and oxygen to inflammatory injuries, ischemia caused due to vessel damage at the wound site.[32] Therefore, the maintenance of cell viability in the wound and continuation of faster healing essentially requires the formation of new vasculature i.e angiogenesis.[33] And as angiogenesis is the synthesis of new blood vessels which arises from dividing differentiated endothelial cells of the local vascular system, mononuclear cells, and bone marrow-derived circulating endothelial cells.[34] Although, it is still debatable that whether or not the circulating cells can give escalate the formation of the luminal endothelium layer. But on the other hand, many of the trials have demonstrated that circulating CD31+ endothelial cells can form new blood vessels.

On this basis we studied the circulating CD31+ cells at the wound site to see the development of new blood vessels. Detailed immunohistochemical staining with CD31+ cells allowed us to determine whether the formation of blood vessel is enhanced in the treated rats or not.

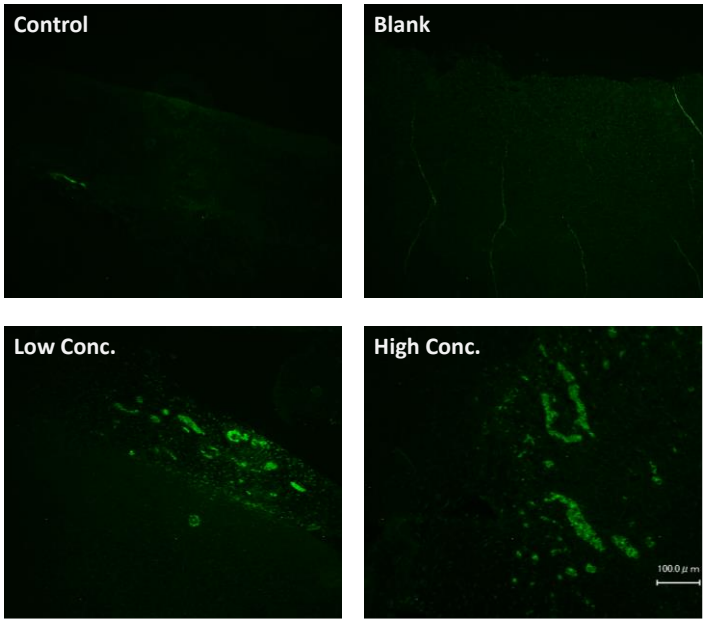

Figure 3.11 Evaluation of angiogenesis through CD31+ cells in the treated rat groups at 8 day.

As seen in the figure 3.11 above the low concentration and high concentration groups showed high degree of CD31+ cells in comparison to the blank and control groups. This clearly shows that our treated groups show angiogenesis around the wounded area which actually approves our hypothesis of better wound healing in treated groups. Although few more studies are required to confirm the angiogenesis as the circulation macrophages also show CD31 positivity. The above results clearly agree with our assumptions of our micelle hydrogel composite aiding to a better wound healing in case of trauma or excision of skin patches.

But an obvious question arises after the above studies that if only one drug in the micelle-hydrogel composite can provide such an enhanced healing why to add two micelles or drug in the composite. This is because the present wounding was done in the controlled condition, which is not always the case naturally, and a second drug is mostly required (which can be a broad spectrum antibiotic or could be a growth factor) to accelerate healing. Moreover, other than this the second micelle in

the composite is required to maintain the structural integrity of the composite via an electrostatic interaction among the micelles. As seen in figure 3.12, the composite synthesized without the PGA-PPA micelles showed a very low storage modulus (G') in range of 10^3 and loss modulus (G'') from order of 10^2 in comparison to the composites with both the micelles were the storage and loss modulus were in the range of 10^5 and 10^4 respectively, which suggests the role of electrostatic interaction between both the micelles in the overall integrity and firmness of the hydrogels.

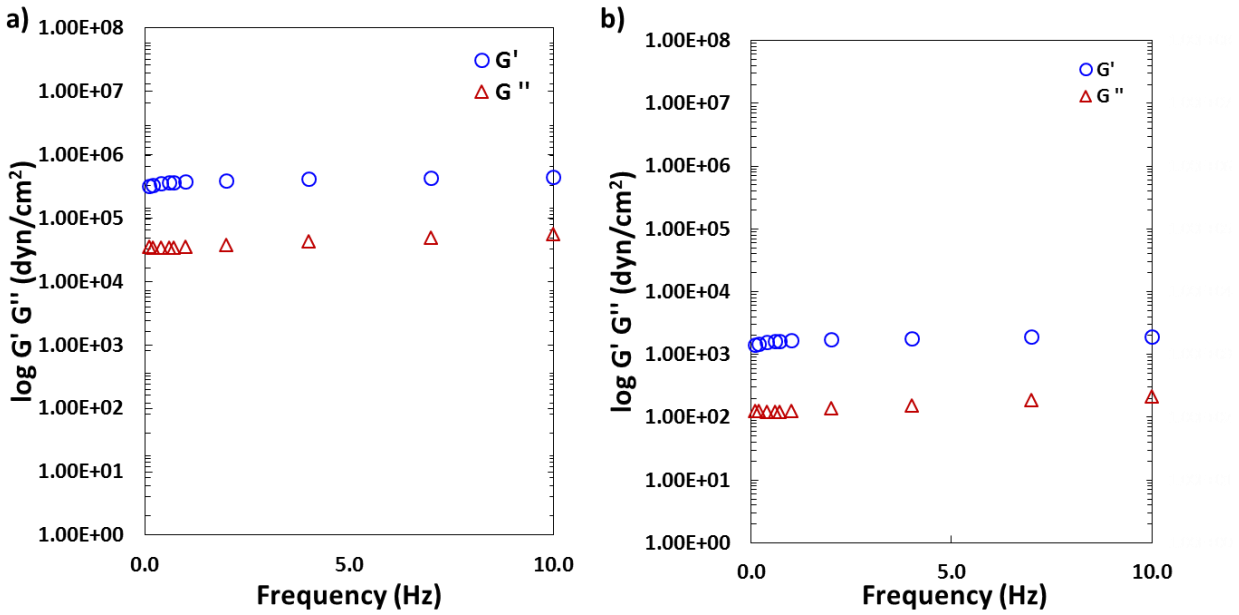

Figure 3.12 Storage and loss modulus of the micelle hydrogel composites a) with PGA-PPA and b) without PGA-PPA at 37°C.

Furthermore, as we know that the hydrophobic core of the micelles in the composite acts as the reservoir of the drugs. It is also hypothesized that the (hydrophobic) drug is associated with some kind of hydrophobic interaction along with the core chains of the micelle. And if, it is so then the overall mechanical strength of the composite should also change along with the drug release as the

core is being loosened with the diffusion of the drug out of it. To evaluate this, a time dependent rheological test was performed on the micelle hydrogel composites. And as seen in the figure 3.13, both storage and loss modulus of the hydrogel gradually decreased with time. This once again support our claim of controlled drug release.

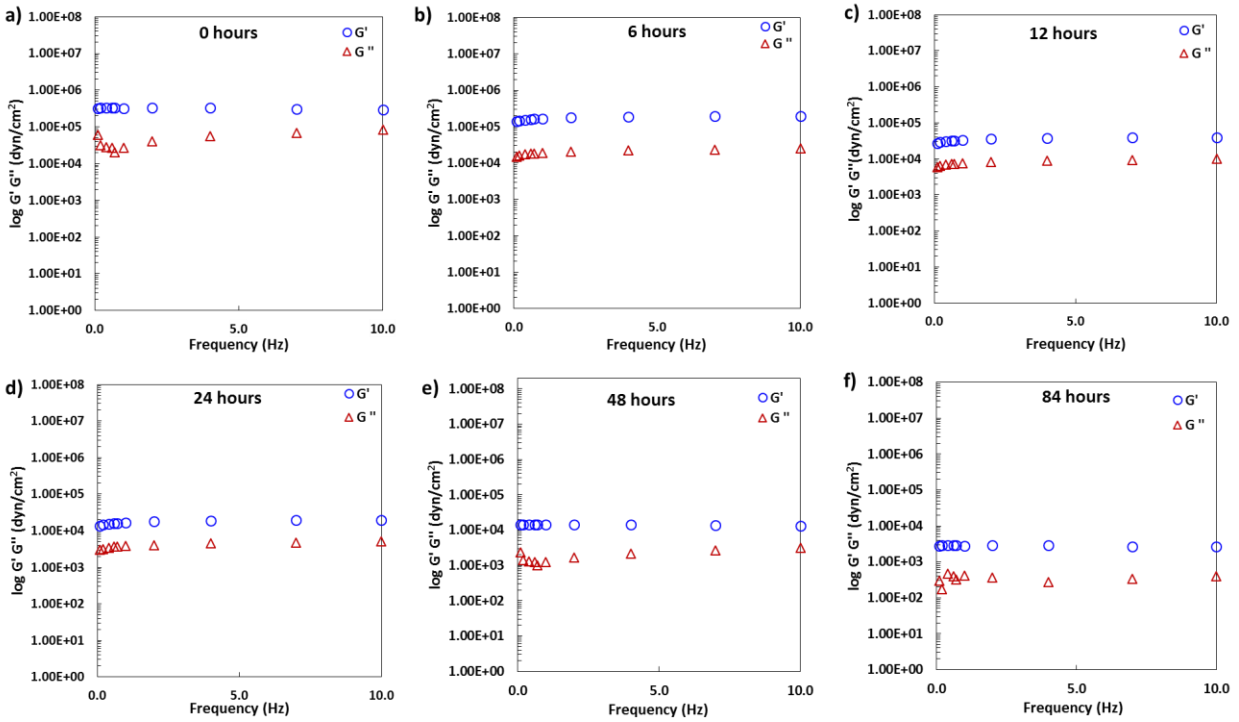

Figure 3.13 Storage and loss modulus of the micelle hydrogel composites at different time intervals after drug release at 37°C.

The above figure clearly shows a decreasing trend in the mechanical modulus of the composites at different time after the drug release. Although not directly related but the gradual decrease in modulus could be an indication of the slow and gradual drug release, which in our case was important as sudden or burst release of curcumin can cause several adverse effects also. As seen in previous researches, a burst or high dose release of curcumin at wound site can cause DNA damage or chromosomal alterations (in rare cases) and can delay wound healing.[35] The mechanical

studies also proved that our micelle-hydrogel system was within the limits of storage modulus of the gel systems used for wound healing and were an ideal candidate for the same.

3.4 Conclusion

In summary, in the light of the experiments conducted and discussed in this chapter, it can be said that these novel micelle-hydrogel composites can serve as an effective would healing materials for enhanced skin repair and regeneration along with controlled release of encapsulated drugs.

These materials showed a positive influence on each stage of wound repair and healing with showing enhanced wound contraction, granulation and re-epithelialization along with a minimal inflammatory response. This also deem these materials extremely biocompatible and non-toxic for animal use.

Although the exact mechanistic effect of these materials on wound healing is still not known but even without any encapsulated drug the blank groups also showed better healing than the control group. Thus further this kind of systems can be optimized better for becoming an enhanced wound healing as well as dressing materials for clinical use.

3.5 Reference

1. a) E. Gelinsky, Bruns' Beitrage zur klinischen Chirurgie **1957**, 194, 51-73; b) V. Patrulea, V. Ostafe, G. Borchard, O. Jordan, European journal of pharmaceutics and biopharmaceutics : official journal of Arbeitsgemeinschaft fur Pharmazeutische Verfahrenstechnik e.V **2015**, 97, 417-426; c) S. E. Wharram, X. Zhang, D. L. Kaplan, S. P. McCarthy, Macromolecular bioscience **2010**, 10, 246-257.
2. a) R. Saraceno, A. Chiricozzi, S. P. Nistico, S. Tiberti, S. Chimenti, *The Journal of dermatological treatment* **2010**, *21*, 363-366; b) N. Yamamoto, T. Kiyosawa, *International wound journal* **2014**, *11*, 616-621; c) R. M. Zadeh Farahani, A. Shahidi, *Journal of tissue viability* **2009**, *18*, 57-58.
3. a) M. I. Khan, J. M. Islam, W. Kabir, A. Rahman, M. Mizan, M. F. Rahman, J. Amin, M. A. Khan, *Materials science & engineering. C, Materials for biological applications* **2016**, *69*, 609-615; b) S. Yanagibayashi, S. Kishimoto, M. Ishihara, K. Murakami, H. Aoki, M. Takikawa, M. Fujita, M. Sekido, T. Kiyosawa, *Bio-medical materials and engineering* **2012**, *22*, 301-310.
4. a) R. Rakhshaei, H. Namazi, Materials science & engineering. C, Materials for biological applications **2017**, 73, 456-464; b) M. Rezvanian, N. Ahmad, M. C. Mohd Amin, S. F. Ng, International journal of biological macromolecules **2017**, 97, 131-140; c) N. Wathoni, K. Motoyama, T. Higashi, M. Okajima, T. Kaneko, H. Arima, International journal of biological macromolecules **2016**, 89, 465-470.
5. a) M. P. Brooks, Journal of the Mississippi State Medical Association **1973**, 14, 385-390; b) K. R. Kirker, G. A. James, APMIS : acta pathologica, microbiologica, et immunologica Scandinavica **2017**, 125, 344-352; c) S. Tejada, A. Manayi, M. Daglia, S.

F. Nabavi, A. Sureda, Z. Hajheydari, O. Gortzi, H. Pazoki-Toroudi, S. M. Nabavi, Current pharmaceutical biotechnology **2016**, 17, 1002-1007.

6. a) B. S. Atiyeh, M. Costagliola, S. N. Hayek, S. A. Dibo, *Burns : journal of the International Society for Burn Injuries* **2007**, *33*, 139-148; b) H. Babavalian, A. M. Latifi, M. A. Shokrgozar, S. Bonakdar, S. Mohammadi, M. Moosazadeh Moghaddam, *Jundishapur journal of microbiology* **2015**, *8*, e28320; c) J. Betts, *Evidence-based nursing* **2003**, *6*, 81.
7. a) M. J. Hudson-Peacock, C. M. Lawrence, *Journal of the American Academy of Dermatology* **1995**, *32*, 627-630; b) G. C. Jagetia, G. K. Rajanikant, *The Journal of surgical research* **2004**, *120*, 127-138; c) G. C. Jagetia, G. K. Rajanikant, *International wound journal* **2012**, *9*, 76-92.
8. A. F. Laplante, L. Germain, F. A. Auger, V. Moulin, FASEB journal : official publication of the Federation of American Societies for Experimental Biology **2001**, 15, 2377-2389.
9. a) D. L. Hunt, *ACP journal club* **2003**, *139*, 16; b) K. H. Kwan, X. Liu, M. K. To, K. W. Yeung, C. M. Ho, K. K. Wong, *Nanomedicine* **2011**, *7*, 497-504; c) A. Mittal, R. Kumar, D. Parsad, N. Kumar, *Journal of tissue engineering and regenerative medicine* **2014**, *8*, 351-363; d) G. Stern, *Pflege Zeitschrift* **2007**, *60*, 201-202.
10. a) M. Boury-Jamot, J. Daraspe, F. Bonte, E. Perrier, S. Schnebert, M. Dumas, J. M. Verbavatz, *Handbook of experimental pharmacology* **2009**, 205-217; b) M. E. Posthauer, *Advances in skin & wound care* **2006**, *19*, 74-76; c) M. G. Rippon, K. Ousey, K. F. Cutting, *Journal of wound care* **2016**, *25*, 68, 70-65.
11. a) M. Ishihara, K. Ono, M. Sato, K. Nakanishi, Y. Saito, H. Yura, T. Matsui, H. Hattori, M. Fujita, M. Kikuchi, A. Kurita, *Wound repair and regeneration : official publication*

of the Wound Healing Society [and] the European Tissue Repair Society **2001**, *9*, 513-521; b) K. Lay-Flurrie, *Professional nurse* **2004**, *19*, 269-273; c) Y. Luo, H. Diao, S. Xia, L. Dong, J. Chen, J. Zhang, *Journal of biomedical materials research. Part A* **2010**, *94*, 193-204.

12. a) A. N. Begum, M. R. Jones, G. P. Lim, T. Morihara, P. Kim, D. D. Heath, C. L. Rock, M. A. Pruitt, F. Yang, B. Hudspeth, S. Hu, K. F. Faull, B. Teter, G. M. Cole, S. A. Frautschy, *The Journal of pharmacology and experimental therapeutics* **2008**, *326*, 196-208; b) F. Payton, P. Sandusky, W. L. Alworth, *Journal of natural products* **2007**, *70*, 143-146; c) U. Singh, A. Barik, B. G. Singh, K. I. Priyadarsini, *Free radical research* **2011**, *45*, 317-325; d) X. H. Zheng, Y. X. Shao, Z. Li, M. Liu, X. Bu, H. B. Luo, X. Hu, *Journal of separation science* **2012**, *35*, 505-512.
13. a) R. De, P. Kundu, S. Swarnakar, T. Ramamurthy, A. Chowdhury, G. B. Nair, A. K. Mukhopadhyay, *Antimicrobial agents and chemotherapy* **2009**, *53*, 1592-1597; b) M. Roy, D. Sinha, S. Mukherjee, J. Biswas, *European journal of cancer prevention : the official journal of the European Cancer Prevention Organisation* **2011**, *20*, 123-131.
14. M. M. Hashem, A. H. Atta, M. S. Arbid, S. A. Nada, G. F. Asaad, Food and chemical toxicology : an international journal published for the British Industrial Biological Research Association **2010**, 48, 1581-1586.
15. A. Ukil, S. Maity, S. Karmakar, N. Datta, J. R. Vedasiromoni, P. K. Das, *British journal of pharmacology* **2003**, *139*, 209-218.
16. a) A. K. Choudhury, S. Raja, S. Mahapatra, K. Nagabhushanam, M. Majeed, *Antioxidants* **2015**, *4*, 750-767; b) W. M. Weber, L. A. Hunsaker, S. F. Abcouwer, L. M. Deck, D. L. Vander Jagt, *Bioorganic & medicinal chemistry* **2005**, *13*, 3811-3820; c) Y.

X. Xu, K. R. Pindolia, N. Janakiraman, C. J. Noth, R. A. Chapman, S. C. Gautam, *Experimental hematology* **1997**, *25*, 413-422.

17. a) N. Chainani-Wu, *Journal of alternative and complementary medicine* **2003**, *9*, 161-168; b) V. P. Menon, A. R. Sudheer, *Advances in experimental medicine and biology* **2007**, *595*, 105-125; c) S. Wessler, P. Muenzner, T. F. Meyer, M. Naumann, *Biological chemistry* **2005**, *386*, 481-490.
18. a) G. Liang, S. Yang, L. Jiang, Y. Zhao, L. Shao, J. Xiao, F. Ye, Y. Li, X. Li, *Chemical & pharmaceutical bulletin* **2008**, *56*, 162-167; b) M. Xie, D. Fan, Z. Zhao, Z. Li, G. Li, Y. Chen, X. He, A. Chen, J. Li, X. Lin, M. Zhi, Y. Li, P. Lan, *International journal of pharmaceutics* **2015**, *496*, 732-740.
19. a) G. Chauhan, G. Rath, A. K. Goyal, *Artificial cells, nanomedicine, and biotechnology* **2013**, *41*, 276-281; b) S. Umar, M. A. Shah, M. T. Munir, M. Yaqoob, M. Fiaz, S. Anjum, K. Kaboudi, M. Bouzouaia, M. Younus, Q. Nisa, M. Iqbal, W. Umar, *Poultry science* **2016**, *95*, 1513-1520.
20. a) P. Lu, Q. Tong, F. Jiang, L. Zheng, F. Chen, F. Zeng, J. Dong, Y. Du, Journal of Huazhong University of Science and Technology. Medical sciences **2005**, 25, 668-670, 678; b) W. Zhang, T. Cui, L. Liu, Q. Wu, L. Sun, L. Li, N. Wang, C. Gong, Journal of biomedical nanotechnology **2015**, 11, 1173-1182.
21. a) R. Freeman, B. King, Journal of clinical pathology **1972**, 25, 912-914; b) R. Marion, Canadian journal of medical technology **1973**, 35, 30-31.
22. H. D. Landahl, Proceedings of the Society for Experimental Biology and Medicine. Society for Experimental Biology and Medicine **1953**, 84, 74-79.
23. C. Stein, S. Kuchler, *Trends in pharmacological sciences* **2013**, *34*, 303-312.

24. a) M. Kiernan, *Community nurse* **1999**, *5*, 47-48; b) H. M. Mori, H. Kawanami, H. Kawahata, M. Aoki, *BMC complementary and alternative medicine* **2016**, *16*, 144.

25. a) V. Moulin, F. A. Auger, D. Garrel, L. Germain, *Burns : journal of the International Society for Burn Injuries* **2000**, *26*, 3-12; b) Raja, K. Sivamani, M. S. Garcia, R. R. Isseroff, *Frontiers in bioscience : a journal and virtual library* **2007**, *12*, 2849-2868.

26. D. F. King, L. A. King, The American Journal of dermatopathology **1986**, 8, 168.

27. a) J. L. Oschman, G. Chevalier, R. Brown, *Journal of inflammation research* **2015**, *8*, 83-96; b) M. Resan, M. Vukosavljevic, D. Vojvodic, B. Pajic-Eggspuehler, B. Pajic, *Clinical ophthalmology* **2016**, *10*, 993-1000; c) W. Suh, K. L. Kim, J. M. Kim, I. S. Shin, Y. S. Lee, J. Y. Lee, H. S. Jang, J. S. Lee, J. Byun, J. H. Choi, E. S. Jeon, D. K. Kim, *Stem cells* **2005**, *23*, 1571-1578.

28. a) X. Y. Gu, S. E. Shen, C. F. Huang, Y. N. Liu, Y. C. Chen, L. Luo, Y. Zeng, A. P. Wang, *Diabetes research and clinical practice* **2013**, *102*, 53-59; b) S. Okizaki, Y. Ito, K. Hosono, K. Oba, H. Ohkubo, K. Kojo, N. Nishizawa, M. Shibuya, M. Shichiri, M. Majima, *The American journal of pathology* **2016**, *186*, 1481-1498.

29. Y. Wang, X. Fu, N. Ma, Zhonghua zheng xing shao shang wai ke za zhi = Zhonghua zheng xing shao shang waikf [i.e. waike] zazhi = Chinese journal of plastic surgery and burns **1996**, 12, 45-47.

30. a) S. R. Doctrow, A. Lopez, A. M. Schock, N. E. Duncan, M. M. Jourdan, E. B. Olasz, J. E. Moulder, B. L. Fish, M. Mader, J. Lazar, Z. Lazarova, *The Journal of investigative dermatology* **2013**, *133*, 1088-1096; b) R. Monteil, G. Biron, *Therapie* **1971**, *26*, 535-544.

31. a) D. M. Douglas, J. C. Forester, R. R. Ogilvie, *The British journal of surgery* **1969**, *56*, 219-222; b) I. Grabska-Liberek, R. Galus, W. Owczarek, K. Wlodarsk, S. Zabielski, J. Malejczyk, D. Sladowski, *Polski merkuriusz lekarski : organ Polskiego Towarzystwa Lekarskiego* **2013**, *35*, 51-54; c) C. S. Kamma-Lorger, C. Boote, S. Hayes, J. Albon, M. E. Boulton, K. M. Meek, *Experimental eye research* **2009**, *88*, 953-959; d) E. Mussini, J. J. Hutton, Jr., S. Udenfriend, *Science* **1967**, *157*, 927-929.

32. a) F. Arnold, D. C. West, *Pharmacology & therapeutics* **1991**, *52*, 407-422; b) S. Yoshida, H. Yoshimoto, A. Hirano, S. Akita, *Plastic and reconstructive surgery* **2016**, *137*, 1486-1497.

33. M. Grunewald, I. Avraham, Y. Dor, E. Bachar-Lustig, A. Itin, S. Jung, S. Chimenti, L. Landsman, R. Abramovitch, E. Keshet, *Cell* **2006**, *124*, 175-189.

34. C. Urbich, S. Dimmeler, *Circulation research* **2004**, *95*, 343-353.

35. a) H. F. Lu, J. S. Yang, K. C. Lai, S. C. Hsu, S. C. Hsueh, Y. L. Chen, J. H. Chiang, C. C. Lu, C. Lo, M. D. Yang, J. G. Chung, *Neurochemical research* **2009**, *34*, 1491-1497; b) H. S. Shang, C. H. Chang, Y. R. Chou, M. Y. Yeh, M. K. Au, H. F. Lu, Y. L. Chu, H. M. Chou, H. C. Chou, Y. L. Shih, J. G. Chung, *Oncology reports* **2016**, *36*, 2207-2215; c) P. Urbina-Cano, L. Bobadilla-Morales, M. A. Ramirez-Herrera, J. R. Corona-Rivera, M. L. Mendoza-Magana, R. Troyo-Sanroman, A. Corona-Rivera, *Journal of applied genetics* **2006**, *47*, 377-382.

CHAPTER 4

Polypeptide Based Microspheres Gels for Cell Encapsulation and Delivery

4.1 Introduction

In recent time trend of encapsulation of drugs,[1] enzymes,[2] and cells[3] within polymeric microspheres[4] has intrigued the field of biomedical and biotechnology due to its vast application possibilities. Although delivery of drug and enzymes is been extensively exploited but still the delivery of cells or the active ingredients from the cells remains a challenge[5]. As scientist in different groups are trying to elucidate and work on this problem, electrospray[6] along with biocompatible polymers has risen as an answer to it. Also, it has provoked interests in clinical uses such as treatment of diabetes islet cells, for releasing insulin from within the encapsulated framework. And encapsulation here can effectively overcome the problems associated with immune system by proving immunoisolation[7] to the trapped cells which would allow transplantation minus the prerequisite for immunosuppression[8] (which is a problem in itself). As this technology develops, many different kinds of polymers[9] have been used for cell encapsulation, and among all those hydrogels are classically the prime material of choice. Due to the fact that they are perfectly suited to biomedical applications, and chiefly for cell encapsulation,[10] due to their close resemblance to the extracellular matrix in structure and high water content resulting in good mass transport properties.[11] Many natural and synthetic polymers such as alginate, poly (ethylene glycol) (PEG)[12] and poly (vinyl alcohol) (PVA)[13] have been used in similar application. And these polymers effectively provide many advantages including high mechanical14 and chemical steadiness,[15] low nonspecific interactions,[16] reproducibility (minimal batch to batch variation), ease of modification,[17] and tunability. But despite of all the benefits these polymers experience some limiting factors when comes to encapsulation of cells, which being need of harsh environments for gelling such as temperatures above physiological optima, non-standard pH or use of organic solvents (being non compatible and detrimental with the enzymes, protein and

cells).[18] So there is a need to develop synthetic encapsulation systems which can provide all the above mentioned benefits along with overcoming the drawbacks.

And as we have seen, in our previous chapters that our polypeptide system was compatible with cells and so here, we concentrate on protein hydrogel formation through covalent cross-linking for cell encapsulation as a model system for clinical use using immersed electrospray technology. Synthetic peptide-based materials, contains amino acids as the basic building blocks of the whole hydrogel system provide additional benefit of site targeting and pH responsiveness inside the body with ionizable side groups, also, they are easy to crosslink and highly biocompatible. Covalent cross-linking of these materials offer precise control over the density and other mechanical properties of the prepared hydrogels matching the stiffness of the cell type or tissue type to be encapsulated.[19]

Till date, a variety of chemical chemistries have been utilized for crosslinking the peptides and/or proteins to form hydrogels such as glutaraldehyde,[20] NHS,[21] genipin[22] etc. In case of amine based crosslinkers N-hydroxysuccinimide (NHS) esters and their water-soluble analogs, sulfo-NHS esters, are most commonly used homofunctional cross-linkers[23] that demonstrate good reactivity at physiological pH along with fast gelation time but they suffer a major drawback of being highly vulnerable to hydrolysis and thus degradation during the cross-linking reaction, which give rises to poor conjugation efficiency and lower controllability.[24] While numerous chemical cross-linkers are commercially obtainable, only a smaller group is cytocompatible; therefore, limiting the flexibility of using such synthetic hydrogel design for cell encapsulation applications.

So to answer this in this study we used, THPC[25] as a tetrafunctional cross-linker for polypeptide-based biomaterials. It reacts with primary and secondary amines through a Mannich-type reaction. (Scheme 4.1)

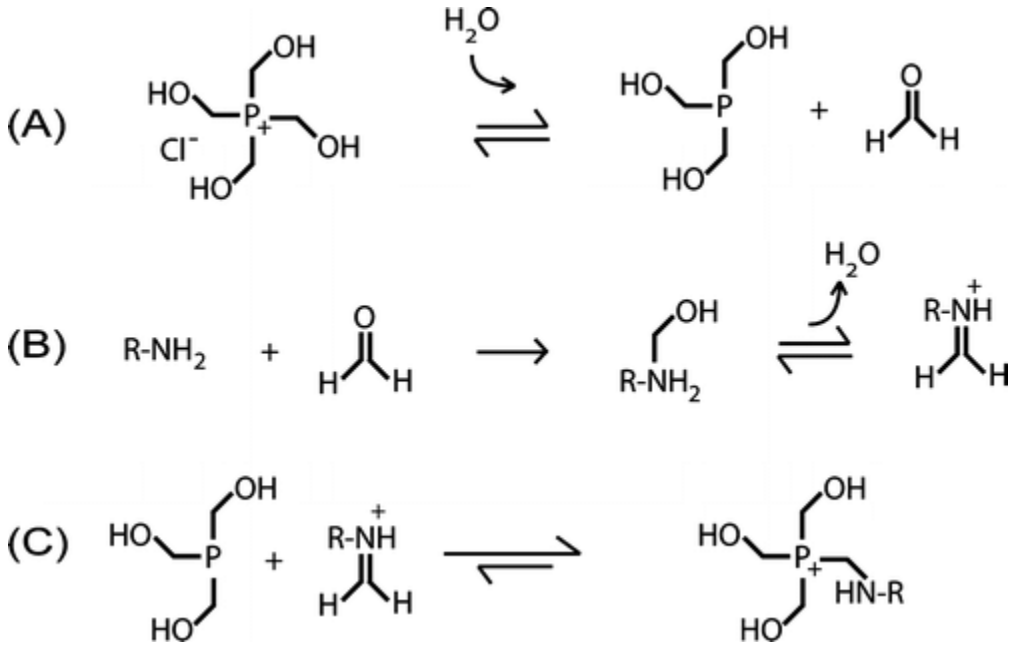

Scheme 4.1 The suggested mechanism of THPC[26]

After solving the issue of a compatible cross linker and polymer the remaining most important criteria for encapsulation was choice of suitable tool for creation of microspheres. So for the fabrication of cell encapsulating microspheres we tried a droplet generating system which would generate cell trapped droplets which could be gelled. Various methods have been used for droplet generation till date such as air jet, [27] jet-cutter,2[8] vibration jet break up,[29] and electrostatic methods,[30] as well as emulsion methods. Amongst these, emulsion type was found most suitable for droplet gelation over time. Recently, Olabisi et al. demonstrated such a photoinduced gelation in emulsion droplets using vortex mixing. However this method enforces a high amount of shear stresses on cells and ends in irregular distribution of cells and a large size variance in the droplets[31]

and these difficulties have consequently restricted the use of these emulsion methods in cell encapsulation.[32] As a substitute technique for producing a controlled emulsion electrospray is being popular these days. Electrospray, as described in literatures is electrostatic atomization, using a high voltage to overcome the surface tension of a fluid meniscus at an orifice, resulting in the generation of fine droplets.[33] It can be generally conducted in air or vacuum, however it is possible to perform ‘‘submerged electrospray’’ in insulating liquids.[34] Both electrospray techniques i.e. in air and more lately submerged electrospray have been tried with cells. Electrospray in air has been used extensively for cell encapsulation with good results and high cell viability.[35] Submerged electrospray has recently been used to spray cells, however not very famous in generation of cell encapsulating microspheres.

So in this chapter I examine the possibility of electro spraying a polypeptide matrix along with cells to generate hydrogel microspheres to encapsulate cells for a clinical use model.

4.2 Materials and Methods

4.2.1 Materials

Polypeptide (poly(lysine-co-glutamic acid) was synthesized by NCA method stated in chapter 2. Sorbitan monooleate (Span 80) were obtained from Sigma Aldrich. Olive oil was used from Nacalai tesque . Phosphate buffered saline (PBS) was made up with 137mM sodium chloride, 2.7mM potassium chloride, 10mM sodium phosphate dibasic, 2mM potassium phosphate monobasic to pH 7.4. Dulbecco's Modified Eagle Medium (DMEM), trypsin, fetal bovine serum were used for cell culture and calcein- AM and propidium iodide were used for cell staining.

4.2.2 Polymer preparation

The co copolymers PZLL-b-P(OBzl)PGA was synthesized as follows: firstly, the equimolar mixture of both amino acids glutamic acid and lysine, 7 mmol Lys (Z)-NCA (2 g) and Glu (OBzl)-NCA (1.8 g) was dissolved in 5 mL dimethylformamide with n-hexylamine (9.5 μL, 0.07 mmol) used as the initiator and stirred for 48 h at room temperature. The reaction mixture was then precipitated with an excess of diethyl ether under vigorous stirring. Then, the viscous polymer was again dissolved in dimethylformamide and re-precipitated with diethyl ether to give a white solid of PZLL-*b*-P(OBzl)PGA. The polymer was dried under vacuum at room temperature. De-protection was performed by dissolving the polymers in trifluoroacetic acid and 33 % HBr/ CH_3COOH followed by stirring for 10 h at room temperature. The de-protected polymers were precipitated with an excess of diethyl ether to obtain white solids that were dried in vacuum at room temperature for 48 h to yield PLL-PGA.

4.2.3 Electrospray Apparatus

The electrospray set up is shown schematically in Figure 1.

The water-in-oil droplet generation system was created by using a prototype electrospray assembly. Laboratory-made glass nozzles (~65 μm orifice diameter) and commercially available glass nozzles (~4 μm orifice diameter) [SIJ Technology, Japan] were used throughout the experiments. A 90-mm glass capillary was used to make nozzles with a Puller machine PC-10 [Narishige, Japan] using a 2-step mode and keeping the heater level between 60 and 50. Tungsten wire was used as an electrode when the large nozzle was used. In the electro spray chamber the earth electrode was a copper ring placed below the tip of needle. An oil phase contained olive oil with 5% span 80. All of the oil mixtures used in the experiments were freshly prepared by vortexing at 2,500 rpm for 5 min and incubating at 30 °C for 30 min.

Microspheres were isolated from the oil by adding PBS to the centrifuge tube and centrifuging at 1,000 rpm for 3 min. The oil was then aspirated and the pellet of beads in PBS was collected by pipette and resuspended in PBS. This washing step was repeated twice. Microspheres were imaged by optical microscopy for morphology. Sizing was done by laser scattering (Mastersizer 2000, Malvern Instruments). All diameters reported are based on volume calculations (means are given as the volume moment mean, D).

4.2.4 Cell Encapsulation

L929 murine fibroblasts were cultured in Dulbecco's Modified Eagle Medium (DMEM) supplemented with 10% fetal bovine serum. When required for experiments, cells were trypsinized and re-suspended in DMEM. Polypeptide (PLL-PGA) was dissolved in sterile PBS and the cell

suspension was added to give a final cell concentration of $1x10^6$ cells/mL and 5 wt% polymer. Sterile THCP was added to a final concentration of 0.05wt% and the solution gently mixed to ensure even cell distribution. The cell/macromer solution was transferred to a capillary nozzle and microsphere formation then proceeded as described previously. Cell encapsulation was performed at 2 kV. Microspheres were separated from the oil as described previously, re-suspended in complete DMEM and incubated at 37°C in 5% CO2. After 3h, 24 h and 3 day viability of cells within the spheres was assessed by Live/Dead staining with calcein-AM and propidium iodide (PI), each at 1mg/mL. Encapsulated cells were incubated in the staining solution in the dark for 10 min, washed with PBS and assessed immediately by microscopy (Keyence Biozero 2000). Viability is expressed as the percentage of live cells compared to total cells.

4.2.5 Characterization

^1H and ^{13}C NMR spectra were obtained at 25 °C on a Bruker AVANCE III 400 spectrometer (Bruker BioSpin Inc., Fällanden, Switzerland) in DMSO-d_6. Gel permeation chromatography (GPC) measurements were performed before de-protection of the polypeptides using a Shodex GPC101 (Yokohama, Japan) with a connection column system of 803 and 807 and equipped with Jasco 830 RI and Jasco UV-2075 plus detectors using pullulan as a molecular weight standard.

4.3 Results and discussions

Before any study the prepared polymers were characterized for the formation with NMR and GPC to evaluate their polydispersity, mass and gelation time (Table 4.1). Based on which the polymer was optimized to be used is marked as *

Table 4.1 Overview of polypeptides synthesized using NCA amino acid polymerization.

Polymer	PLL	PGA	M_n X 10^3	PDI[b]	Gelation Time (min)
PLL_{50}-PGA_{50}	50	50	22.14	1.12	21
*PLL_{75}-PGA_{75}	75	75	33.71	1.19	12
PLL_{100}-PGA_{100}	100	100	45.39	1.27	5

For the submerged electrospray setup the setup was established as illustrated in Figure 4.1. The aqueous mixture of fluids polypeptide, THPC (with or without cells) were introduced into the lumen of a glass needle. The nozzle was implanted with platinum wire for conduction of the current to the tip and under an open electric field, drops of the fluid at the tip of the needle was allowed to break and sprayed into an immersed bath of olive oil and was incubated at room temperature for 15 min to gel.

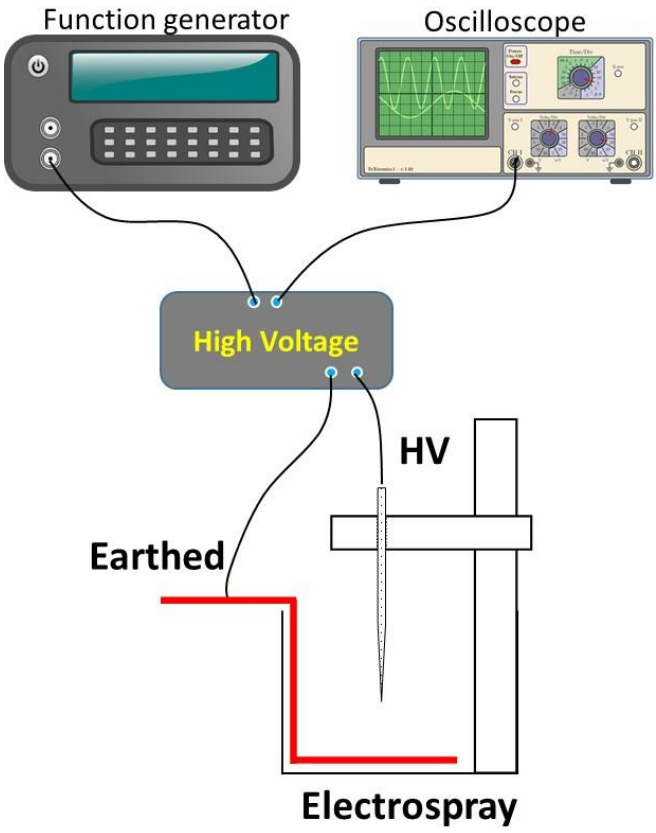

Figure 4.1. Schematic illustration of setup of immersed electrospray apparatus for generation of microspheres

Typical phase contrast (DIC) and light micrographs were used to demonstrate the formation of microspheres without cells. As seen in figure 4.2 the size of microspheres can be tuned to requirements by changing the nozzle size and resultant voltage applied to the system. The resultant microspheres varied from the 10 to approximately 300 μm in diameter.

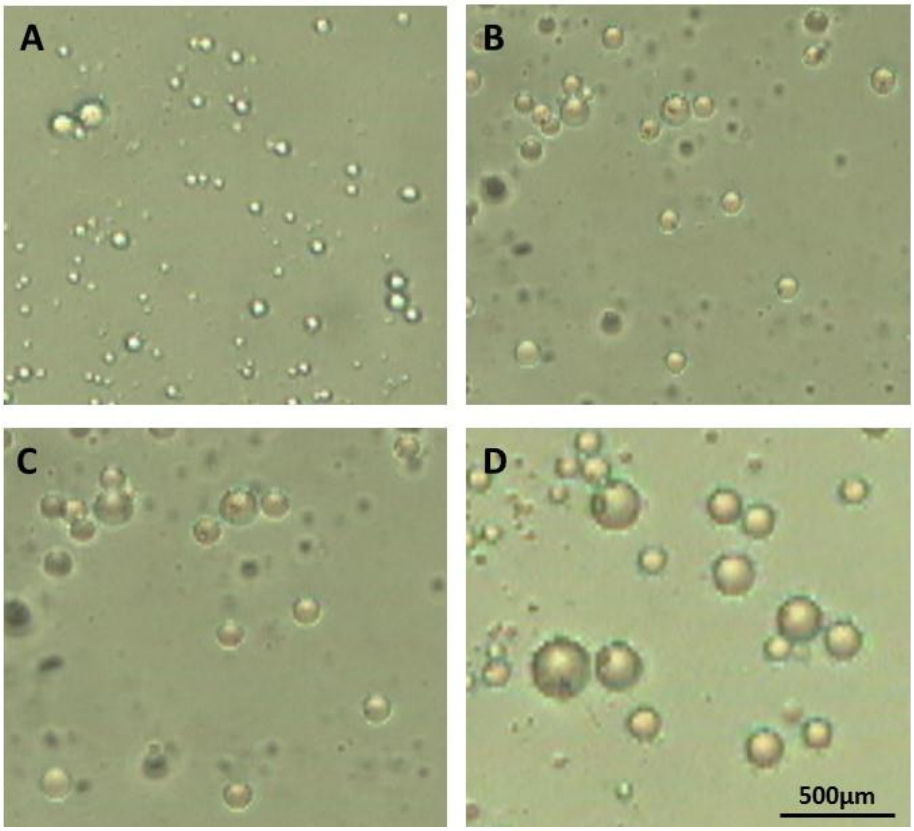

Figure 4.2 Different sizes of microspheres formed with varying voltage and nozzle sizes.

Evaluating the different sizes of nozzle and applied voltage (figure 4.3), the microsphere size is optimized at appox. 250µm which was easily achieved by applying 2 kV of voltage with 250µm nozzle diameter. As seen in the figure, the nozzle size and applied voltage both are crucially important parameters to control the size of the resulting microspheres. For a constant nozzle size, as the voltage increases the size of resulting microsphere decreases. It could be understood over the fact that as the higher voltage is applied the breaking force at the meniscus is higher,[36] which eventually leads to the breaking of meniscus layer into smaller droplets. And hence resulting smaller microspheres.

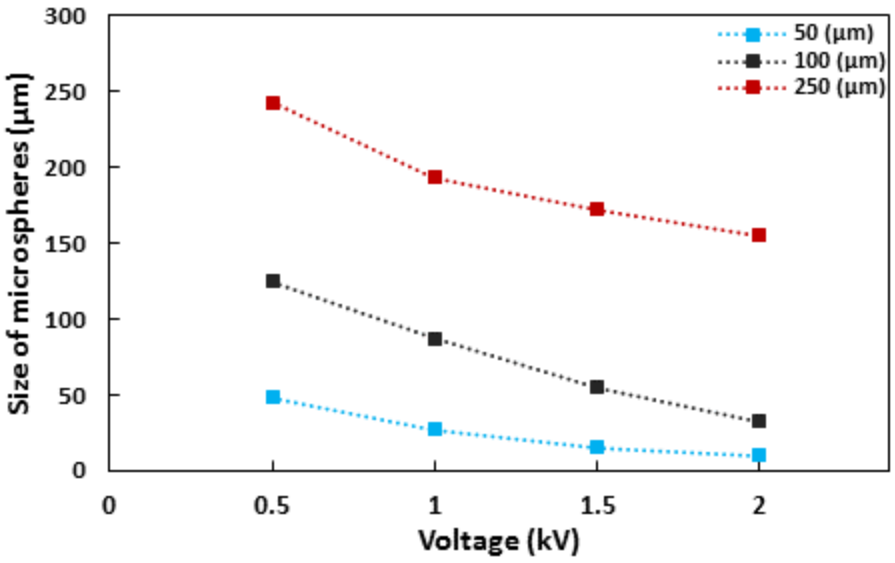

Figure 4.3 Dependence of nozzle size and voltage over the microsphere diameter.

Further for cell encapsulation, L929 cells were suspended in the core fluid at a density of 1 x 10^6 cells/ml and electrospray was done under the influence of 2 kV of applied voltage in an immersed olive oil bath. And under the optimized conditions, the resultant cell-laden microspheres were found to be of size 287 ± 27 µm in diameter (slightly larger than microspheres without cells (figure 4.4)). And as there were very few literatures citing the use of THPC, which is relatively new in arena of crosslinking, it was a valid consideration to evaluate the cyto-compatibility of the THPC as a cross linker. To study that we performed the cell viability assay of L929 cells in the polypeptide microspheres.

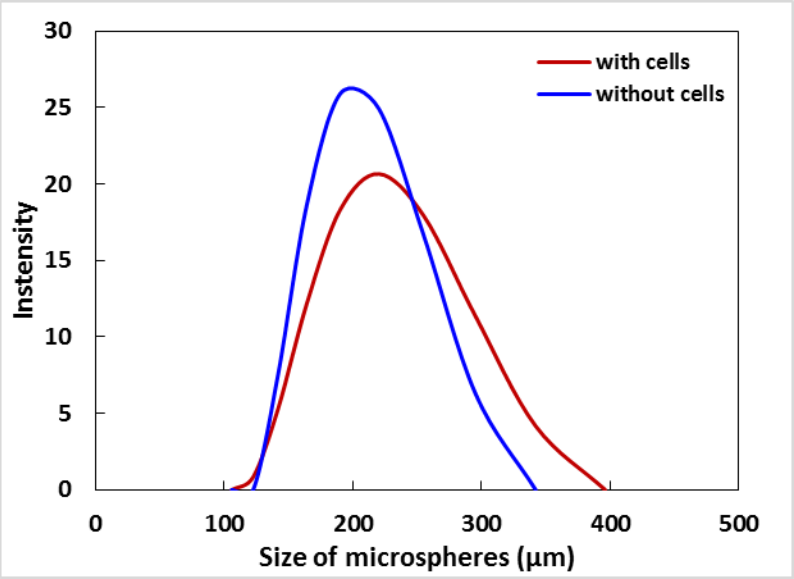

Figure 4.4. Size distribution of microspheres with and without encapsulated cells

As it can be seen in the figure 4.5, the THPC showed high cyto-compatibility with the cells as more than 80% of the live cell density was found even after three days of encapsulation. For lower THPC percentages such as 0.05, 0.1 and 0.5 the cell viability was relatively very high, whereas moving to higher percentage of THCP the cell viability decreases slightly which would be attributed to the high stiffness[37] of the gel encapsulating the cells causing stress and eventually cell death.

Also, when the percent of cross linker goes as high as 2% the cell viability decreases drastically which is due to that the gelation of the polypeptide solution takes place within the nozzle and microsphere formation is seized. And thus the viability cannot be recorded for percentage higher than 2%.

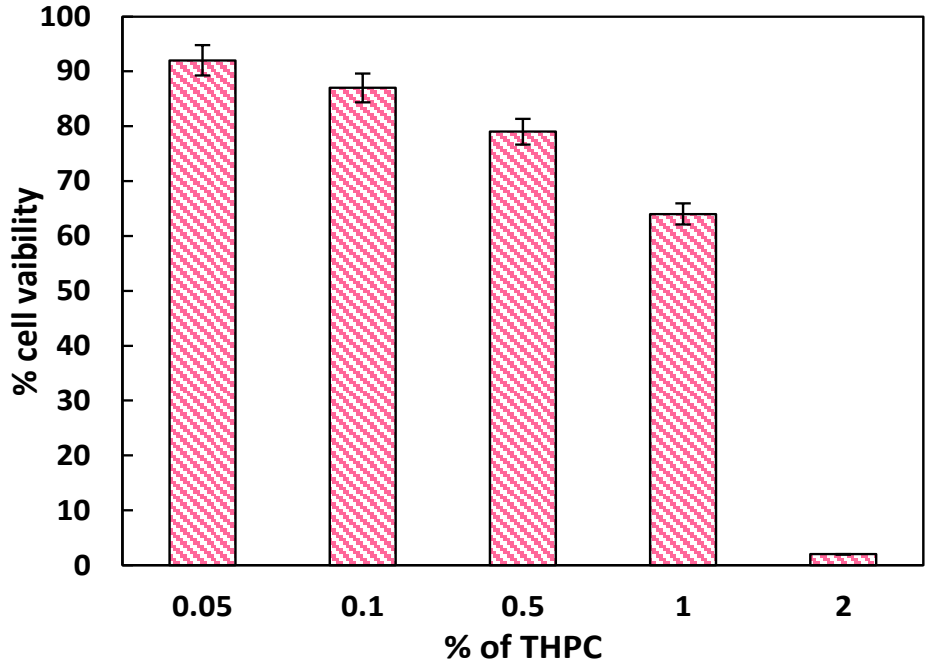

Figure 4.5 Cell viability with different percent of THPC

Seeing this behavior of rapid gelation on higher cross linker percentage and difficulty in formation of microspheres, we optimized the gelation time by varying the cross linker concentration.

Table 4.2 Optimization of gelation time with THPC

% of THPC	Critical Gelation Time
0.05	12 min
0.1	10 min
0.5	6 min
1	3 min
2	1 min

As seen, with increasing the cross linker concentration the gelation time decreases gradually till 2% where gelation is almost immediate to the mixing. Of the basis of the table above and study of gelation time, the ideal cross linker concentration was taken as 0.05% for the entire study unless

otherwise stated to make sure uniform mixing and spraying time for the solution before being gelled into hydrogel microspheres.

The figure 4.6, shows the microspheres with the encapsulated L929 cells under light microscope and after live dead assay.

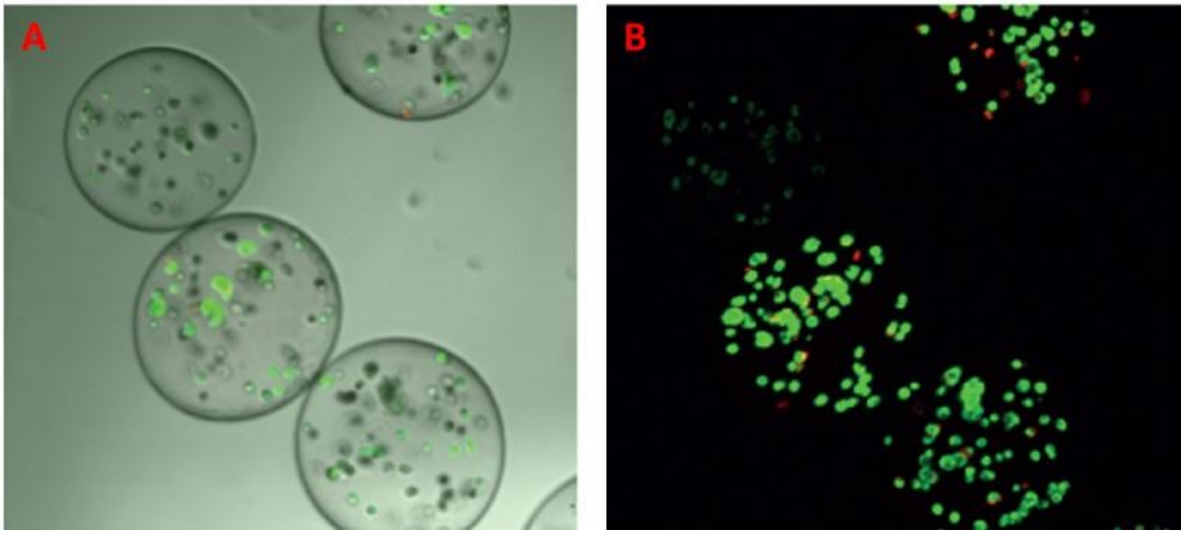

Figure 4.6 The image of L929 cells encapsulated in polypeptide microspheres A. light microscopic image B. after live dead assay

As this is a model study, first of kind with synthetic polypeptide polymer it was essential to optimize other parameters of the microsphere formation. As we have already seen that concentration of cross linker influence the formation of microspheres. So it was a valid consideration to estimate the effect of polymer concentration.

As we have seen in previous chapter (chapter 3) that the electrostatic interaction between the oppositely charged groups of the polypeptide chain effects the mechanistic properties of the gel on bulk scale. So decided to investigate that whether changing the polymer concentration i.e. varying

the electrostatic interactions would impose any influence on the size or formation of the cell containing microspheres.

For this we tried to vary the concentration of the polymer keeping all other parameters of the observation constant, to evaluate the effect of polymer concentration or density over the process.

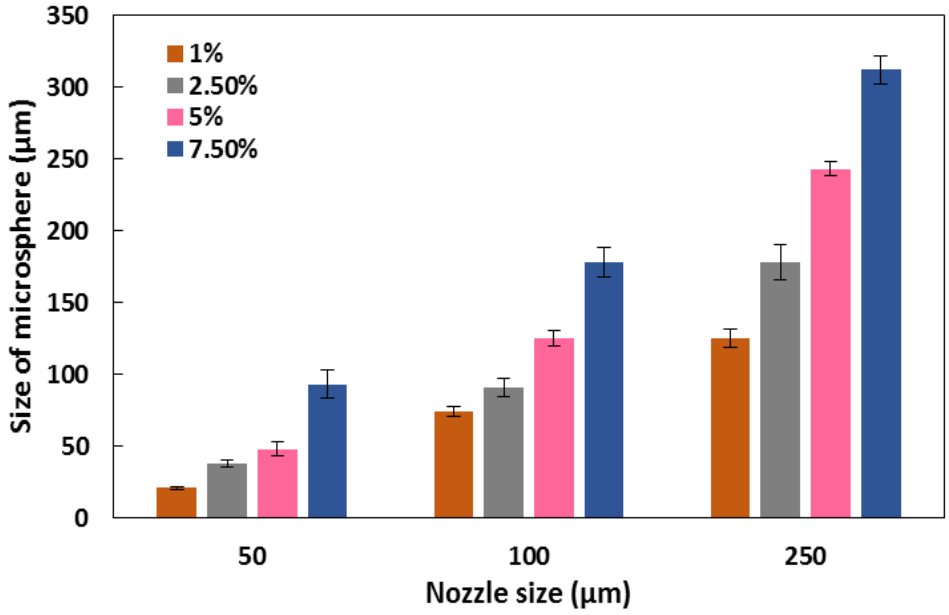

Figure 4.7 The effect of polymer concentration over formation of microspheres

As observed in the figure 4.7, keeping the other parameters constant for each nozzle value, with increasing the polymer concentration the size of microspheres increased significantly. Also, taking the visible parameters in consideration the polymer solution from 1% to 7.5% showed visible change in viscosity, i.e. higher the polymer concentration higher the viscosity was observed. This could be due to increased attractions among the oppositely charged groups of polymer chains causing inter as well as intra chain interaction[38] leading to higher viscosity of the solution. And as the previous literature quotes that higher viscosity of the solution in nozzle requires higher force

to separate the meniscus layer from the bulk. And as most of the force applied by the electric current is utilized in breaking the meniscus the remnant force[39] left to break the sprayed liquid into the droplets is reduced causing formation of larger droplets and hence bigger microspheres.

Further, as high voltage was being employed in generation of the microspheres, it was an obvious question that whether the cells are susceptible to this voltage or whether they can sustain to such stringent voltage conditions. For this we performed live/dead assay of the cell containing microspheres after 4 hours (day 0) and day 3 after the microsphere generation.

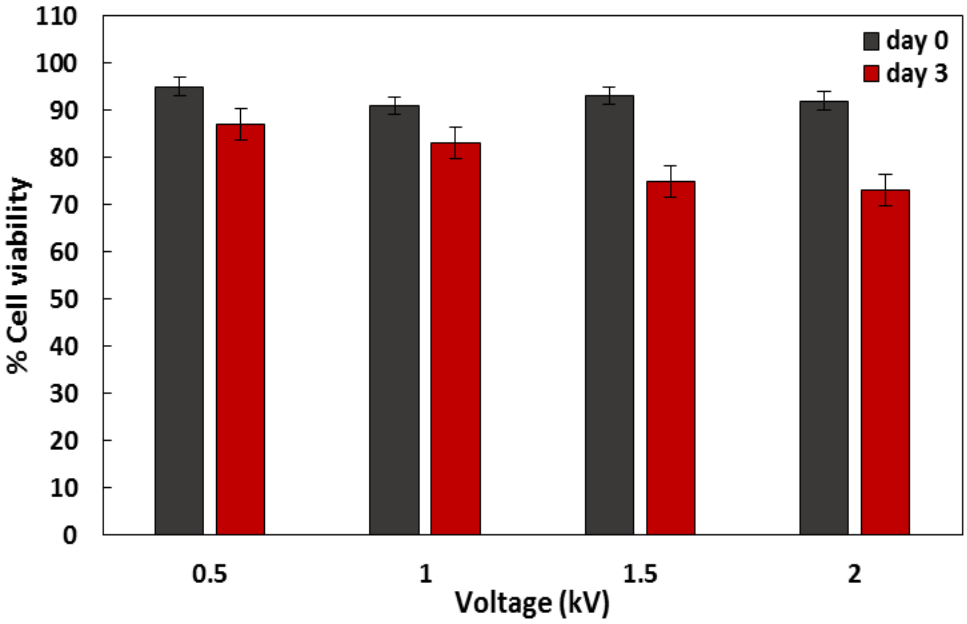

Figure 4.8 The cell viability at different applied voltages at day 0 and day 3 of microsphere generation.

As evident by figure 4.8, in all the samples tested the cell viability at day 0 was >90% showing that the high voltage eventually doesn't affect viability. Although the viability dropped at day 3 of microsphere generation but still was found to be considerably high being close 70-80%.

And it was interesting to see that cells sustained high level of viability even at such high voltages. Thus proving that this model study can be successfully applied to different cell lines for clinical purposes. Although this study can be vastly elaborated to evaluate the release of entrapped cell as specific sites or to study the release of bioactive molecules from the entrapped cell into the system.

This study although successful, still keeps different arena for trials open and can be continued further towards a conclusive approach.

4.4 Conclusion

Protein-based hydrogel systems serve as attractive in vitro systems to investigate cell response to environmental cues. The identification of new, cyto-compatible cross-linkers allows for greater flexibility of hydrogel design. Here, we have introduced THPC as an inexpensive, aqueous cross-linker for 3D cell encapsulation in peptide-based hydrogels. In this chapter we successfully formulated, entirely polypeptide based microspheres for cell encapsulation which can be tuned for their size over a range of parameters.

These microspheres were able to entrap cells successfully and showed cyto-compatibility with retention of cell growth and phenotype in the microsphere hydrogel system.

4.5 References

1 a) T. J. Nelson, A. Martinez-Fernandez, A. Terzic, *Nat Rev Cardiol* **2010**, *7*, 700-710; b) M. Mimeault, R. Hauke, S. K. Batra, *Clin Pharmacol Ther* **2007**, *82*, 252-264; c) G. Keller, *Gene Dev* **2005**, 19, 1129-1155.

2 a) K. R. Boheler, J. Czyz, D. Tweedie, H. T. Yang, S. V. Anisimov, A. M. Wobus, *Circ Res* **2002**, 91. 189-201; b) J. Kramer, C. Hegert, K. Guan, A. M. Wobus, P. K. Muller, J. Rohwedel, *Mechanisms of development* **2000**, *92*, 193-205.

3 a) Y. S. Pek, A. C. A. Wan, J. Y. Ying, *Biomaterials* **2010**, *31*, 385-39; b) J. K. Choi, X. He, *PLoS One* **2013**, *8*, e56158; b) T. W. Sadler, Langman's medical embryology 12th Ed. Lippincott Williams & Wilkins: Philadelphia

4 a) D. T. Scadden, *Nature* **2006**, *441*, 1075-9; b) E. Cukierman, R. Pankov, D. R. Stevens, K. M. Yamada, *Science* **2001**, *294*, 1708-12; c) L. G. Griffith, M. A. Swartz, *Nat Rev Mol Cell Biol* **2006**, 7, 211-24.

5 B. S. Yoon, S. J. Yoo, J. E. Lee, S. You, H. T. Lee, H. S. Yoon, *Differentiation* **2006,** *74*, 49-159; b) D. E. Kehoe, D. H. Jing, L. T. Lock, E. S. Tzanakakis, *Tissue Eng Pt A* **2010**, *16*, 405-421.

6 A. Faulkner-Jones, S. Greenhough, J. A. King, J. Gardner, A. Courtney, W. M. Shu, *Biofabrication* **2013**, 5.

7 J. Park, C. H. Cho, N. Parashurama, Y. W. Li, F. Berthiaume, M. Toner, A. W. Tilles, M. L. Yarmush,, *Lab Chip* **2007**, *7*, 1018-1028

8 a) A. M. Bratt-Leal, R. L. Carpenedo, T. C. McDevitt, *Biotechnol Prog* **2009**, *25*, 43-51; b) H. Kurosawa, *J Biosci Bioeng* **2007**, *103*, 389-98

9 a) M. Shafa, B. Day, A. Yamashita, G. Meng, S. Liu, R. Krawetz, D. E. Rancourt, *Nat Methods* **2012**, *9*, 465-6.

10 D. A. Fluri, P. D. Tonge, H. Song, R. P. Baptista, N. Shakiba, S. Shukla, G. Clarke, A. Nagy, P. W. Zandstra, *Nat Methods* **2012**, *9*, 509-16.

11 Y. S. Hwang, B. G. Chung, D. Ortmann, N. Hattori, H. C. Moeller, A. Khademhosseini, *Proc Natl Acad Sci U S A* **2009**, *106*, 16978-83

12 a) N. S. Hwang, S. Varghese, Z. Zhang, J. Elisseeff, *Tissue Eng* **2006**, *12*, 2695-2706; b) H. Park, J. S. Temenoff, Y. Tabata, A. I. Caplan, A. G. Mikos, *Biomaterials* **2007**, *28*, 3217-3227

13 G. Orive, R. M. Hernandez, A. R. Gascon, R. Calafiore, T. M. S. Chang, P. De Vos, G. Hortelano, D. Hunkeler, I. Lacik, A. M. J. Shapiro, J. L. Pedraz, *Nat Med* **2003**, *9*, 104-107.

14 H. Liu, J. Lin, K. Roy, *Biomaterials* **2006**, *27*, 5978-89

15 K. Y. Lee, D. J. Mooney, *Prog Polym Sci* **2012**, *37*, 106-126; b) A. D. Augst, H. J. Kong, D. J. Mooney, *Macromol Biosci* **2006**, *6*, 623-33; c)W. Zhang, X. He, *J Biomech Eng* **2009**, *131*, 074515.

16 a) Y. H. Lee, F. Mei, M. Y. Bai, S. Zhao, D. R. Chen, *J Control Release* **2010**, *145*, 58-65; b) J. Kim, P. Sachdev, K. Sidhu, *Stem cell research* **2013**, *11*, 978-989

17 F. Chen, Y. Zhan, T. Geng, H. Lian, P. Xu, C. Lu, *Anal Chem* **2011**, 8816-20

18 Y. Wu, I. C. Liao, S. J. Kennedy, J. Du, J. Wang, K. W. Leong, R. L. Clark, *Chem Commun (Camb)* **2010**, *46*, 4743-5,

19 L. Zhang, J. Huang, T. Si, R. X. Xu, *Expert Rev Med Devices* **2012**, *9*, 595-61236.

20 D. B. Shenoy, A. A. Antipov, G. B. Sukhorukov, H. Mohwald, *Biomacromolecules* **2003**, *4*, 265-72,

21 T. Maguire, E. Novik, R. Schloss, M. Yarmush, *Biotechnol Bioeng* **2006**, *93*, 581-91.

22 W. Zhang, S. Zhao, W. Rao, J. Snyder, J. K. Choi, J. Wang, I. A. Khan, N. B. Saleh, P. J. Mohler, J. Yu, T. J. Hund, C. Tang, X. He, *J Mater Chem B Mater Biol Med* **2013**, *2013*, 1002-1009

23 X. Wang, W. Wang, J. Ma, X. Guo, X. Yu, X. Ma, *Biotechnol Prog* **2006**, *22*, 791-800.

24 S. Sakai, I. Hashimoto, K. Kawakami, *Biotechnol Bioeng* **2008**, *99*, 235-43.

25 a) S. Sakai, S. Ito, K. Kawakami, *Acta Biomater* **2010**, *6*, 3132-7; b) C. Kim, S. Chung, Y. E. Kim, K. S. Lee, S. H. Lee, K. W. Oh, J. Y. Kang, *Lab Chip* **2011**, *11*, 246-52.

26 a) P. Agarwal, S. Zhao, P. Bielecki, W. Rao, J. K. Choi, Y. Zhao, J. Yu, W. Zhang, X. He, *Lab Chip* **2013**, *13*, 4525-33; b) Y. C. Tung, A. Y. Hsiao, S. G. Allen, Y. S. Torisawa, M. Ho, S. Takayama, *Analyst* **2011**, *136*, 473-8.

27 a) J. Choi, P. Agarwal, H. Huang, S. Zhao, X. He, *Biomaterials* **2014**, *35*, 5122-5128; b) D. R. Cole, M. Waterfall, M. McIntyre, J. D. Baird, *Diabetologia* **1992**, *35*, 231-7.

28 P. de Vos, C. G. van Hoogmoed, B. J. de Haan, H. J. Busscher, *J Biomed Mater Res* **2002**, *62*, 430-7.

29 W. Dou, D. Wei, H. Li, H. Li, M. M. Rahman, J. Shi, Z. Xu, Y. Ma, *Carbohydrate polymers* **2013**, *98*, 1476-82.

30 J. C. Duarte, *Fems Microbiol Rev* **1994**, *13*, 121-121; b) D. M. Updegraf, Semimicro *Anal Biochem* **1969**, *32*, 420-427.

31 C. K. Griffith, C. Miller, R. C. A. Sainson, J. W. Calvert, N. L. Jeon, C. C. W. Hughes, S. C. George, *Tissue Eng* **2005**, *11*, 257-266; b) M. Zhang, D. Methot, V. Poppa, Y. Fujio, K. Walsh, C. E. Murry, *J Mol Cell Cardiol* **2001**, *33*, 907-921.

32 M. Amit, I. Laevsky, Y. Miropolsky, K. Shariki, M. Peri, J. Itskovitz-Eldor, *Nature protocols* **2011**, *6*, 572-9.

33 R. Zweigerdt, R. Olmer, H. Singh, A. Haverich, U. Martin, *Nature protocols* **2011**, *6*, 689-700; b) M. P. Storm, C. B. Orchard, H. K. Bone, J. B. Chaudhuri, M. J. Welham, *Biotechnol Bioeng* **2010**, *107*, 683-95.

34 P. W. Burridge, S. Thompson, M. A. Millrod, S. Weinberg, X. A. Yuan, A. Peters, V. Mahairaki, V. E. Koliatsos, L. Tung, E. T. Zambidis, *PLoS One* **2011**, *6*.

35 S. J. Kattman, A. D. Witty, M. Gagliardi, N. C. Dubois, M. Niapour, A. Hotta, J. Ellis, G. Keller, *Cell Stem Cell* **2011**, *8*, 228-240.

36 a) S. S. Y. Wong, H. S. Bernstein, *Regen Med* **2010**, *5*, 763-775; b) P. B. Zhang, J. A. Li, Z. J. Tan, C. Y. Wang, T. Liu, L. Chen, J. Yong, W. Jiang, X. M. Sun, L. Y. Du, M. X. Ding, H. K. Deng, *Blood* **2008**, *111*, 1933-1941.

37 B. I. Jugdutt, *Circulation* **2003**, *108*, 1395-403; b) K. Song, Y. J. Nam, X. Luo, X. Qi, W. Tan, G. N. Huang, A. Acharya, C. L. Smith, M. D. Tallquist, E. G. Neilson, J. A. Hill, R. Bassel-Duby, E. N. Olson, *Nature* **2012**, *485*, 599-604.

38 a) R. G. Gourdie, N. J. Severs, C. R. Green, S. Rothery, P. Germroth, R. P. Thompson, *Journal of cell science* 1**993**, *105* (Pt 4). 985-91; b) L. F. Lemanski, *The Journal of cell biology* **1979**, *82*, 227-38;

39 Z. Ai, A. Fischer, D. C. Spray, A. M. Brown, G. I. Fishman, *The Journal of clinical investigation* **2000**, *105*, 161-71.

CHAPTER 5

General Conclusion

4.1 Summary of the thesis

The work reported in this thesis emphasizes over the use of synthetic polypeptide materials over drug and cell delivery for clinical use. This thesis addresses the possibility of synthetic polypeptide materials to be employed for various biomaterial and clinical applications. The polypeptides used in this work were synthesized using the ring opening polymerization of NCA monomers with controlled PDI and mass. These polypeptide materials show tremendous scope toward being used in various clinical approaches.

Chapter 2, of this work presents the research employed in formulating an entirely polypeptide based material as a dual drug releasing hydrogel. . I used simple amino acid block peptides to synthesize who different kinds of micelle precisely PLL-PPA and PGA-PPA. This work used the strategy of utilizing these two oppositely charged micelle and encapsulating drugs in the hydrophobic core of the micelles. Further the micelles were cross linked to form a stable hydrogel and the drug release profile from these micelles were studied. In results, it was found that these micelles can be efficiently tuned over a range of parameters to switch there drug release profiles according to the tailored need. Such a phenomenon can be of use in field of controlled and simultaneous drug release for wound healing purposes.

In chapter 3, I presented the research I employed to test these micelle-hydrogel composites prepared in chapter 2 for their wound healing efficiency on animal models, for which curcumin was used as a model drug for the study. To be precise, this chapter talks about *in vivo* experiments conducted over a batch of rat models to test the efficacy of previously created micelle-hydrogel composite. For this rat models were divided in 4 groups of control, blank, low conc., and high conc. and were given an excision wound. The created wound were either implanted with hydrogels

laden with/without drug or just gauge bandage. In this study it was found that the synthesized composites are not only biocompatible but also showed an enhanced wound healing efficiency on almost all the parameters than blank and control groups. Wound healing indicators such as granulation, re-epithelialization, inflammation, angiogenesis, and wound closure was studied along with biochemical test to determine the content of SOD, catalase and collagen in the wounded tissue. The study revealed that the composites were very efficient toward wound healing. Also, the mechanical study was performed to evaluate the loss and storage modulus of the gels to develop a better understanding towards the drug delivery process.

Further, **in chapter 4**, I tried to explore a new area with these synthetic polypeptides. As in previous chapter these polypeptides were proven to be cyto-compatible so, we tried to explore these polypeptide for cell encapsulation. In this chapter we employed microfluidic technique of electrospray to form spherical shaped microsphere entrapping cells. For this study L929 cells were used. In the results, the cells showed high viability within the entrapped microsphere. Also, it was found that microsphere size can be tuned on the various parameters such nozzle size, voltage and concentration of polymer.

4.2 Future prospectus

In chapter 4 we are working on the cell delivery, although we received few promising results in preliminary study like cell were actively surviving, and proliferating. Even at high voltage the cell were surviving. We further plan to evaluate cell release from this microspheres as well as develop a strategy to release the active molecules such as cytokines and other growth factors from the encapsulated cell into the surroundings.